

L-628
19930093663

MR Jan. 1944

NATIONAL ADVISORY COMMITTEE FOR AERONAUTICS

WARTIME REPORT

ORIGINALLY ISSUED

January 1944 as
Memorandum Report

TESTS OF THE NORTHRUP MX-33¹/4 GLIDER AIRPLANE

IN THE NACA FULL-SCALE TUNNEL

By Gerald W. Brewer

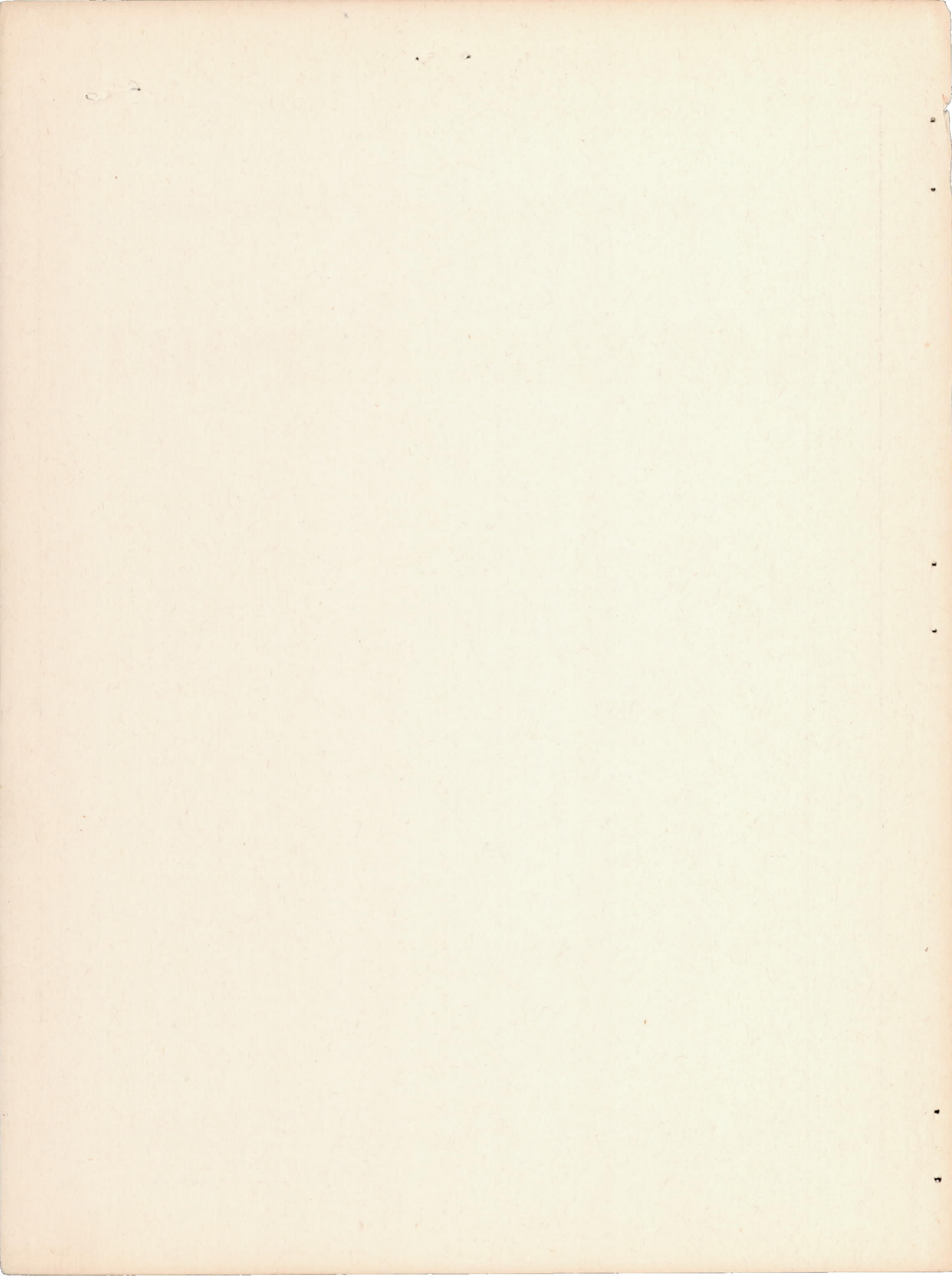
Langley Memorial Aeronautical Laboratory
Langley Field, Va.

PROPERTY OF
E-SYSTEMS INC.
GARLAND DIVISION
LIBRARY



WASHINGTON

NACA WARTIME REPORTS are reprints of papers originally issued to provide rapid distribution of advance research results to an authorized group requiring them for the war effort. They were previously held under a security status but are now unclassified. Some of these reports were not technically edited. All have been reproduced without change in order to expedite general distribution.



NATIONAL ADVISORY COMMITTEE FOR AERONAUTICS

MEMORANDUM REPORT

for the

Army Air Forces, Materiel Command

TESTS OF THE NORTHROP MX-334 GLIDER AIRPLANE

IN THE NACA FULL-SCALE TUNNEL

By Gerald W. Brewer

INTRODUCTION

Tests of the Northrop MX-334 airplane have been made in the NACA full-scale tunnel at the request of the Army Air Forces, Materiel Command. The results of this investigation are of particular interest since the MX-334 is an all-wing glider-type airplane having neither a conventional fuselage nor vertical surfaces.

The primary purpose of these tests was to obtain sufficient data with which to determine the longitudinal and lateral stability and control characteristics of the airplane. In addition to the stability and control study, this memorandum report contains the results of tests that were made to (1) determine a suitable wing-tip leading-edge slat arrangement which would improve the static longitudinal stability of the airplane as well as increase the maximum lift coefficient; (2) establish a value of the minimum drag coefficient for the basic wing and determine the additional drag caused by the leading-edge slats; (3) determine the effects on the directional stability characteristics of the airplane of the addition of vertical fins; (4) measure the effectiveness of the air-operated directional control system.

SYMBOLS

C_D drag coefficient ($X/q_0 S$)

C_Y lateral-force coefficient ($Y/q_0 S$)

C_L	lift coefficient ($Z/q_0 S$)
C_l	rolling-moment coefficient ($L/q_0 Sb$)
C_m	pitching-moment coefficient ($M/q_0 Sc$)
C_n	yawing-moment coefficient ($N/q_0 Sb$)
C_{he}	elevator hinge-moment coefficient ($H_e/q_0 b_e \bar{c}_e^2$)
C_{ha}	aileron hinge-moment coefficient ($H_a/q_0 b_a \bar{c}_a^2$)

where

X	force along X axis, positive when directed backward
Y	force along Y axis, positive when directed to right
Z	force along Z axis, positive when directed upward
L	rolling moment about X axis, positive when it tends to depress the right wing
M	pitching moment about Y axis, positive when it tends to depress the trailing edge
N	yawing moment about the Z axis, positive when it tends to retard the right wing
H_e	elevator hinge moment, positive when the trailing edge is directed downward
H_a	aileron hinge moment, positive when the trailing edge is directed downward
q_0	free-stream dynamic pressure $(\frac{1}{2} \rho V_0^2)$
ρ	mass density of air
V_0	free-stream velocity
S	wing area (250 square feet)
b	wing span (36 feet)
c	wing mean chord (6.95 feet)
b_e	elevator span (9.7 feet)

b_a	aileron span (9.7 feet)
b_t	elevon tab span (2 feet)
\bar{c}_e	root-mean-square elevator chord (0.833 foot)
\bar{c}_a	root-mean-square aileron chord (0.833 foot)
\bar{c}_t	root-mean-square tab chord (0.167 foot)
Q/V_o	relative air-flow quantity
Q	volume rate of air flow
$p b/2V$	helix angle
p	rolling velocity, radians per second
V	indicated airspeed
F_e	elevator stick force
F_a	aileron stick force
Δp	difference in static pressure between the inside and outside of the rudder bellows
c_{d_0}	section profile-drag coefficient
H_o	free-stream total pressure
H_l	total pressure in the field of the airfoil
y	vertical distance from the wake center
F	a correction factor, usually about 0.8 to 0.9
α	angle of attack of thrust axis, degrees
ψ	angle of yaw, degrees; positive when the right wing is retarded
δ_e	elevator deflection (with respect to the wing chord), degrees; positive when the trailing edge is deflected downward
δ_a	aileron deflection, degrees; positive when the trailing edge is deflected downward

$\Delta\delta_a$ total deflection of both ailerons, degrees
 δ_r rudder deflection, degrees (subscript L indicates left rudder)
 δ_t tab deflection, degrees; positive when the trailing edge is directed downward

DESCRIPTION OF MODEL

The Northrop MX-334 as tested in the NACA full-scale tunnel is a single-place, all-wing, glider-type airplane. Figure 1 shows the airplane mounted on the balance system. The more important characteristics of the airplane are summarized in the following table:

Gross weight, pounds	2960
Total wing area, square feet	250
Wing span, feet	36
Mean aerodynamic chord, feet	8.21
Airfoil section (constant along the span). NACA 66,2-018	
Proposed center-of-gravity location,	
percent M.A.C.	27.5
Angle of incidence relative to thrust	
line, degrees	0
Angle of sweepback of the quarter chord	
line, degrees	21.8
Geometric twist, degrees	0
Dihedral angle, degrees	1

The general arrangement of the wing and control surfaces and the over-all dimensions of the airplane are shown in figure 2. The airplane was also equipped with fixed wing-tip slats which are not shown in the figure. The pilot's cockpit in this airplane is an integral part of the wing and is located in the center section of the wing near the leading edge. The wheel-type control column, which is operated from a prone position, is housed in the extended section at the leading edge.

The outboard control surfaces, classified as elevons, serve the dual purpose of elevators and ailerons. The elevons for this airplane were sealed and internally balanced. The general arrangement of the balance is

given in figure 3. It was necessary to install additional seals at the hinges and at the inboard and outboard ends of the elevons prior to the tests to obtain a completely sealed control surface.

The inboard surfaces are the air-operated bellows type and provide both dive braking and directional control. Each surface was divided into two parts to simplify the structure at the joint between the wing and center section. The mechanical linkage between these two surfaces is such that the upper and lower surfaces have identical angular travel. Neither surface can be operated individually. The ducting for this system consists of a passage from a leading-edge inlet through a venturi section to a trailing-edge outlet and a second duct leading from the venturi throat to the bellows. The pressure and air flow for the bellows are regulated by means of a butterfly control valve placed in the venturi section.

METHODS AND TESTS

During preliminary tests of the airplane with the slats removed the wing tips stalled at high angles of attack. Due to the high sweepback of the wing this tip stall caused a serious longitudinal instability. The development was therefore undertaken of a leading-edge slat configuration that would eliminate the inherent longitudinal instability of the wing.

The three slat arrangements that were tested include (1) the original slat (fig. 4), (2) the original slat moved closer to the wing leading-edge contour (fig. 4), and (3) a large-span slat with the revised slot. The original and the large-span slats extended 20 and 36.6 percent of the wing span, respectively (figs. 1 and 5). Force and moment measurements were made through a large range of angles of attack for the basic wing and for the three slat configurations. To supplement the force tests, tuft observations were made to determine the stalling characteristics of the wing as affected by these slat configurations.

In order to provide a check on the force-test results, the minimum drag of the airplane was also obtained by measuring the loss of total pressure in the wake behind

the wing. These measurements were made at numerous stations along the span at a distance approximately 0.30c behind the wing with the airplane at the zero lift attitude.

In order to obtain data for the determination of the longitudinal stability and control characteristics of the airplane, aerodynamic moments and forces on the airplane and elevon hinge moments were determined for a large range of elevon deflections and angles of attack. The changes in the hinge moments resulting from deflection of the elevon tab, removal of the added seals at the hinges and ends of the elevons, and the installation of a beveled trailing-edge elevon were also determined.

For the determination of the lateral stability characteristics of the airplane, forces and moments were measured at several angles of attack for angles of yaw ranging from 0 to 18.6. Some additional tests were made to determine the effect on the directional stability of the airplane of installing two sets of vertical fins on the upper and lower surfaces at the airplane center line. One set projected 12 inches from the wing contour and extended 4 feet on either side of the center-of-gravity position; the second set, of equal side area (16 square feet), extended 4 feet rearward from the center of gravity. Figure 6 shows the arrangement of the fins on the airplane.

Due to the unconventional method of rudder and brake control, tests were made to determine the effectiveness of the duct system. The air-flow quantity and the bellows pressures were obtained for four control-valve positions with the original and the modified leading-edge duct inlet. A sketch of the inlet modification is shown in figure 7.

The data are presented in standard NACA force and moment coefficient form and are corrected for jet-boundary and blocking effects by the methods discussed in references 1 and 2. The moments have been computed about a center of gravity located at 27.5 percent of the mean aerodynamic chord and on the root chord line. The results of the tests have been referred to conventional stability axes. The X axis always lies in the plane of symmetry of the airplane and is oriented to coincide with the relative wind direction at zero yaw and with the projection of the relative wind on the plane of symmetry at any angle of yaw.

RESULTS AND DISCUSSION

Aerodynamic Characteristics of the Airplane

Lift and pitching moments. - The lift and pitching-moment characteristics of the airplane, with the leading-edge wing slat removed and with the original and large-span slats installed, are given in figure 8. The results of tuft observations, which supplement the force test data, are shown in figures 9 and 10. The pitching-moment variation for the basic wing shows approximately neutral stability for lift coefficients up to the stall with the center of gravity located at 27.5 percent mean aerodynamic chord. At the stall the loss of lift at the wing tips increases the positive pitching-moment coefficient and causes serious longitudinal instability. It was evident that, before further investigation of the aerodynamic characteristics of the airplane were justified, improvement of the static longitudinal stability of the wing near the stall was necessary.

The most effective method for eliminating the instability appeared to be the control of the stalling pattern with suitable wing-tip slats and, accordingly, the three slat configurations previously described were tested. Each slat configuration progressively improved the stalling characteristics of the wing, as shown by the continuous decrease in wing-tip stall in the tuft surveys, and by the decrease in positive pitching moments at angles of attack near the stall in figure 8. The large-span slats with the revised slot retarded the flow breakdown at the tip section until after the center section had stalled, thus eliminating the cause of the instability. They also increased the maximum lift coefficient from a value of 1.15 to 1.26. The unstable pitching-moment variation at low lift coefficients for this condition is probably due to the interference effects of the slats on the air flow over the wing at low angles of attack.

Drag. - The drag data from these tests are presented in figure 11. The minimum drag coefficient for the basic wing was 0.0100. The original slats with the revised slot increased this value to 0.0118; the large-span slats with the revised slot, to 0.0146.

In order to determine the section drag coefficients and to check the minimum drag of the basic wing, wake

surveys were made. The section profile-drag coefficients were calculated by the relation

$$c_{d_0} = \frac{F}{c} \int_{\text{wake}} \left(\frac{H_0 - H_1}{H_0} \right) dy$$

which is discussed in more detail in reference 3. The results of these calculations are presented as the variation of $c_{d_0} c$ with spanwise station in figure 12. The shaded areas on this figure represent the portion of the total measured drag that was contributed by the interference of the support struts and fairings. Integration of the section drag coefficients along the span, excluding the 22-inch center section, gave a drag coefficient of 0.0074. A detailed survey of this center section gave a further contribution of 0.0019 to the total drag of the wing. This latter increment includes the profile drag of the center section as well as the drag corresponding to the energy losses of the air passing through the duct system. The sum of these values gives a total drag coefficient of the airplane of 0.0093, as measured by the momentum method.

The minimum drag coefficient obtained by force tests is greater than the drag coefficient determined from the wake surveys by 0.0007. This difference is somewhat greater than the expected experimental inaccuracy (reference 4). Further analytical investigation showed that the difference arises from the induced drag resulting from variations of lift across the span of the wings. Evidence for such spanwise variation of the lift was furnished by the wake surveys which showed appreciable vertical displacements of the wake relative to the trailing edge, corresponding to appreciable local downwash and upwash angles. The displacement of the wake was particularly noticeable behind the center section, and at a location about 4 feet to the right of the center. By an analysis of these angles, which are assumed to be given by the ratio of the vertical displacement to the distance from the trailing edge, an induced-drag coefficient of 0.0005 was computed. The addition of this value to that found for the profile-drag coefficient gives a total of 0.0098 which is in satisfactory agreement with the value of 0.0100 determined by the force tests.

Static Longitudinal Stability and Control

Elevator effectiveness. - The results of tests made with the sealed elevons operated as elevators are given in figures 13 and 14 which show the variation of C_L , C_m , and C_{he} with elevator deflection. The data are presented for the basic wing and for the wing with the large-span slats installed. At low angles of attack the elevator effectiveness $dC_m/d\delta_e$, measured at $C_m = 0$, is -0.0047 with the slats removed and is -0.0041 with the large-span slats installed. Although $dC_m/d\delta_e$ is decreased at high lift coefficients for the slats-removed condition to -0.0034, the value of $dC_m/d\delta_e$ for the slats-installed condition remains unchanged. Similarly, the values of $dC_{he}/d\delta_e$, measured at $C_{he} = 0$, are lower at low lift coefficients and higher at high lift coefficients with the slats installed than with the slats removed. For the slats-removed condition $dC_{he}/d\delta_e$ is -0.0055 at a C_L of 0.34 and -0.0035 at a C_L of 0.90; with the slats installed, $dC_{he}/d\delta_e$ is -0.0050 at a C_L of 0.33 and -0.0043 at a C_L of 0.92.

In order to compare the stick-fixed longitudinal stability of the airplane with and without slats, curves showing the variation of elevator deflections for trim with lift coefficient have been obtained from the test results and are given in figure 15. With the slats removed, the airplane is unstable from a C_L of 0.1 to 0.4 and is neutrally stable from a C_L of 0.4 to 0.9. At higher lift coefficients there is a large degree of instability since increases of down-elevator deflections are required to reduce the forward speed of the airplane. With the large-span slats installed, however, the airplane is stable at all lift coefficients above 0.6 but is approximately neutrally stable at lower lift coefficients.

A criterion for satisfactory stability requires a stable stick-free pitching-moment variation. The results in figure 16 show that the airplane with slats removed is very unstable, stick free. With the airplane trimmed at the same lift coefficient, it is shown that the large-span slats decreased this instability slightly and that the large positive pitching-moment variation at high lift coefficients was reduced.

It has already been shown that by eliminating wing-tip stall the large-span slats increased the static longitudinal stability of the airplane at high angles of attack, but, in addition, the improvement of air flow over the wing-tip section decreased the trailing-edge-up floating tendency of the elevons. Figure 17 shows lower elevon floating angles throughout the lift-coefficient range with the slats installed. Near the stall, the effect of the slats is to reduce the floating angle from the maximum up-elevator deflection of 13° up to an angle of approximately 5° .

Another measure of the stability of the airplane is the variation of stick force for trim with flight speed. The stick forces were computed from the relation

$$F_e = \frac{1}{57.3} \frac{d\delta_e}{dx} q b_e c_e^2 C_{he}$$

where $d\delta_e/dx$ is the variation of elevator deflection with stick travel which may be obtained from the calibration given in figure 18. The elevator stick forces required to trim the airplane through the speed range for level flight are presented in figure 19. Evidence of the instability of the airplane, without slats, is given by the stick-force variation which shows pull forces at speeds above the trim speed and push forces, below the trim speed. Although the large-span slats greatly improved the variation of trim stick forces with speed, the stick-force gradient is very low. With the airplane trimmed at 100 miles per hour, however, an unstable stick-force variation still exists. This unstable condition can be alleviated somewhat by artificial means.

In the previous sections it has been shown that for the design center-of-gravity location of 27.5 percent mean aerodynamic chord the airplane is unstable with slats removed and stable at lift coefficient above 0.6 with the large-span slats installed. The most rearward center-of-gravity positions for neutral stability are shown in figure 20 for the two configurations. The airplane with slats installed will be stable at all lift coefficients for a center-of-gravity position of 26 percent mean aerodynamic chord. With the slats removed the airplane will be longitudinally stable up to a lift coefficient of 1.0 for a center-of-gravity location of 25 percent mean aerodynamic chord. At higher lift coefficients the neutral point moves forward rapidly.

Tab effectiveness. - The results of elevator effectiveness tests made for tab deflections of $\pm 10^\circ$ and $\pm 20^\circ$ with the large-span slats installed are given in figure 21. These curves show the variation of C_L , C_m , and C_{he} with δ_e for three angles of attack. The values of $dC_m/d\delta_e$ and $dC_{he}/d\delta_e$ are both approximately -0.0040 for the range of lift coefficients and tab deflections tested.

The longitudinal stability and control characteristics of the airplane with the tab deflected are compared with the results of the preceding section for the zero tab setting in figures 22 to 25. For the range of lift coefficients tested, the variation of elevator deflection for trim with lift coefficient (fig. 22) is stable for tab deflections of 10° and $\pm 20^\circ$. The variation of δ_e for trim with C_L with the tab deflected -10° is approximately the same as that with the tab neutral.

The instability of the airplane, stick free, is generally the same with the tab deflected as with the tab neutral (fig. 23). At the larger positive tab deflection and at high angles of attack the instability increases, probably on account of tab stalling.

It is shown in figure 24 that the elevator with the tab deflected -10° floats about 1° more nose up at a C_L of 0.3 and 3° more at a C_L of 1.2 than with the tab neutral. Above a lift coefficient of 0.6 the nose-up floating angle is less with the tab deflected -20° than for a deflection of -10° . Deflecting the tab 10° and 20° progressively decreased the nose-up floating angle of the elevator.

The curve of elevator stick force for trim against indicated airspeed at sea level (fig. 25) shows that the airplane is trimmed at approximately the same speed, 100 miles per hour, for either -10° or -20° tab settings. For these trim tab settings, however, the airplane is unstable inasmuch as pull forces are required at speeds above the trim speed and push forces below the trim speed.

Although the airplane can be trimmed for zero stick force, it will be unstable for this condition. Also, the stick-free longitudinal instability is decreased very little with the tab deflected. This tab is ineffective at large tab deflections.

Elevator effectiveness with modified elevon. - The variation of C_L , C_m , and C_{he} with δ_e obtained for tests with the elevon seal removed and with the slats removed are given in figure 26. These results show very little change in $dC_m/d\delta_e$ and $dC_{he}/d\delta_e$ resulting from the removal of the elevon seal. For this condition $dC_m/d\delta_e$ increased slightly from -0.0040 at a C_L of 0.1 to -0.0043 at a C_L of 0.92 and $dC_{he}/d\delta_e$ decreased from -0.0050 at a C_L of 0.1 to -0.0038 at a C_L of 0.85.

The effect of the seal on the elevon free-floating angles and stick forces are shown in figures 27 and 28. The sealed elevon floats about 3° more tail-heavy than when unsealed throughout the lift-coefficient range. Although the airplane is longitudinally unstable with the slats removed in either case, the sealed elevon increases this instability and changes the trim speed from about 210 to 100 miles per hour.

Aerodynamic forces and moments were also measured for tests with the original elevon beveled and unsealed and with the large-span slats installed. The test results are given in figure 29. Figure 30 shows the detail of the bevel on the original internally balanced elevon. The elevon hinge moments for the new surface were computed for the increased dimensions of chord and area. For this condition, $dC_m/d\delta_e$ increased slightly from -0.0042 at a C_L of 0.1 to -0.0046 at a C_L of 1.1 and $dC_{he}/d\delta_e$ increased from -0.0055 at a C_L of 0.1 to -0.0067 at a C_L of 1.05.

Inasmuch as the test with the beveled elevon was made with slats installed and elevon seal removed, it was necessary to assume that the effect of the seal with the large-span slats installed would be the same as that with the slats removed in order to estimate the effect of the bevel on the elevator floating angles. With this assumption in mind, it is seen in figure 31 that the bevel succeeded in making the elevator somewhat more tail-heavy. The comparison of stick forces for the original and beveled elevon in figure 32 shows approximately the same variation with speed.

Lateral Stability and Control

Aerodynamic characteristics in yaw. - The results of tests made with the airplane yawed 0° , 2.9° , 5.6° , 9.5° , 14.5° , and 18.6° are presented in figures 33 to 35. The data include the variations of C_l , C_n , C_y , and C_{ha} with total aileron deflection for four angles of attack at each angle of yaw. The variations of C_l , C_n , and C_y with ψ , which were obtained by cross-plotting the original data at zero aileron deflection, are shown in figure 36.

As shown by the low value of $dC_l/d\psi$ at an angle of attack of 3.3° , the airplane will have practically no effective dihedral in the low angle-of-attack range. It is important to note that $dC_l/d\psi$ increases rapidly with increasing lift coefficient. At an angle of attack of 16.9° , for example, $dC_l/d\psi$ is approximately 0.0016, which corresponds to an effective dihedral angle of about 8° . This large increase in effective dihedral with lift coefficient is attributed to the large angle of sweepback of the wing.

The airplane will have almost no weathercock stability at low angles of attack as shown by the small value of $dC_n/d\psi$ (-0.0002) at an angle of attack of 3.3° . As was the case for the dihedral effect, the weathercock stability increases rapidly with increases in lift coefficient. At an angle of attack of 16.9° , $dC_n/d\psi$ is approximately -0.0010 per degree.

The variation of lateral-force coefficient with ψ is also very small at low angles of attack. The value of $dC_y/d\psi$ shows a stable variation for angles of attack below the stall up to a yaw angle of 15° where the values of $dC_y/d\psi$ begin to reverse sign with further increases of ψ . At the stall, there is a reversal in the side force from positive to negative at $\psi = 7^\circ$.

The variation of lift coefficient and pitching-moment coefficient with angle of yaw is shown in figure 37 for four angles of attack. The changes in pitching-moment coefficient with angles of yaw are small and somewhat irregular. The decrease of lift coefficient with angle of yaw was small for the range of yaw angles tested.

Since an undesirable side-force reversal occurs at angles of yaw above 15° , fins were attached to the wing center section in an attempt to correct this condition. The variation of C_l , C_n , and C_y with C_L for the airplane with fins installed is shown in figure 38 for yaw angles of 5.6° and 18.6° . A summary of the test data, giving a comparison of the results for the airplane with and without fins attached, is shown in table I.

Relatively small changes in C_n and C_l were measured at the maximum angle of yaw for either fin arrangement although lower values of C_l were obtained with the full-chord fin than with either the half-chord fin or the basic wing. The unfavorable side-force variation at the higher yaw angles was eliminated by both types of fins. At an angle of attack of 16.9° the lateral-force coefficient for the fin-removed condition was increased from -0.0027 to 0.0330 with the half-chord fin and to 0.0380 with the full-chord fin arrangement.

The variation of C_m , C_D , and α with C_L for airplane with slats attached and controls neutral at $\psi = 14.5^\circ$ are shown in figure 39. The airplane lift, drag, and pitching-moment characteristics are similar with the airplane yawed 0° and 14.5° although for the latter condition there is some irregularity in the lift curve at higher angles of attack.

Aileron effectiveness and control. - The data necessary for the determination of lateral control (fig. 40) show the variation of C_l , C_n , and G_{ha} with total aileron deflection (tab neutral) for the airplane at zero yaw with and without slats attached. Computations have been made of the helix angle $pb/2V$ which represents the lateral displacement of the wing tip in a given forward travel of the airplane as a function of total aileron deflection. A requirement of satisfactory lateral control, as discussed in reference 5, is that the value of $pb/2V$ in flight should not be less than 0.07. The helix angles were computed by the relation

$$\frac{pb}{2V} = \frac{C_l}{C_{l_p}}$$

where C_l is the total rolling-moment coefficient due to deflection of both ailerons and C_{l_p} is the rate of

28

change of C_l with $pb/2V$ and is dependent only upon the geometric characteristics of the airplane. The variation of helix angle with total aileron deflection for the two airplane conditions is shown in figure 41. Extrapolation of these results shows that for the maximum aileron deflection of 24° the value of $pb/2V$ is about 0.055 at 248 miles per hour and 0.070 at 70 miles per hour, slats installed, and is approximately 0.065 at 229 miles per hour and 0.068 at 72 miles per hour, slats removed. These values have been calculated from wind-tunnel data, but it should be noted at this point that in flight the adverse yaw at low speeds and the effects of compressibility and wing twist at high speeds would probably lower these values by about 20 percent.

Aileron stick forces for the required $pb/2V$ have been computed for different aileron deflections and flight speeds, and the results are given in figure 42. The forces were obtained from the relation

$$F_a = \frac{qb_a \bar{c}_a^2}{57.3} \left[-\frac{d\delta_{au}}{dx} \left(C_{hau} + \frac{dC_{hau}}{da} \Delta a \right) - \frac{d\delta_{ad}}{dx} \left(C_{had} - \frac{dC_{had}}{da} \Delta a \right) \right]$$

where C_{hau} and C_{had} are the aileron hinge-moment coefficients for a given up and down aileron deflection, respectively, and $d\delta_{au}/dx$ and $d\delta_{ad}/dx$ are the variation of aileron deflection with stick travel obtained from figure 43. The value Δa is the change in effective angle of attack of the down-going wing.

The aileron-control-force variation with aileron deflection shows no reversal of forces and an increase in force with increased aileron deflection. The force for maximum aileron deflection is about 75 pounds at 248 miles per hour with slats installed and 90 pounds at 229 miles per hour, slats removed. Forces of this magnitude will be excessive for a wheel-type control operated from a prone position. At landing speed, the control force is of the order of 3 pounds for maximum aileron deflection.

Directional Control System Operation

During the preliminary investigation of the stalling characteristics of the airplane, indications of the inadequacy of the rudder-control duct system were noticeable. The tufts around the duct inlets were observed to be very unsteady as the angle of attack was increased and, above an angle of attack of about 14° , it was found that the air flow was directed out rather than into the inlet. Furthermore, before rudder effectiveness tests were made, a trial test was conducted to determine the operational effectiveness of the control valve and bellows. It was impossible to hold a given rudder deflection and, probably due to poor air flow through the duct system, the rudder would fluctuate with changes in angles of attack for a given setting of the control valve. External locks were therefore used for all rudder tests and, later, tests were made to determine bellows pressures, air-flow quantity, and effectiveness of the butterfly control valve.

The variations of C_n , C_l , and C_y with rudder deflection for a range of angles of attack are shown in figure 44. Similar measurements were made for combinations of right and left rudder deflections and the results are shown in figure 45. The rudder effectiveness $dC_n/d\delta_r$ measured at $C_n = 0$ was -0.00006 for most angles of attack. It is apparent from the results in figure 44 that the system proposed for trimming the airplane in yaw is inadequate; that is, the value of C_n developed by maximum rudder deflection will not be sufficient to trim out the adverse yaw due to maximum aileron deflection.

The results of tests made by fixing the butterfly-valve position and measuring the rudder deflection at various angles of attack are shown in figure 46. The findings of the tests with the original inlet substantiate the tuft observations because the rudder deflections began to decrease rapidly above an angle of attack of about 12° . These results also show the irregular control-surface fluctuations as the angle of attack is increased. Furthermore, there is a marked variation of the deflections of inboard and outboard sections for any given condition. It was realized that for adequate control, especially at high angles of attack, the air flow at the inlet should be improved. The original inlet was modified

by (1) reducing the sweepback of the leading-edge inlet to zero degrees and by (2) providing an initial negative angle of attack of about 14° at the face of the inlet (fig. 7).

Results similar to that obtained for the original inlet were obtained for the modified inlet except that greater rudder deflections were obtained and the tendency to stall at the inlet was delayed several degrees (fig. 46). The measurements made to estimate the quantity of air flow through the duct system (fig. 47) show similar characteristics of the effectiveness of the two inlets. Air flowed out of the system at an angle of attack of 15° for the original inlet and at 24° for the modified inlet. In both cases the available quantity decreased rapidly with change in angle of attack from the high-speed attitude.

The variation of deflection of the inboard and outboard sections of the rudder is caused by an uneven distribution of pressure in the two sections of the rudder as shown by the variations of the pressure differential across the bellows with angle of attack in figure 48. The effectiveness of the butterfly valve is shown in figure 49 for each inlet type. It is important to note that the rate of change of valve position with rudder deflection varies considerably and that the valve is most sensitive when about one-half closed. Paralleling the results in the previous figures, it is shown that, when the inlet is stalled, the full range of valve setting will not change the rudder deflection.

The over-all efficiency of the bellows and duct system was determined by measuring the time lag for maximum surface deflection with instantaneous full-rudder control. The minimum time interval for the best condition was about 4 seconds. Since the inlet and duct system do not provide adequate quantity of air flow through the ducts and pressure within the bellows and since the control-valve operation was not effective, the directional control system such as tested in this model is very unsatisfactory.

SUMMARY OF RESULTS

1. At the design center-of-gravity location of 27.5 percent mean aerodynamic chord, the airplane with

slats removed will have an unstable stick force and elevator-trim-angle variation with speed; the instability is very pronounced near the stall.

2. Installation of large-span slats to the leading edge of the wing provided static longitudinal stability at lift coefficients greater than 0.6. The variation of stick force with speed, however, is unstable with the airplane trimmed for zero stick force at 100 miles per hour.

3. The airplane, with slats installed, will be longitudinally stable at all lift coefficients for a center-of-gravity position of 26 percent mean aerodynamic chord. With the slats removed, the airplane will be stable up to a lift coefficient of 1.0 for a center-of-gravity location of 25 percent mean aerodynamic chord. At higher lift coefficients the neutral point moves forward rapidly.

4. The large-span slats not only improved the static longitudinal stability of the airplane at high lift coefficients but also increased the maximum lift coefficient from 1.15 to 1.26.

5. The value of the minimum drag coefficient for the basic wing is 0.0100; the addition of the large-span slats increased this value to 0.0146.

6. The effective dihedral $dC_l/d\psi$ and the weather-cock stability $dC_n/d\psi$ are practically zero at low angles of attack. The value of $dC_l/d\psi$ and $dC_n/d\psi$ increase rapidly with angle of attack such that at an angle of attack of 16.9° $dC_l/d\psi$ is approximately 0.0016 and $dC_n/d\psi$, -0.0010.

7. The lateral force developed in yaw is small and at angles of yaw above 15° the slope of the curve of lateral-force coefficient against angle of yaw changes from positive to negative.

8. The installation of vertical fins at the wing center section resulted in a large improvement in the lateral-force characteristics at high angles of yaw.

9. The stick forces for maximum aileron deflection in flight at low lift coefficients may be excessive for control operation from a prone position.

10. The method for obtaining directional control is entirely inadequate. The yawing moment developed by maximum rudder deflection will not be sufficient to trim out the total adverse yaw resulting from maximum aileron deflection.

11. If the present directional control system is to be used, the design of the duct system must be revised to obtain satisfactory performance. Modifications to the inlets, the ducting, and the butterfly control valve are required, and, if possible, the control surfaces should not be sectioned.

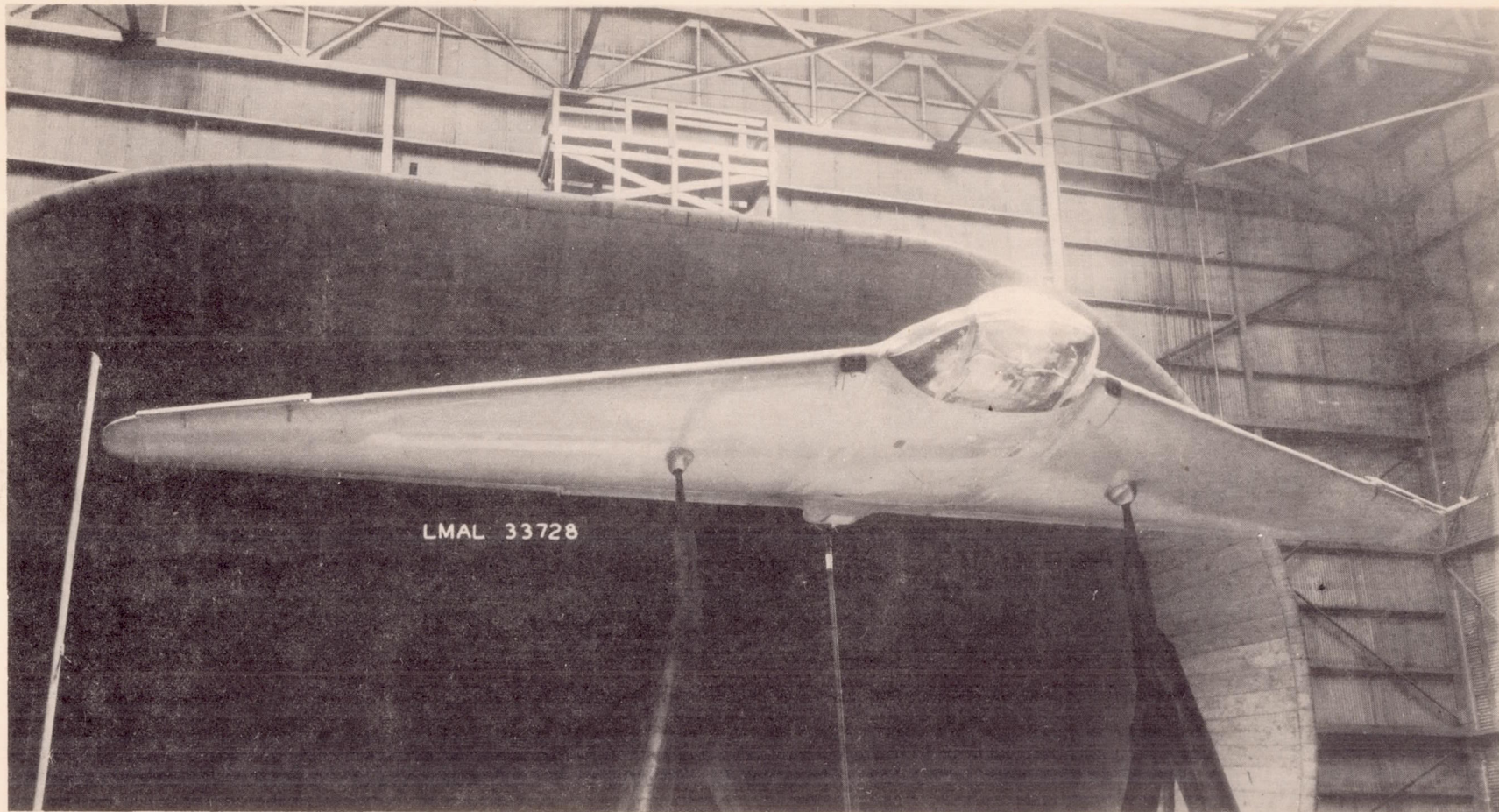
Langley Memorial Aeronautical Laboratory,
National Advisory Committee for Aeronautics,
Langley Field, Va., January 13, 1944.

REFERENCES

1. Silverstein, Abe, and Katzoff, S.: Experimental Investigation of Wind-Tunnel Interference on the Downwash behind an Airfoil. Rep. No. 609, NACA, 1937.
2. Theodorsen, Theodore, and Silverstein, Abe: Experimental Verification of the Theory of Wind-Tunnel Boundary Interference. Rep. No. 478, NACA, 1934.
3. Silverstein, A., and Katzoff, S.: A Simplified Method for Determining Wing Profile Drag in Flight. Jour. Aero. Sci., vol. 7, no. 7, May 1940, pp. 295-301.
4. Goett, Harry J., and Bullivant, W. Kenneth: Tests of N.A.C.A. 0009, 0012, and 0018 Airfoils in the Full-Scale Tunnel. Rep. No. 647, NACA, 1938.
5. Gilruth, R. R., and Turner, W. N.: Lateral Control Required for Satisfactory Flying Qualities Based on Flight Test of Numerous Airplanes. Rep. No. 715, NACA, 1941.

TABLE I
EFFECT OF SLATS AND FINS ON THE AERODYNAMIC CHARACTERISTICS OF
THE MX-334 AIRPLANE YAWED AT 5.6° AND 18.6°

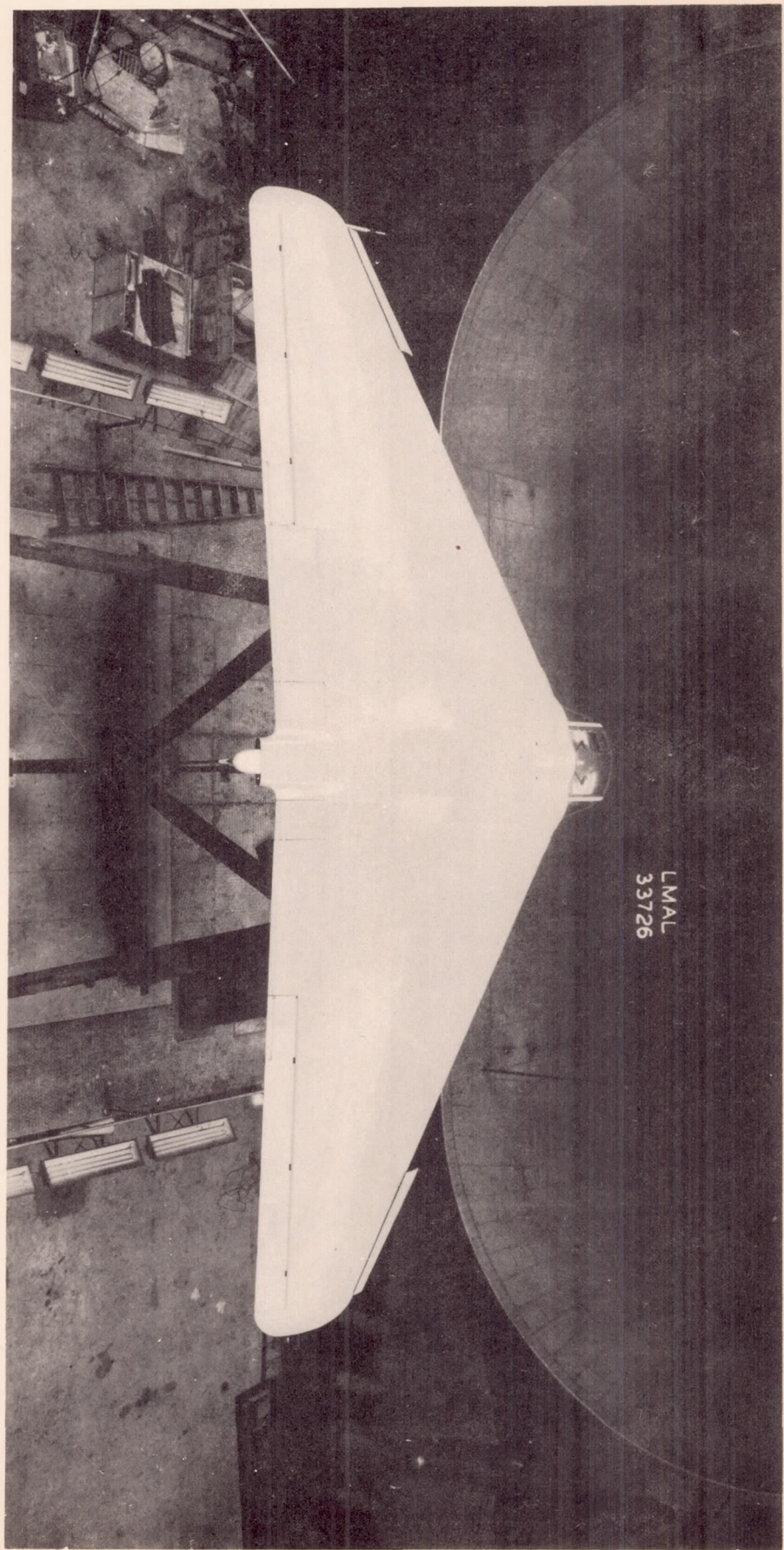
ψ , deg	5.6°				18.6°				Slats	Fins
α , deg	3.3	10.6	16.9	21.6	3.3	10.6	16.9	21.6		
c_l	-----	-----	-----	-----	0.0080	0.0200	0.0340	1.0700	off	Off
	0.0008	0.0002	0.0010	0.0010	.0078	.0180	.0350	.0520	on	Off
	.0015	.0035	.0050	.0065	.0065	.0173	.0258	.0360	on	Full chord
	-----	-----	-----	-----	.0075	.0280	.0450	.0560	on	Half chord
c_n	-----	-----	-----	-----	-0.0023	-0.0068	-0.0146	-0.0075	off	Off
	-0.0003	-0.0010	-0.0050	-0.0075	-.0027	-.0068	-.0160	-.0230	on	Off
	-.0005	-.0018	-.0035	-.0063	-.0002	-.0050	-.0130	-.0200	on	Full chord
	-----	-----	-----	-----	-.0040	-.0080	-.0160	-.0235	on	Half chord
c_Y	-----	-----	-----	-----	0.0038	-0.0010	-0.0060	-0.0450	off	Off
	0.0005	0.0015	0.0005	0.0062	.0052	.0027	-.0027	-.0173	on	Off
	.0095	.0095	.0095	.0045	.0460	.0415	.0380	.0360	on	Full chord
	-----	-----	-----	-----	.0500	.0430	.0330	.0220	on	Half chord



(a) Three-quarter front view.

Figure 1.- The MX-334 airplane mounted for tests in the NACA full-scale tunnel.
Original slats installed.

L MAL
33726

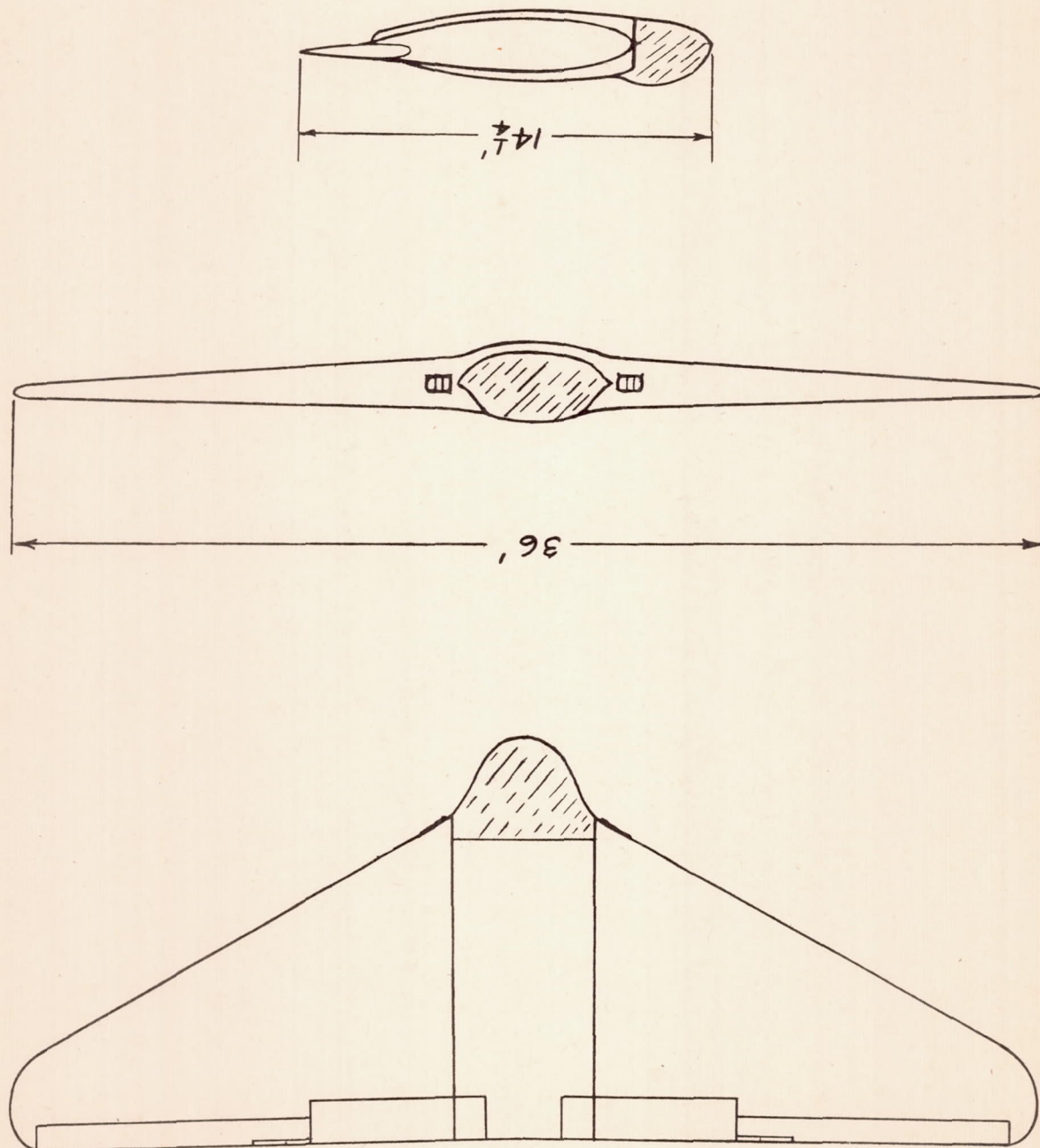


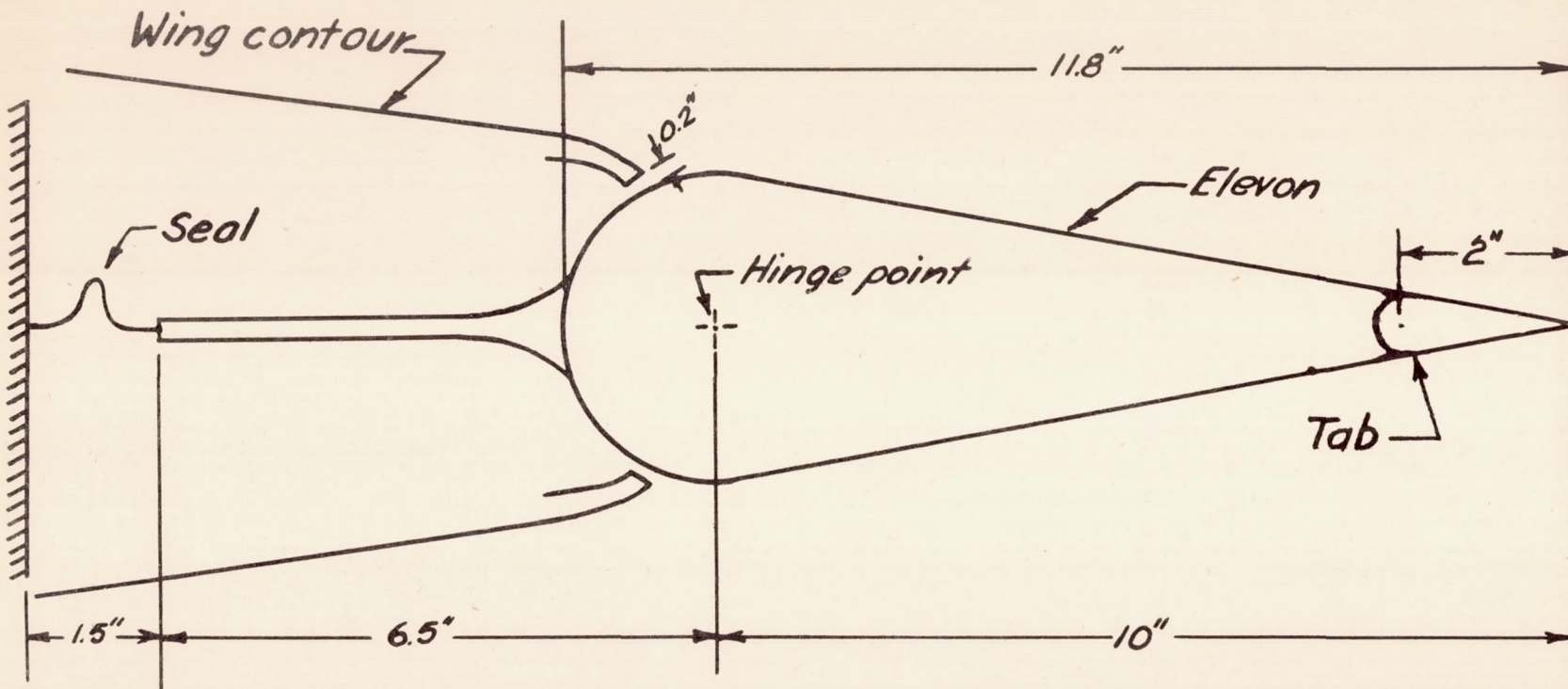
(b) Rear View.

Figure 1.- Concluded.

Figure 2.-Three-view drawing of the MX-334 airplane.

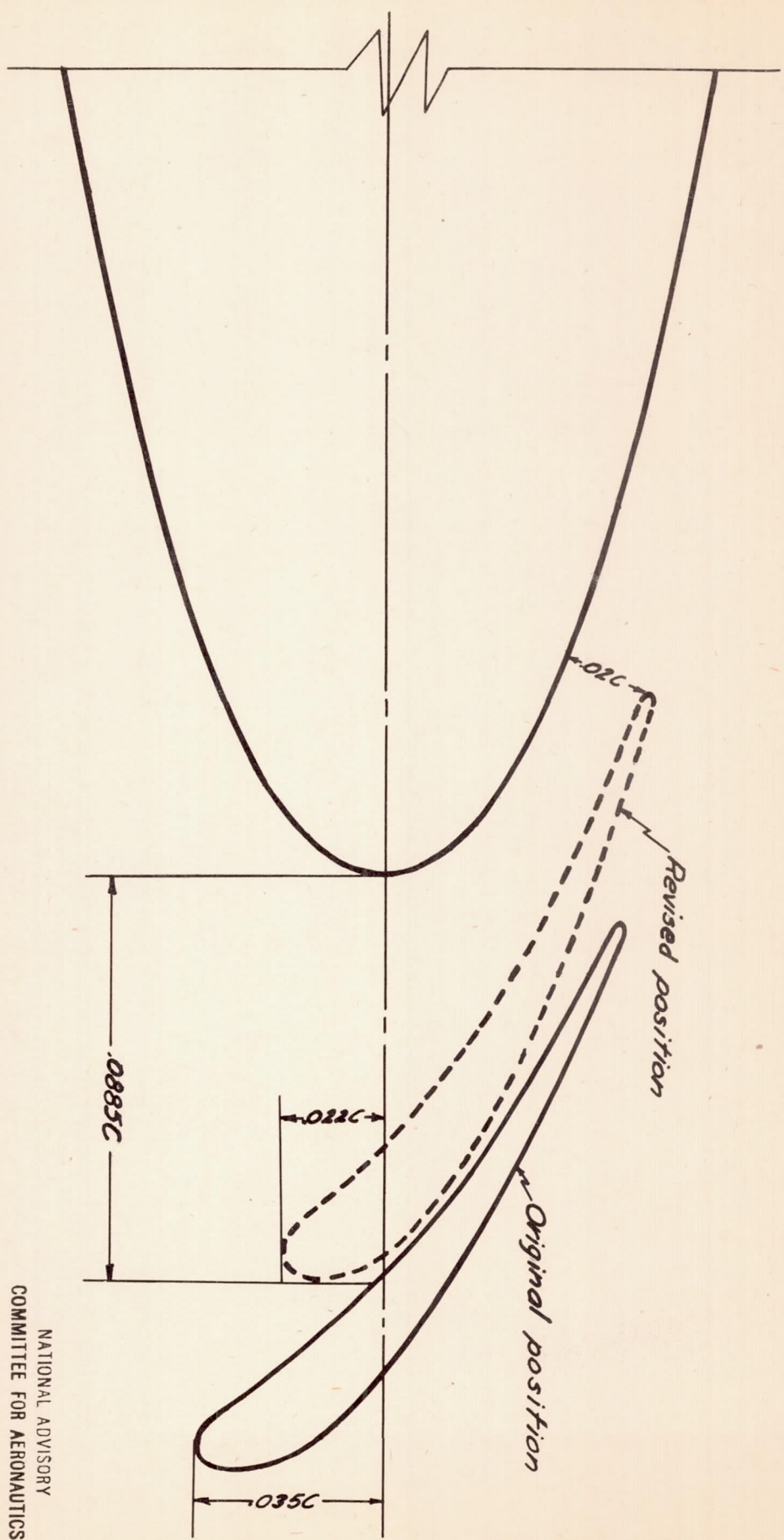
NATIONAL ADVISORY
COMMITTEE FOR AERONAUTICS





NATIONAL ADVISORY
COMMITTEE FOR AERONAUTICS

Figure 3:- Diagram of internal balance for the elevon of the MX-334 airplane.

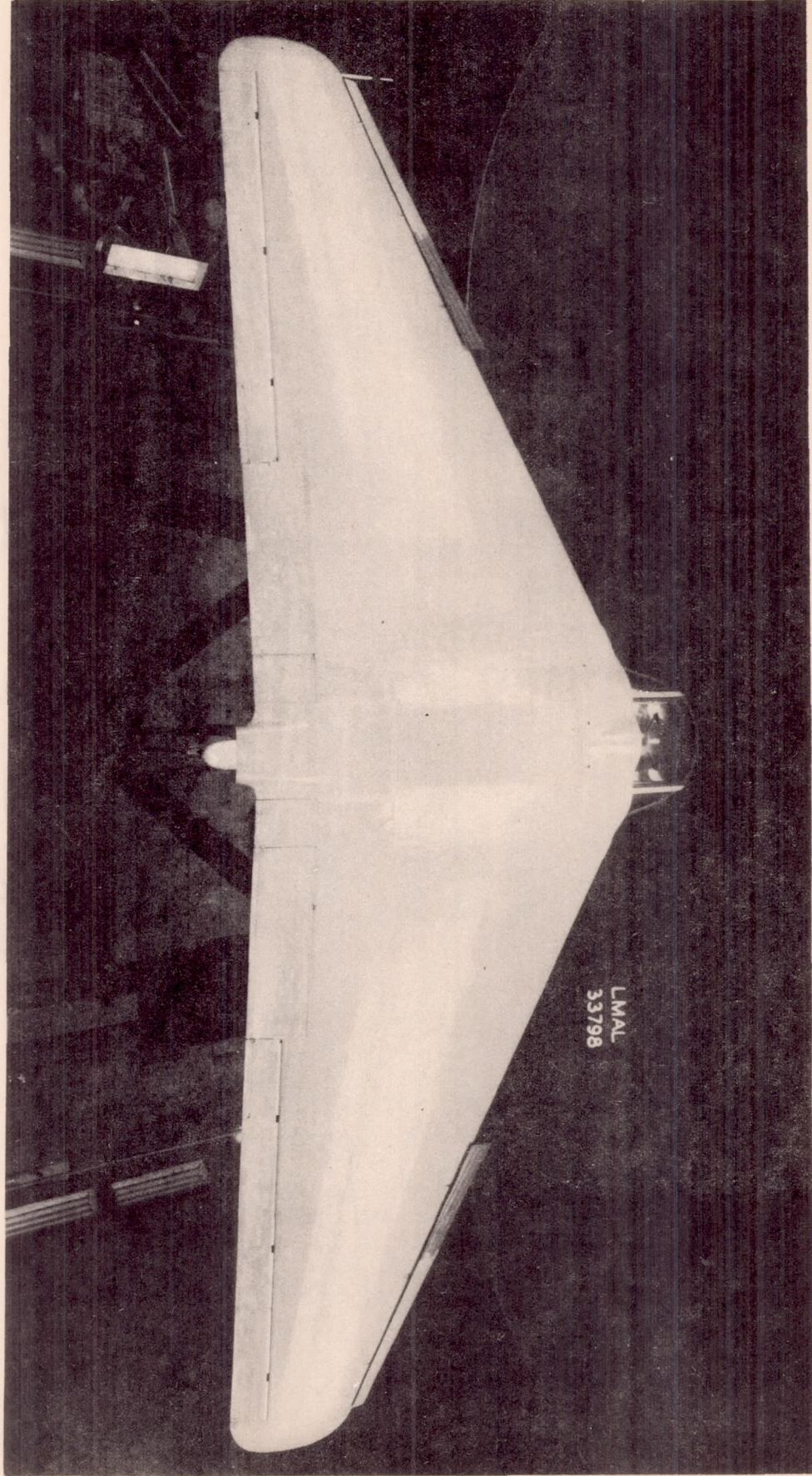


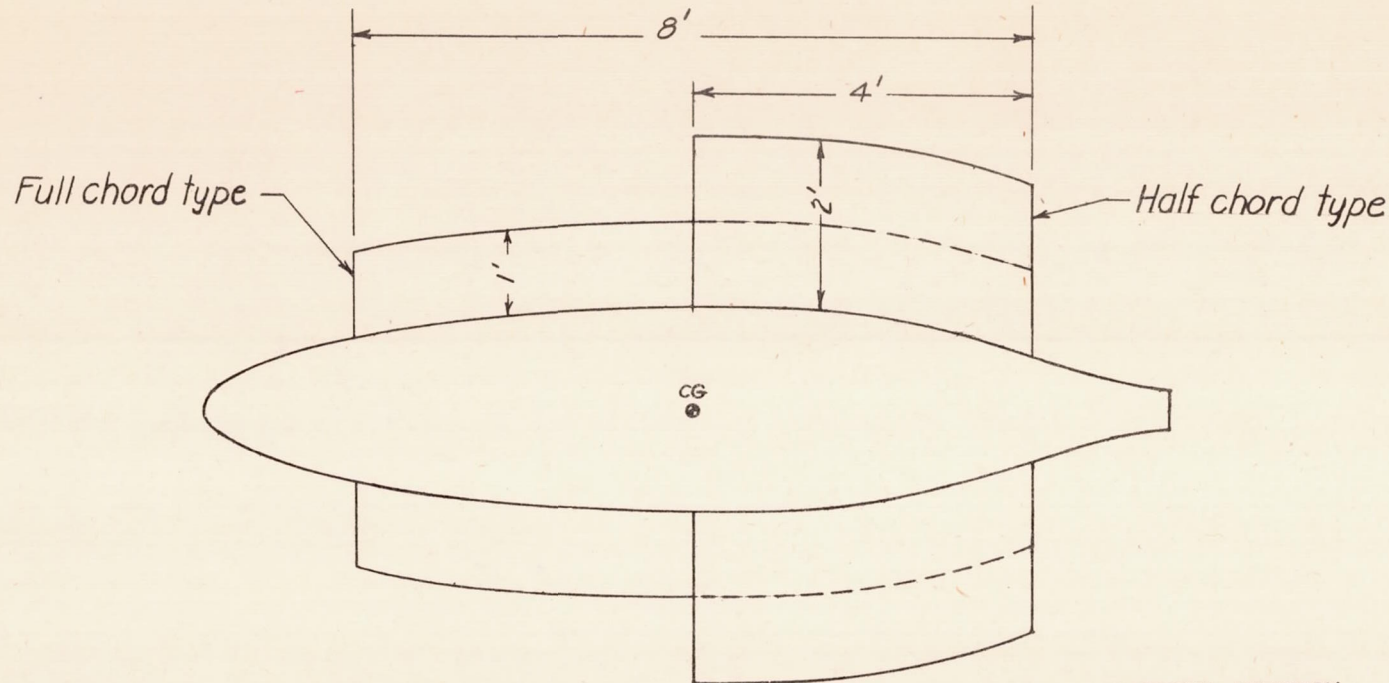
$\frac{1}{4}$
 $\frac{1}{2}$
 $\frac{3}{4}$
one inch

Figure 4.-Final slot configuration for MX-334 glider

section at the outboard support station.

Figure 5.- The MX-334 airplane with large-span slats installed.

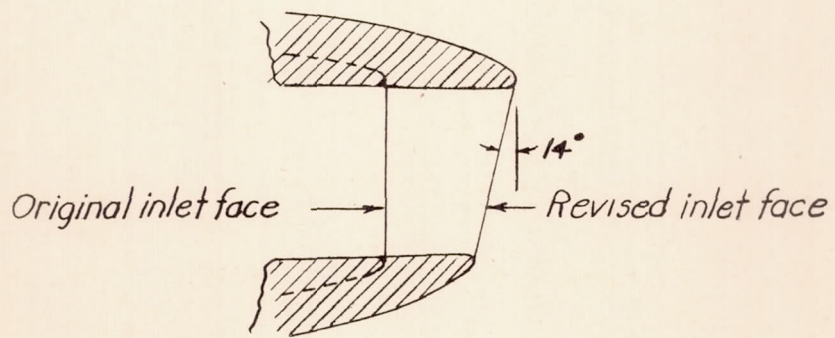
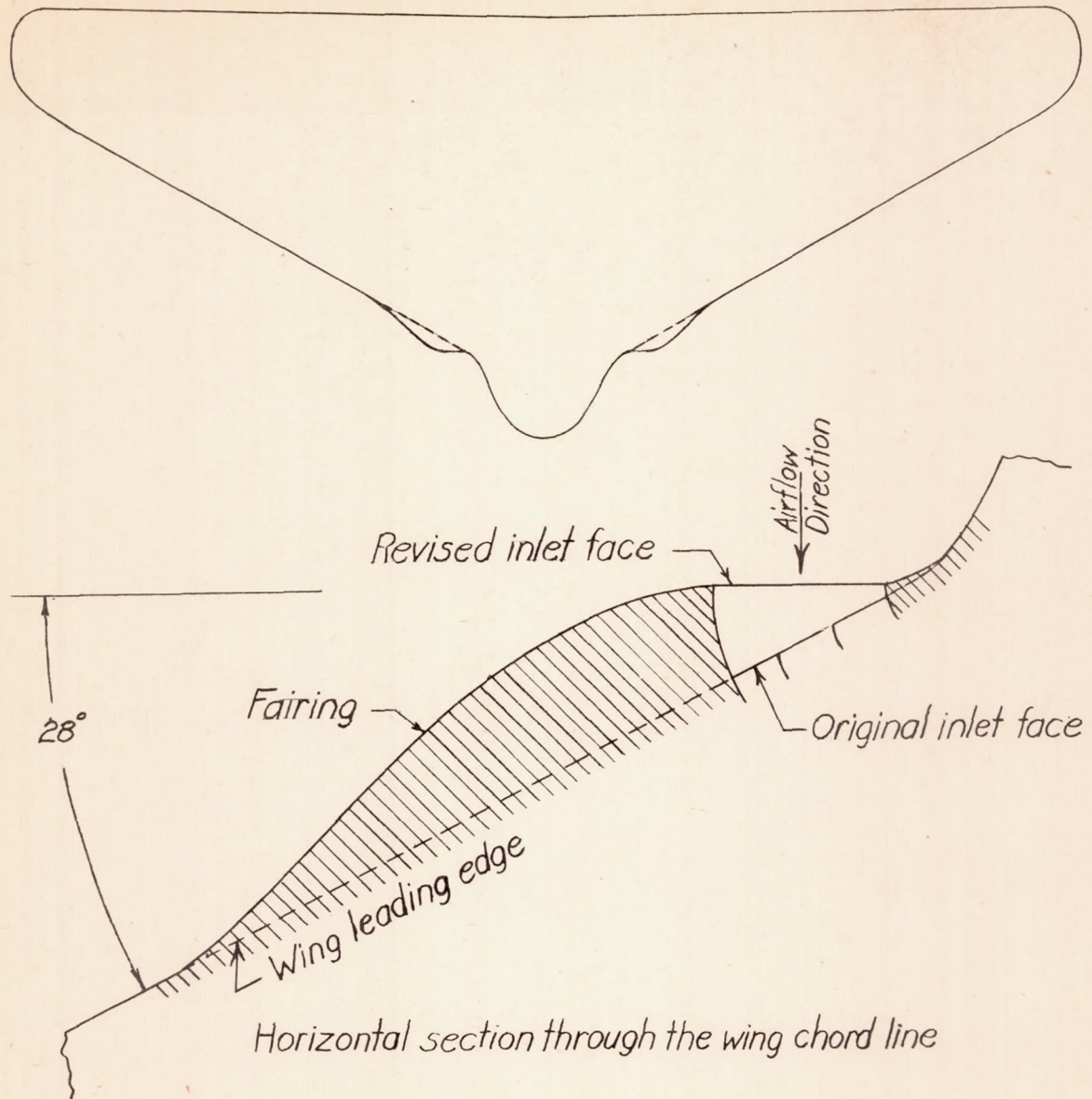




NATIONAL ADVISORY
COMMITTEE FOR AERONAUTICS

Section at centerline of the airplane

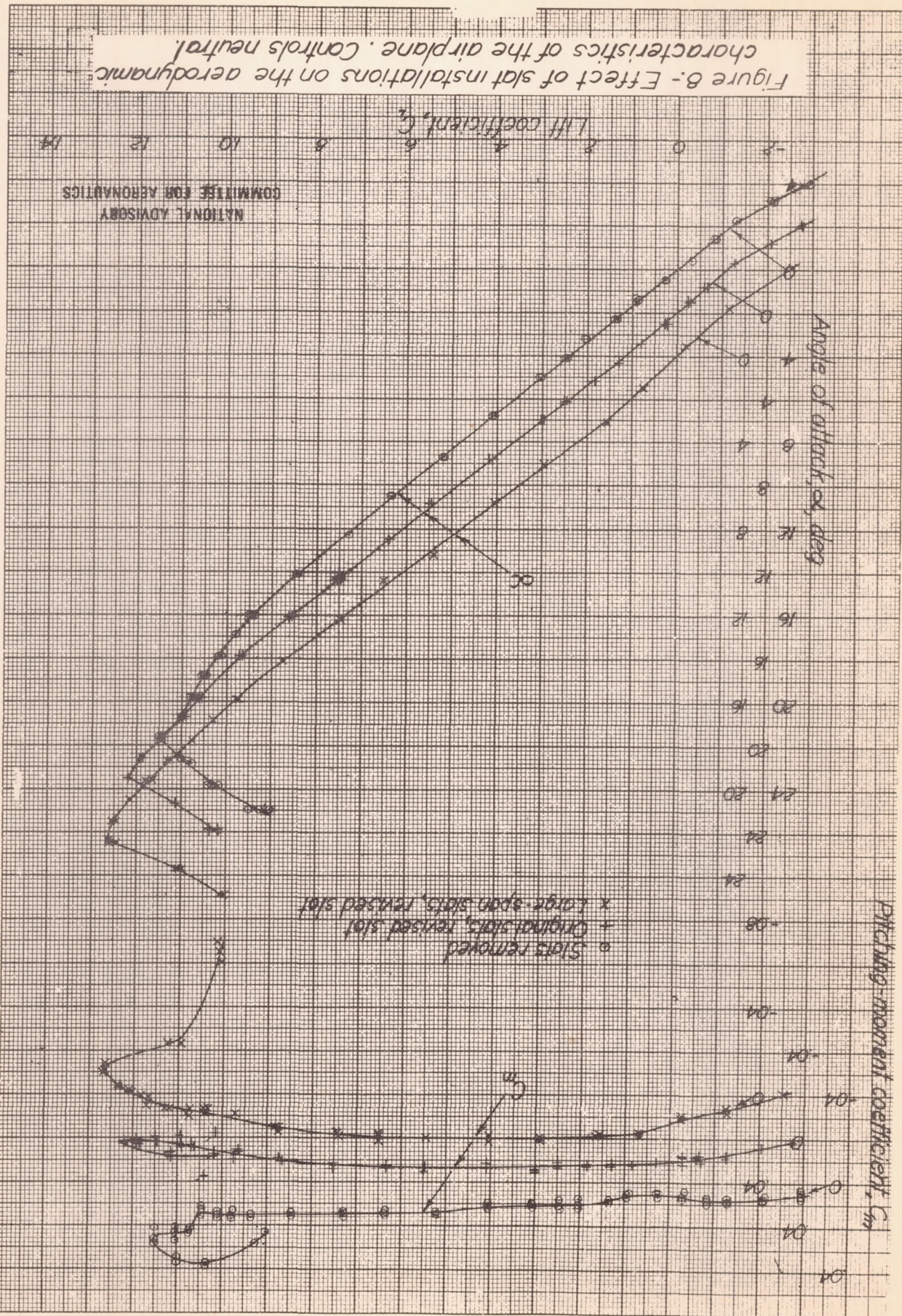
Figure 6.- Arrangement of fins on the MX-334 airplane.



Vertical section of the duct inlet

NATIONAL ADVISORY
COMMITTEE FOR AERONAUTICS

Figure 7.-Inlet modification for the MX-334 airplane.

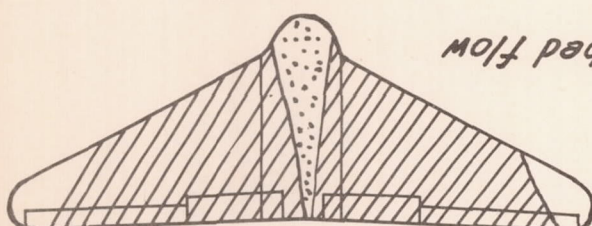


Glider airframe: L, approximately 63 m.s.h.
 Figure 9 - Flow characteristics over the MX-334

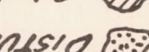
(a) Original slots

(b) Slots removed

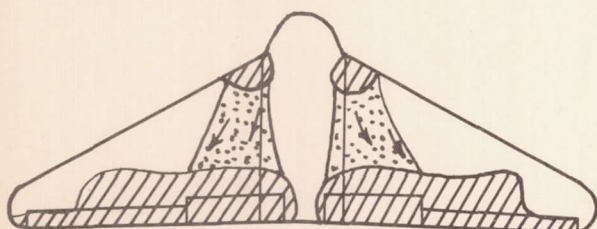
$\alpha, 23.8^\circ$



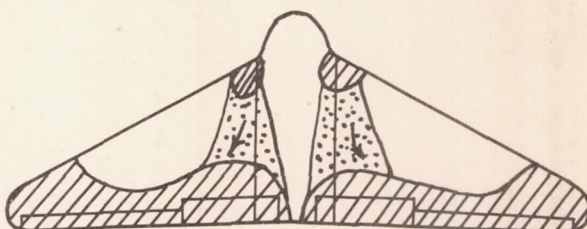
$\alpha, 23.8^\circ$ STALL



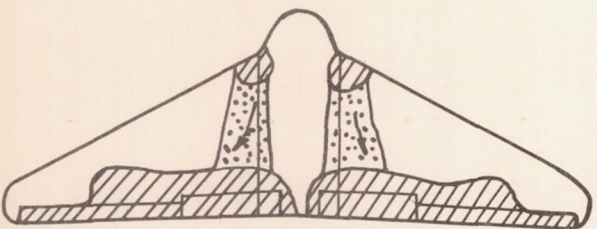
$\alpha, 21.6^\circ$



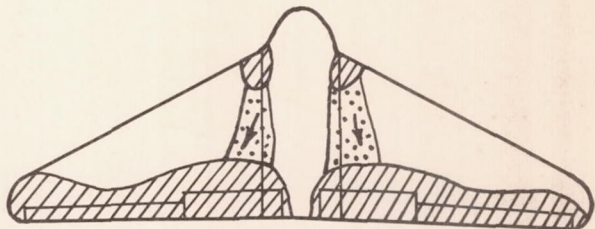
$\alpha, 21.6^\circ$



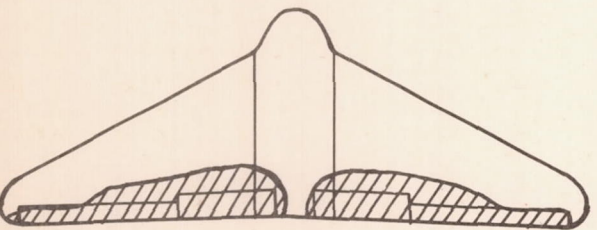
$\alpha, 20.5^\circ$



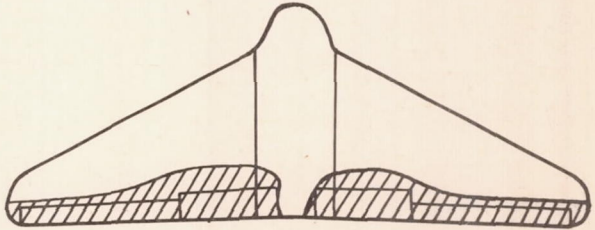
$\alpha, 19.8^\circ$



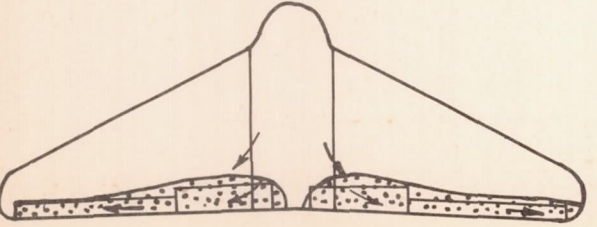
$\alpha, 18.7^\circ$



$\alpha, 17.9^\circ$



$\alpha, 10.5^\circ$



$\alpha, 10.5^\circ$

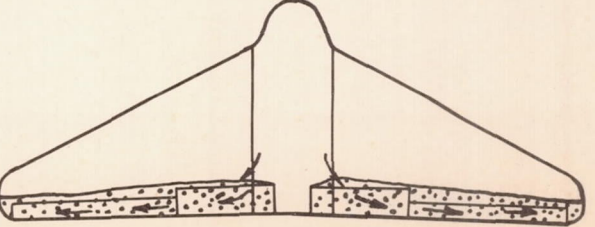
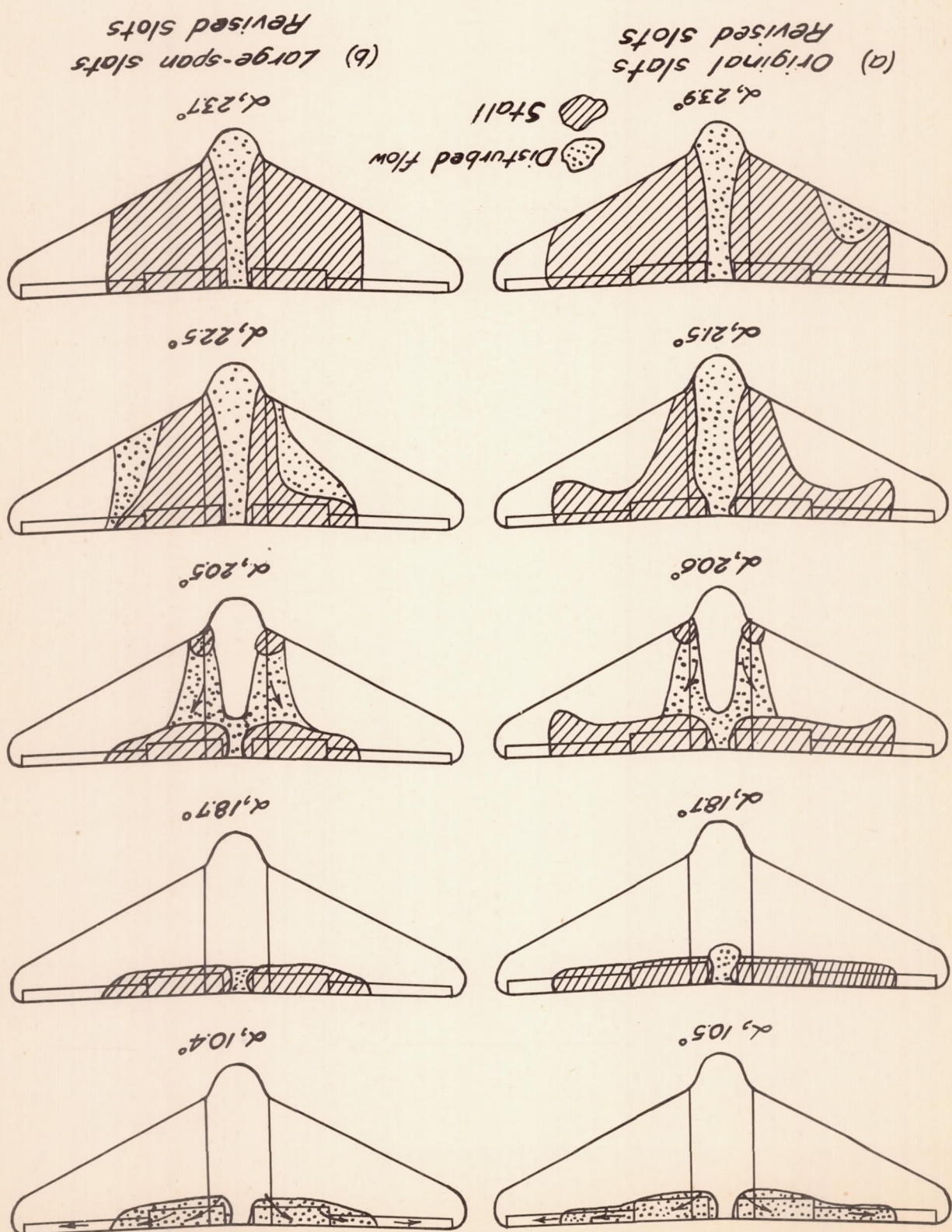


FIGURE 10 - FLOW CHARACTERISTICS OVER THE MX-334 GLIDER
airplane, at approximately 63 mph.



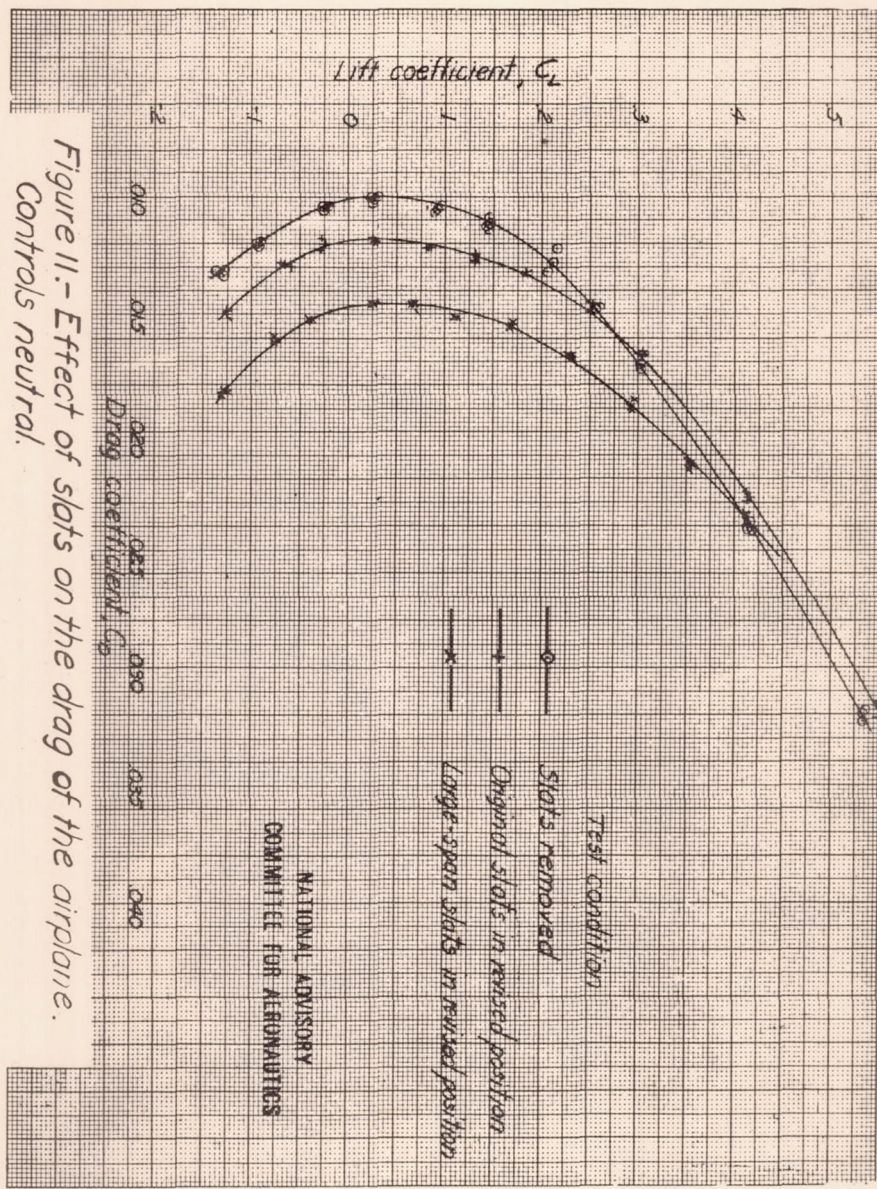


Figure 11.—Effect of slots on the drag of the airplane.
Controls neutral.

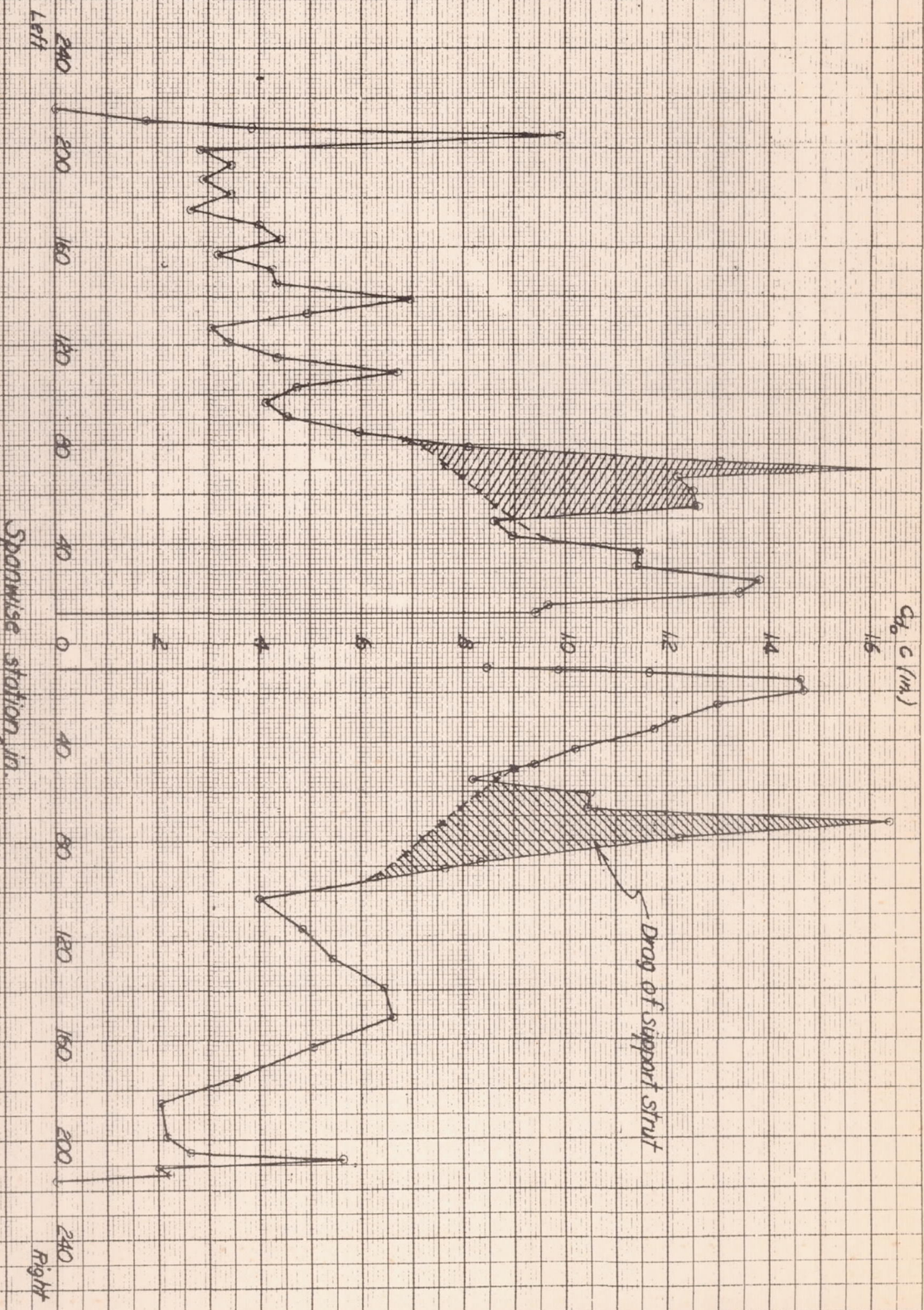
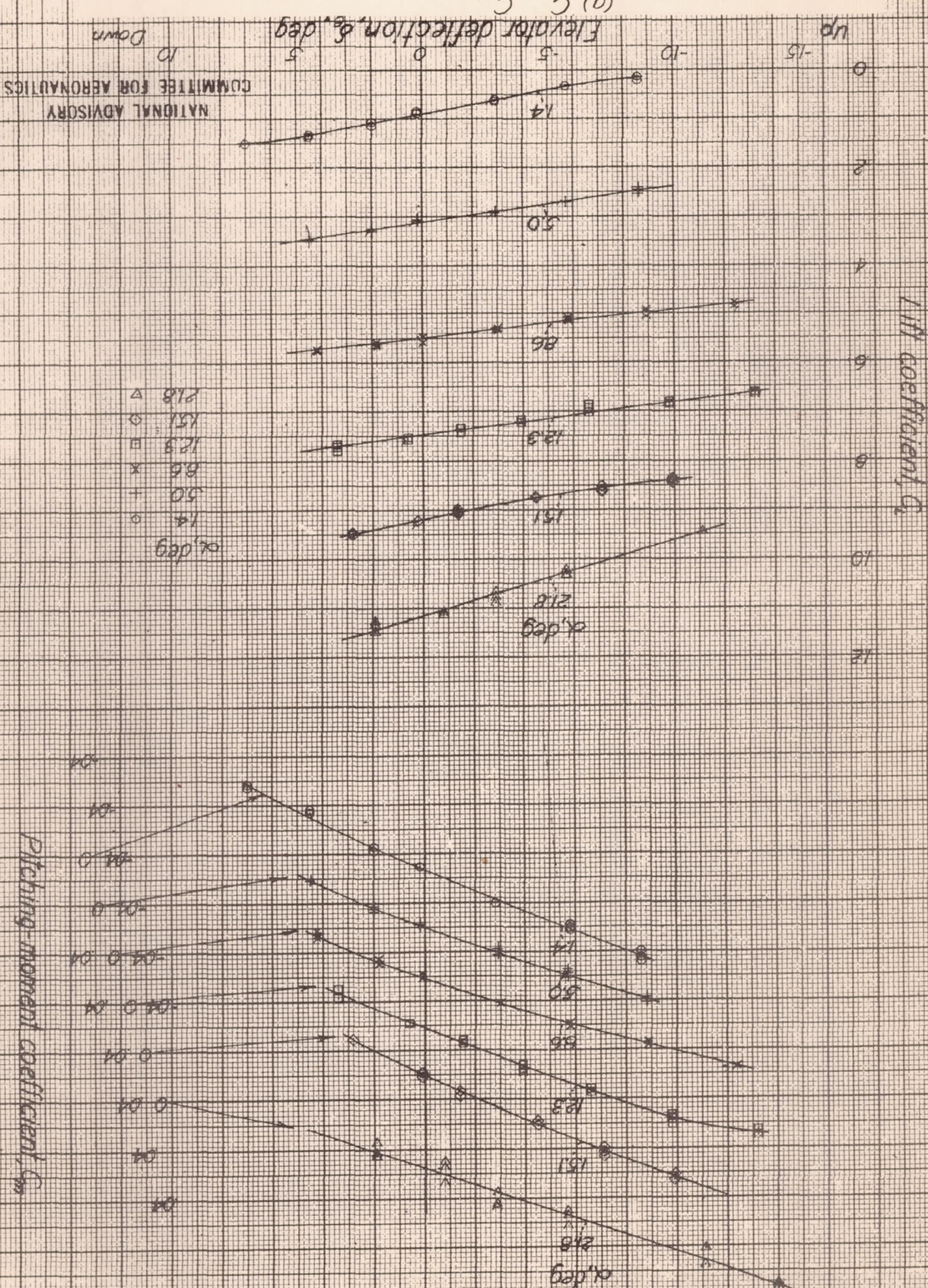


Figure 12.—Variation of C_d/c with spanwise station. C_d/c , V approximately 22 mph.

NATIONAL ADVISORY
COMMITTEE FOR AERONAUTICS

Figure 13.- Effect of elevator deflection on the aero-dynamic characteristics of the airfoil. Slats removed; elevon sealed; tab neutral.



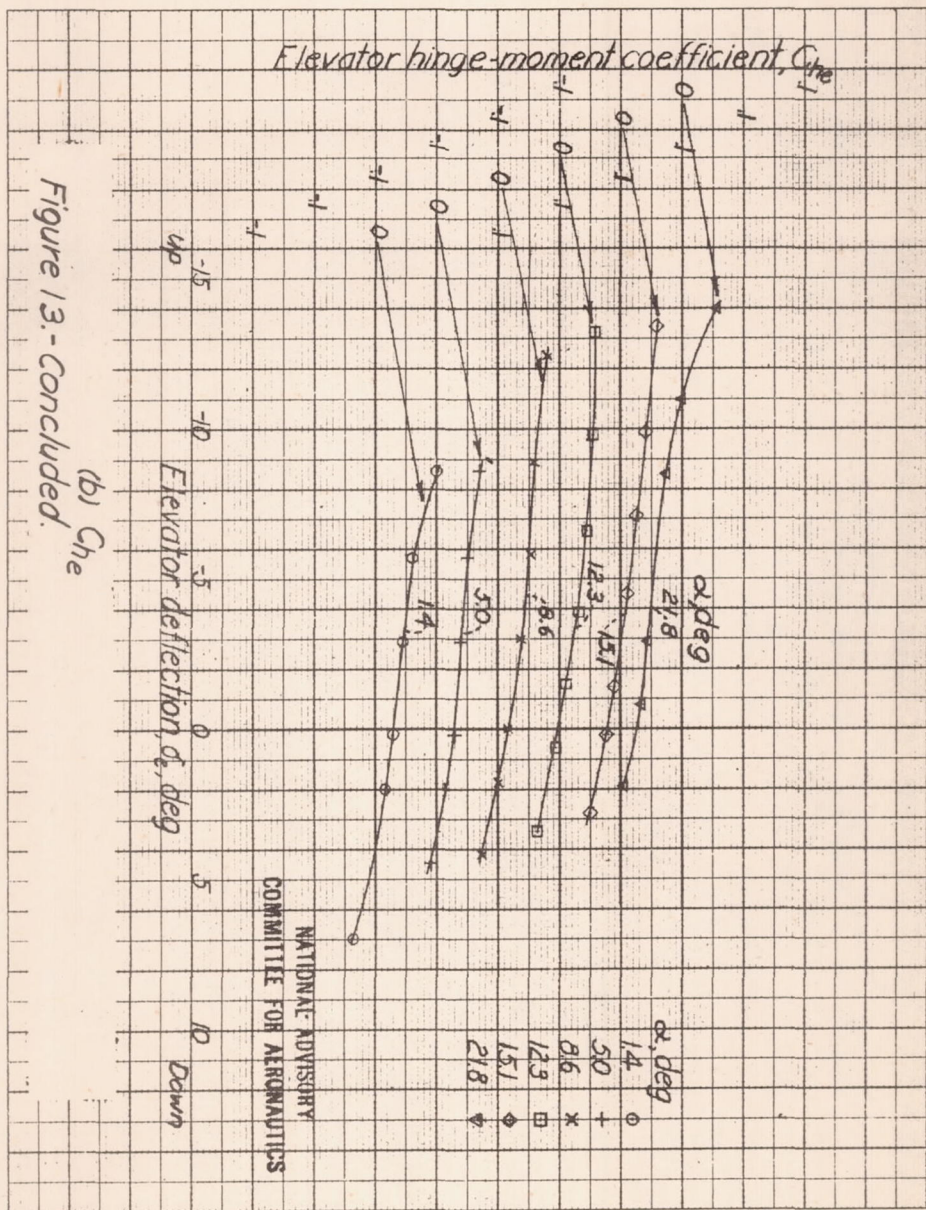
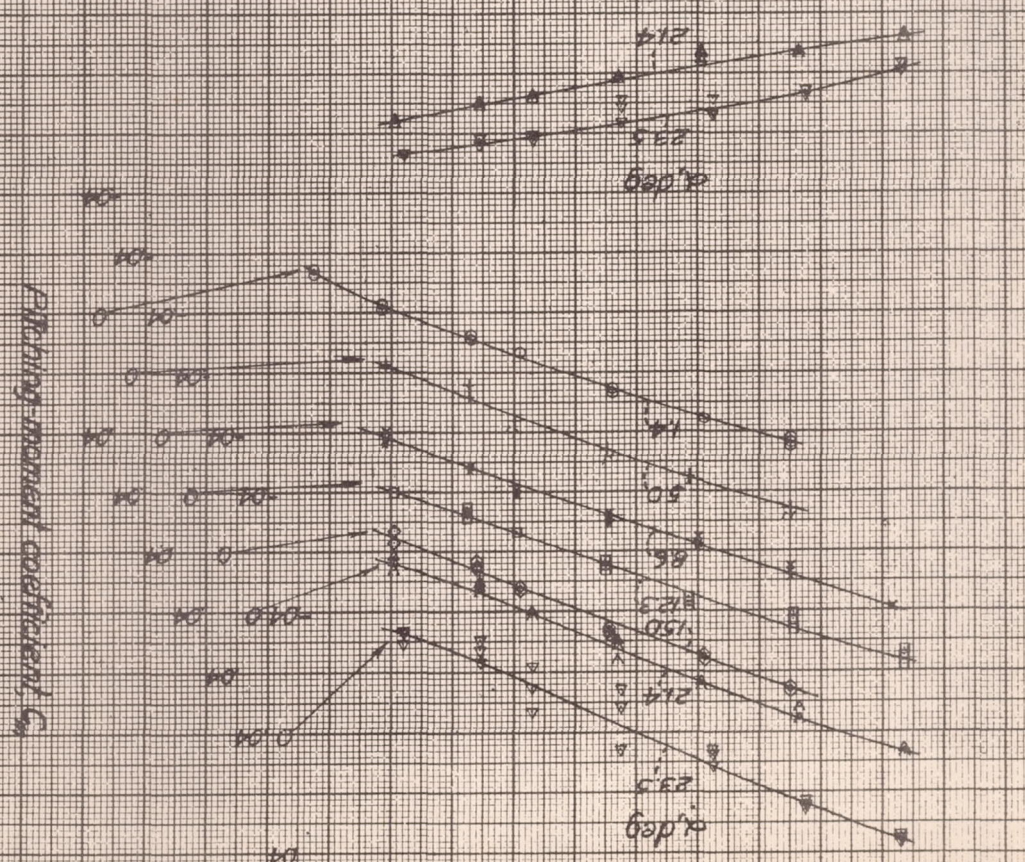
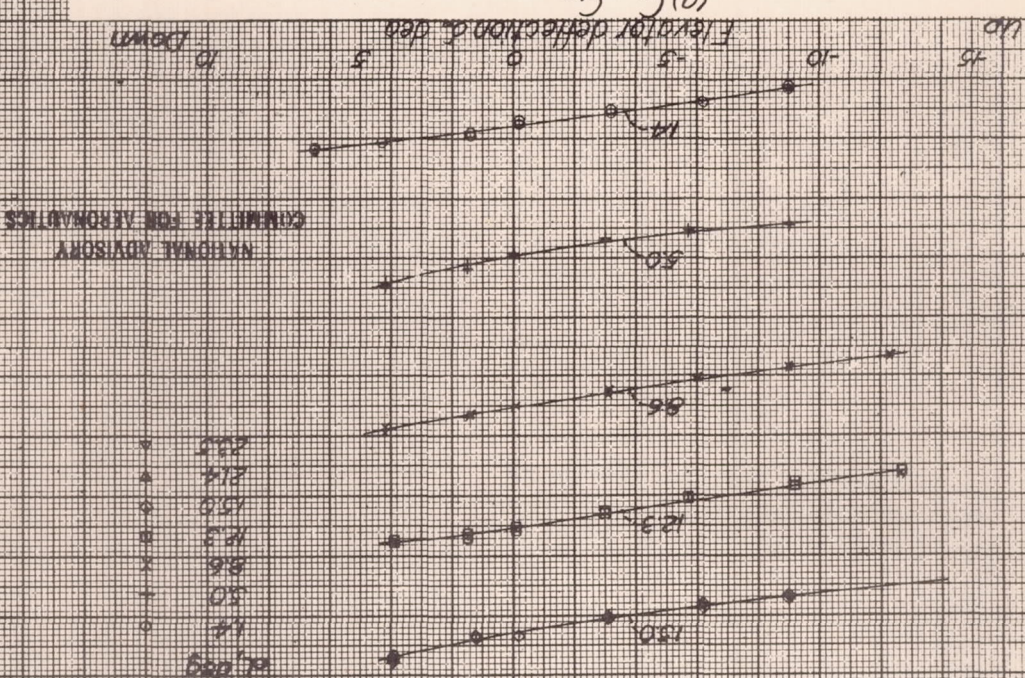


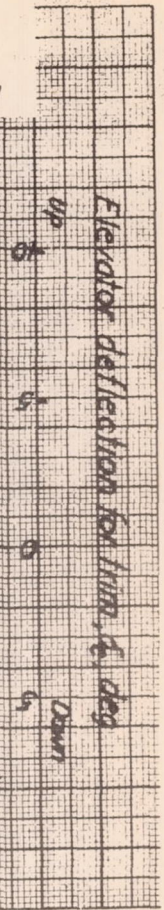
Figure 13.- Concluded.
(b) C_{he}

Figure 14.—Effect of elevator deflection on the aerodynamic characteristics of the airplane. Large-span slots installed; elevon sealed; tail neutral.



Pitching moment coefficient, C_m

Elevator deflection for trim, δ_e , deg



27.5 percent MAC

angle with lift coefficient. Tab neutral; center of gravity at
figure 15.-Effect of slats on the variation of elevator trim

lift coefficient C_L

COMMITTEE FOR AERONAUTICS
NATIONAL ADVISORY

Elevator hinge moment coefficient, C_m

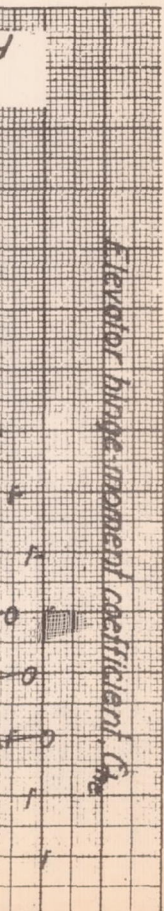
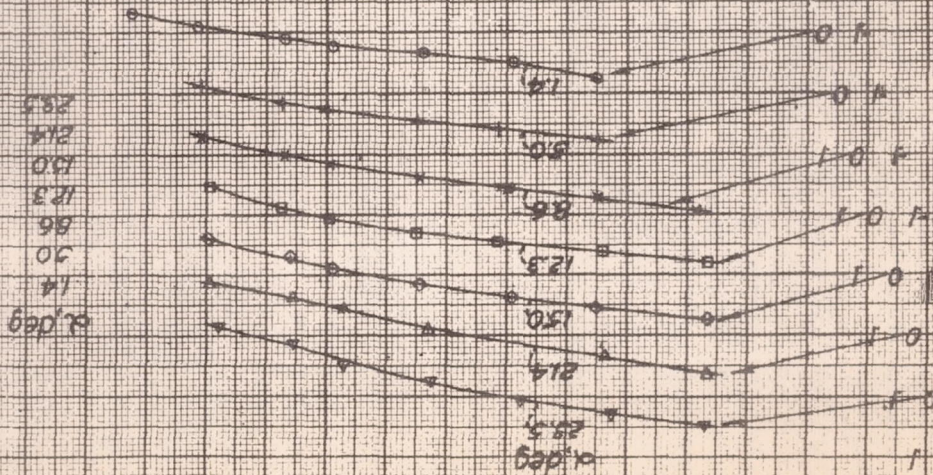


Figure 14.-Concluded.
(b) C_m

Elevator deflection for trim

Down 0 2 4 6 8 10 12 14

COMMITTEE FOR AERONAUTICS
NATIONAL ADVISORY



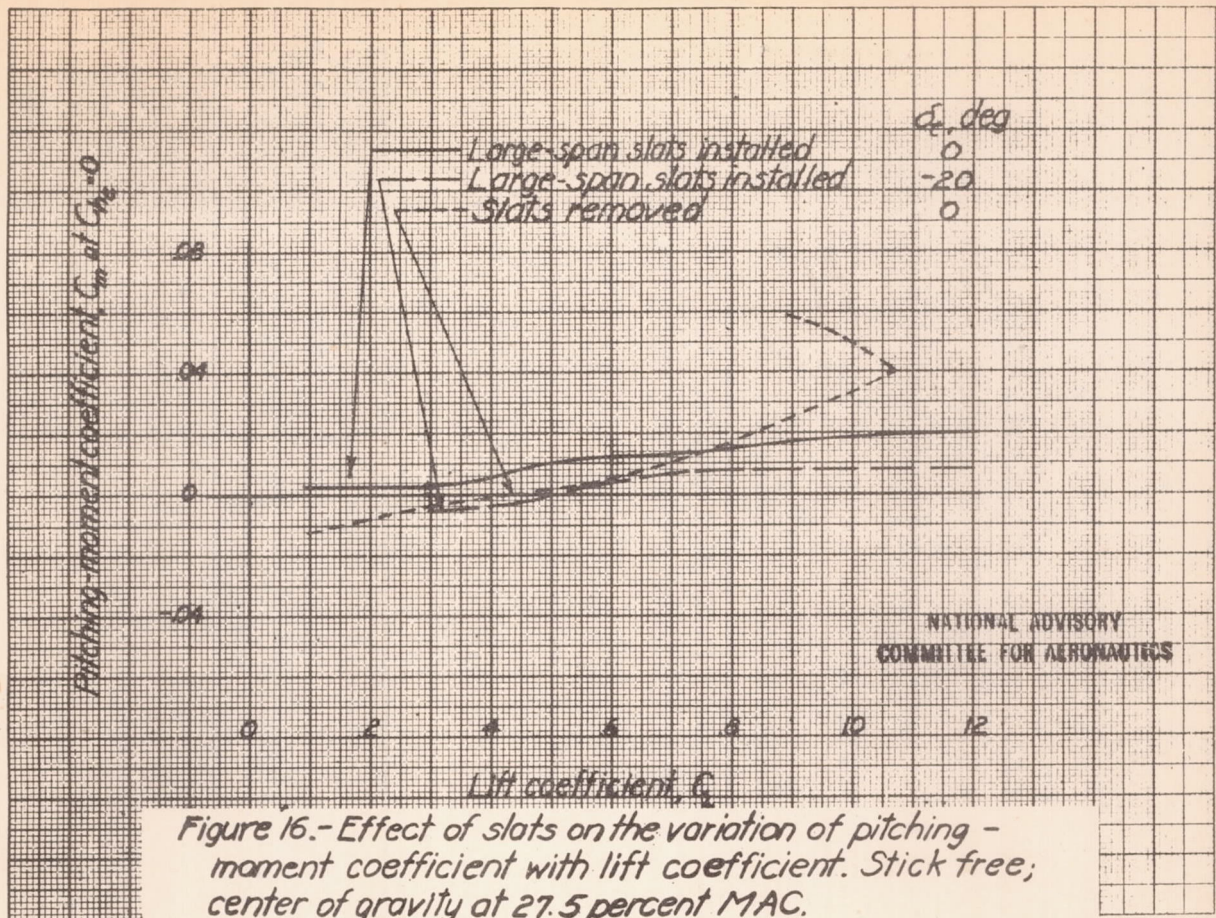


Figure 16.-Effect of slats on the variation of pitching-moment coefficient with lift coefficient. Stick free; center of gravity at 27.5 percent MAC.

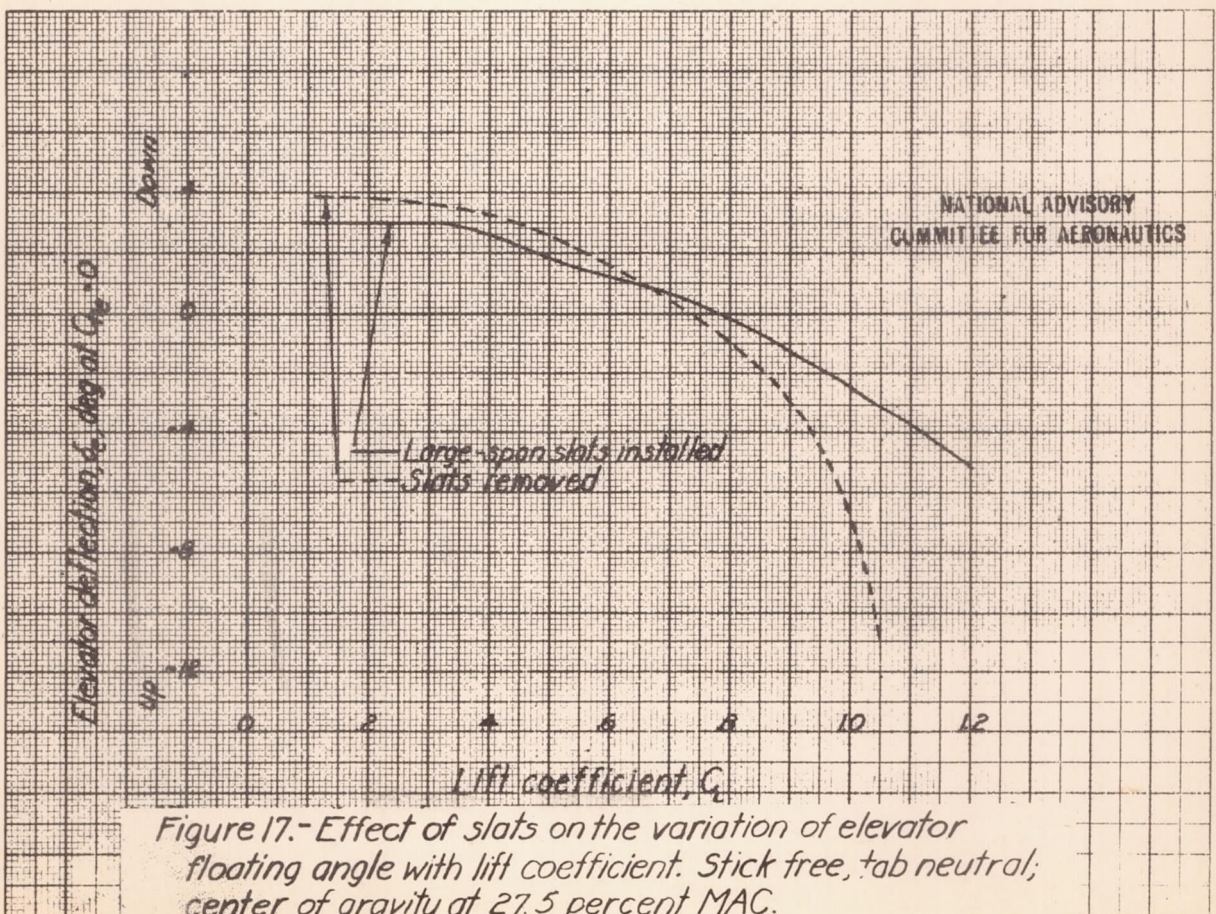
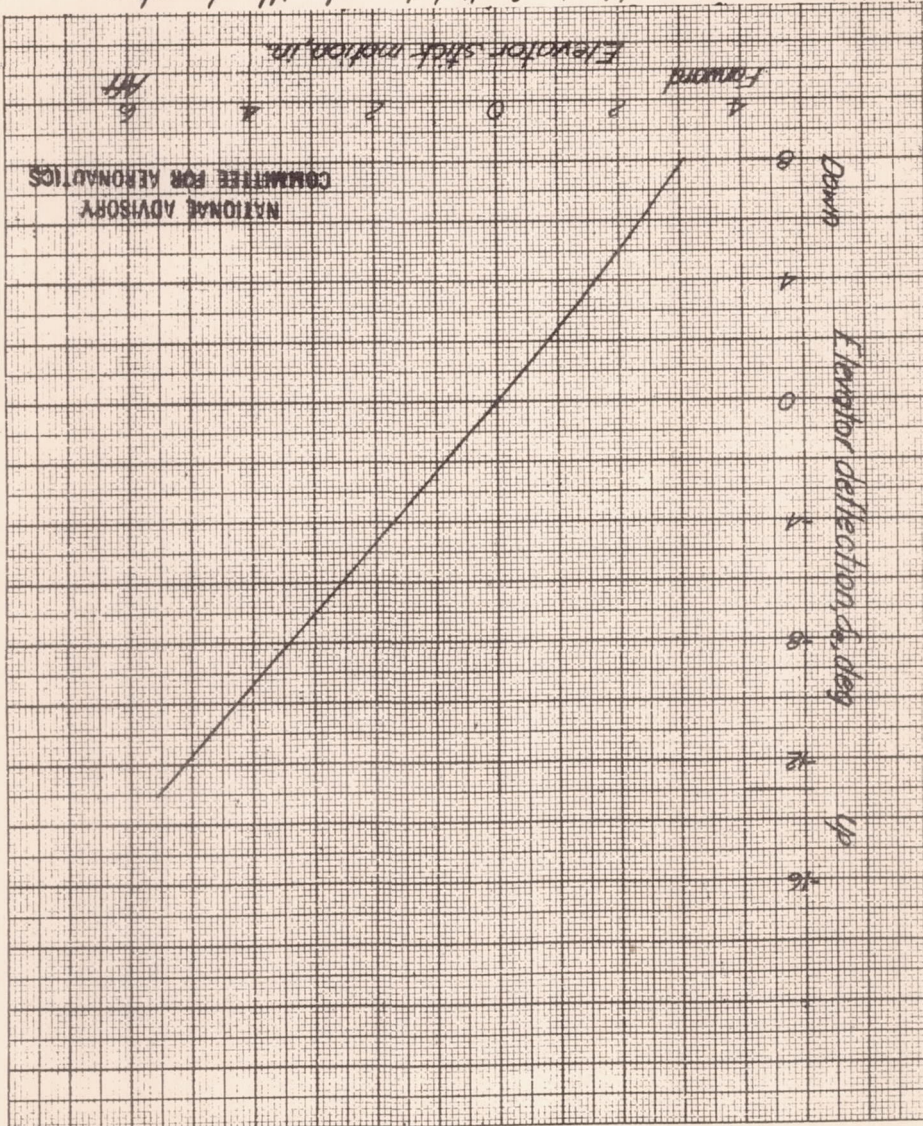


Figure 17.-Effect of slats on the variation of elevator floating angle with lift coefficient. Stick free, tab neutral; center of gravity at 27.5 percent MAC.

Figure 18.-Variation of pitch travel with elevator deflection for the MX-334 airplane.



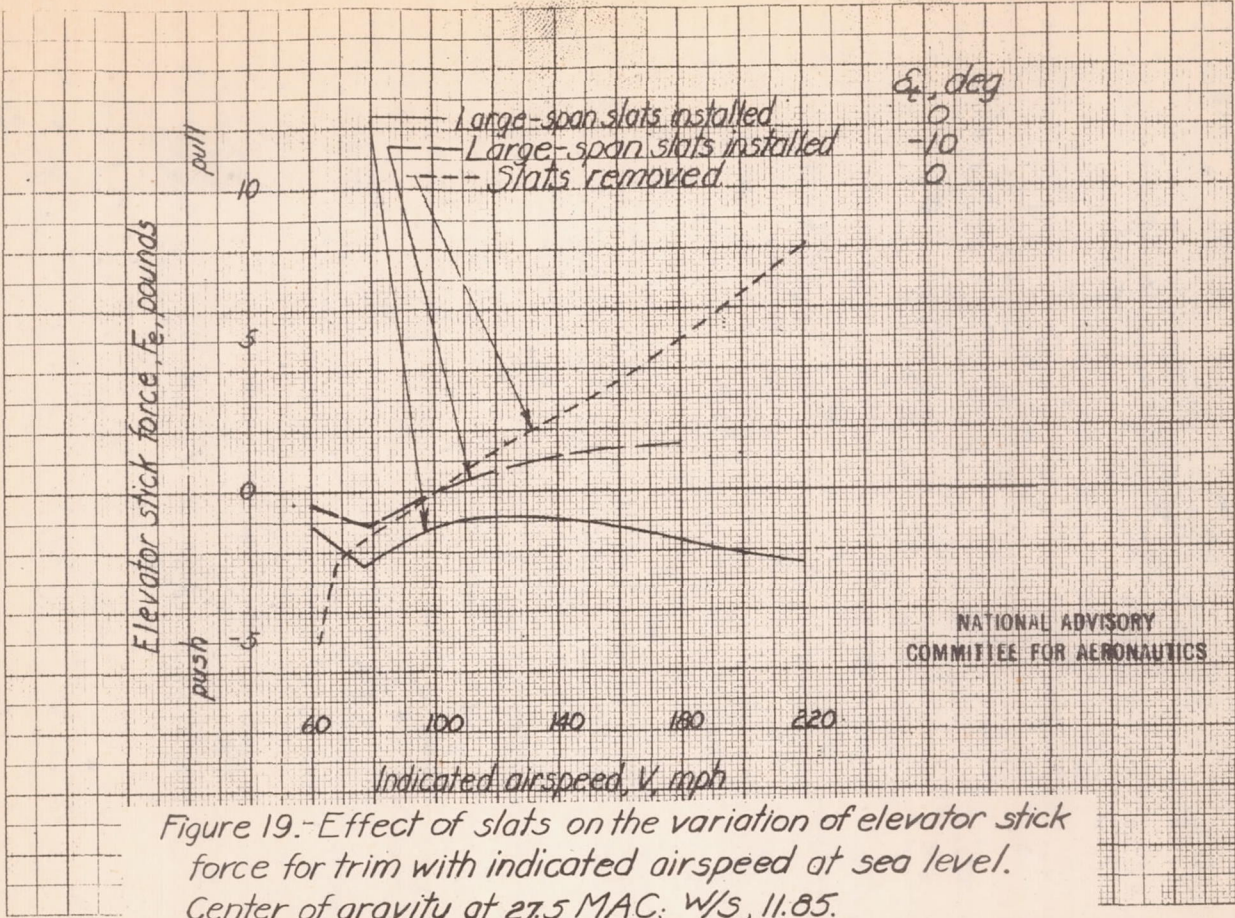


Figure 19.-Effect of slats on the variation of elevator stick force for trim with indicated airspeed at sea level.
Center of gravity at 27.5 MAC; W/S, 11.85.

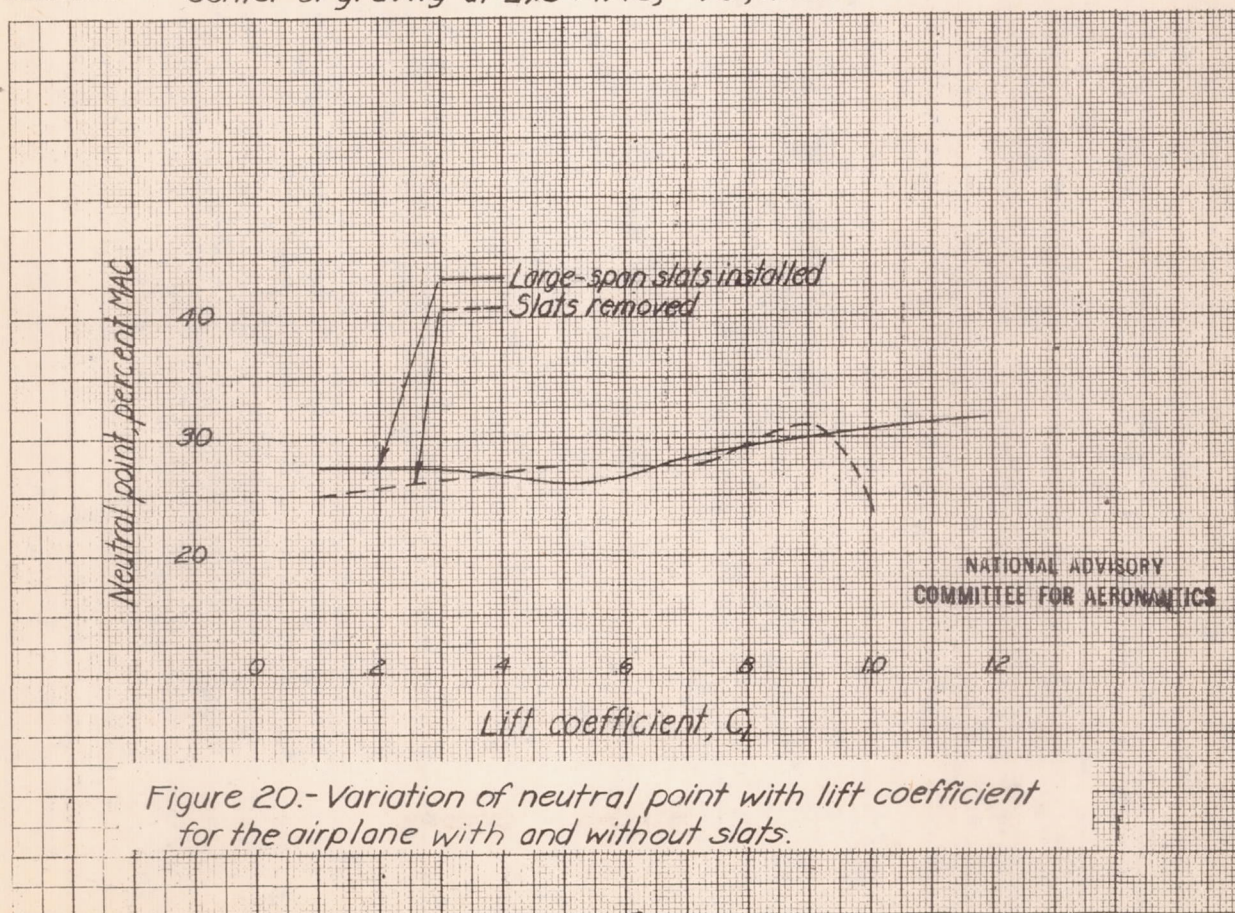
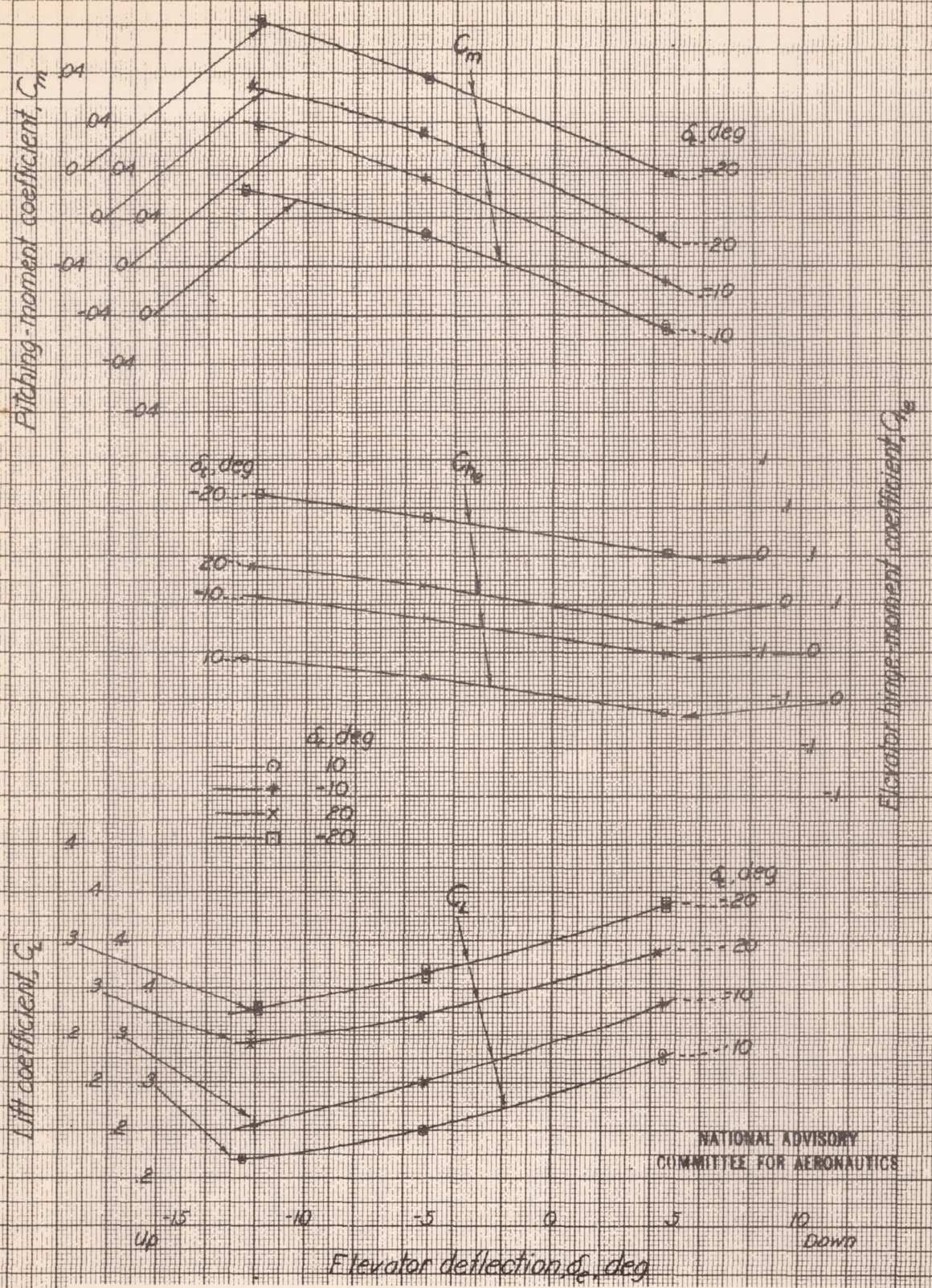


Figure 20.-Variation of neutral point with lift coefficient for the airplane with and without slats.



(a) $\alpha = 5.1^\circ$
 Figure 21.- Effect of elevator deflection and elevator tab setting on the aerodynamic characteristics of the airplane. Large-span slats installed; elevon sealed.

Lift coefficient, C_L

Pitching-moment coefficient, C_m

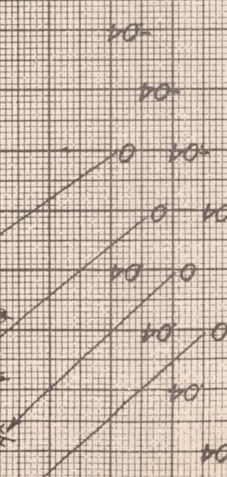
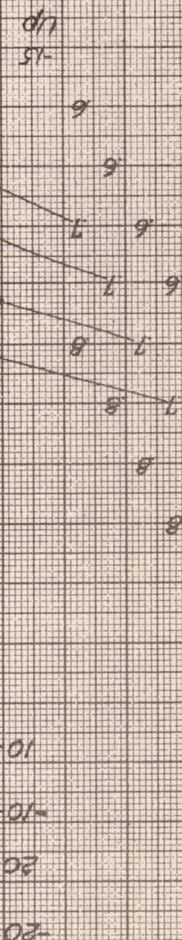


Figure 21.- Continued.
(b) $\alpha, 12.4^\circ$

Elevator deflection, δ_e , deg

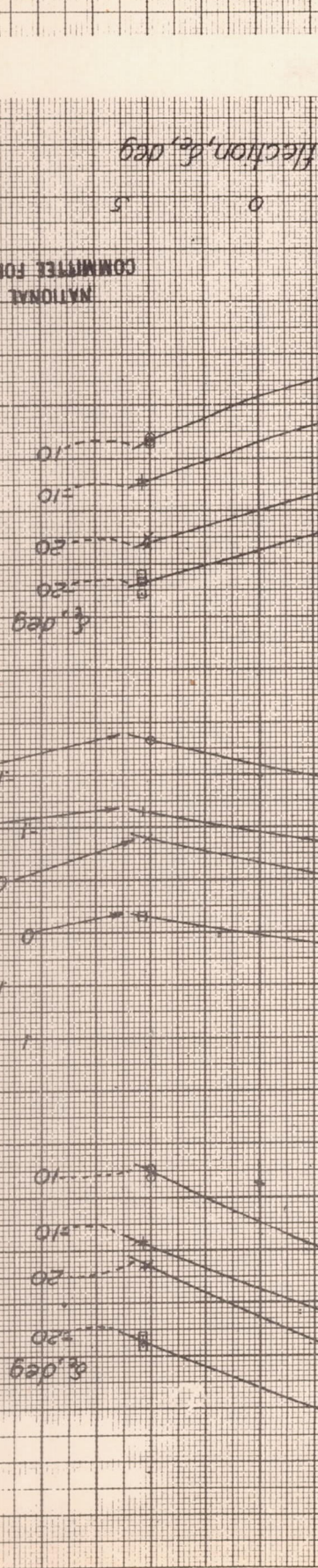
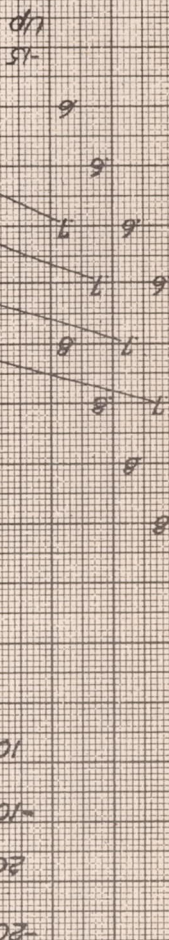
Down

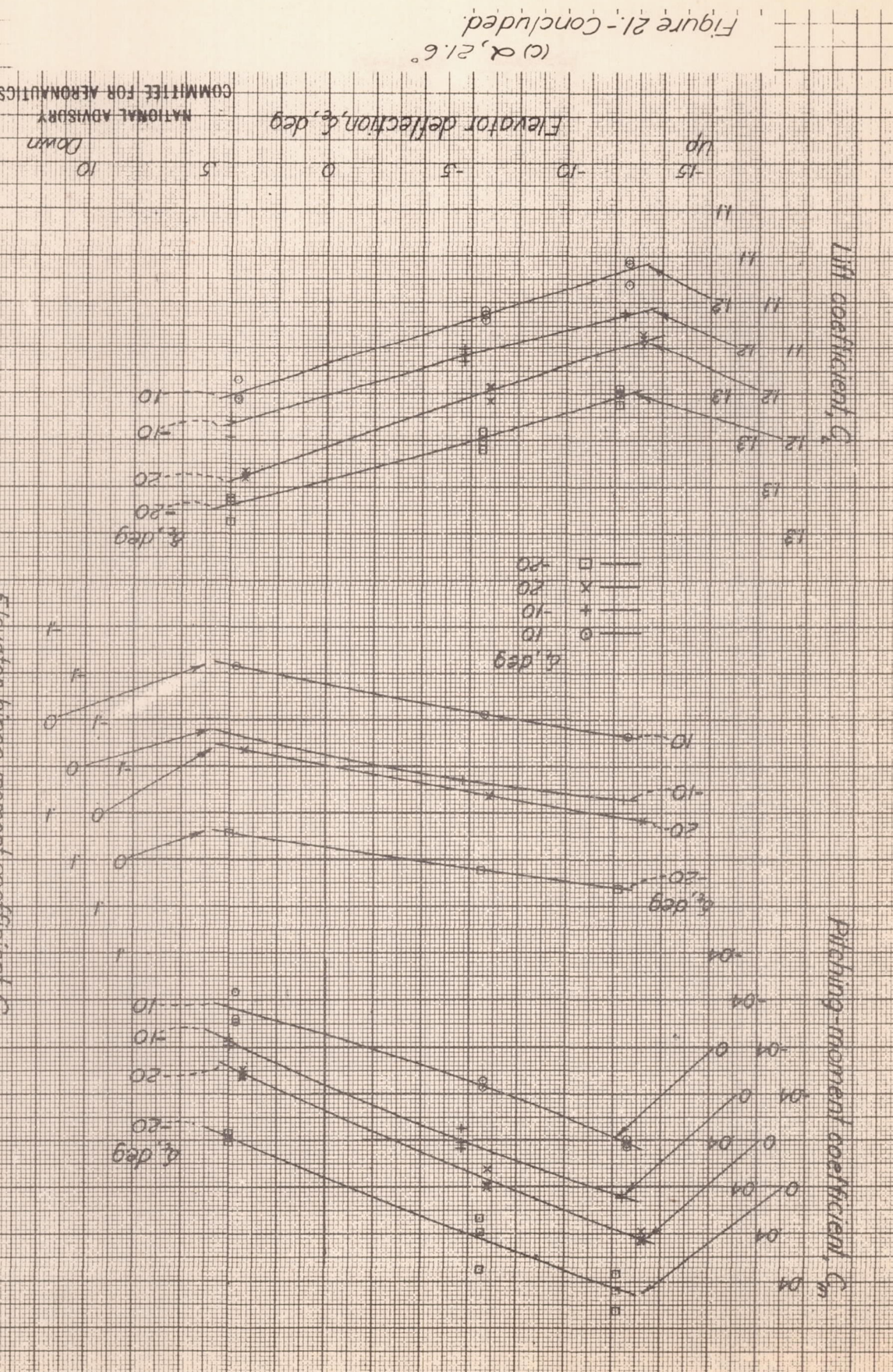
-10 -5 0 5 10

COMMITTEE FOR AERONAUTICS
NATIONAL ADVISORY

Elevator hinge moment coefficient, C_h

Up





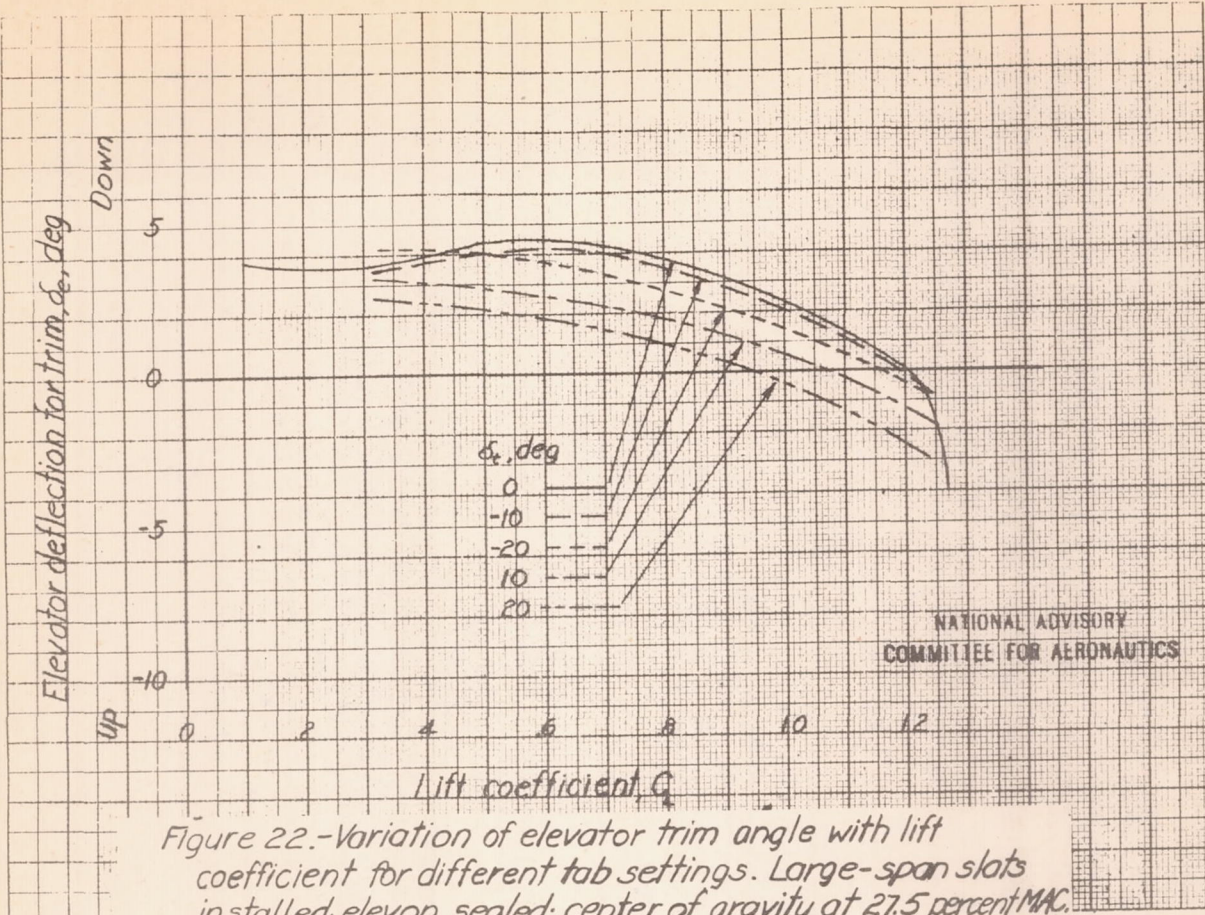


Figure 22.-Variation of elevator trim angle with lift coefficient for different tab settings. Large-span slats installed; elevon sealed; center of gravity at 27.5 percent MAC.

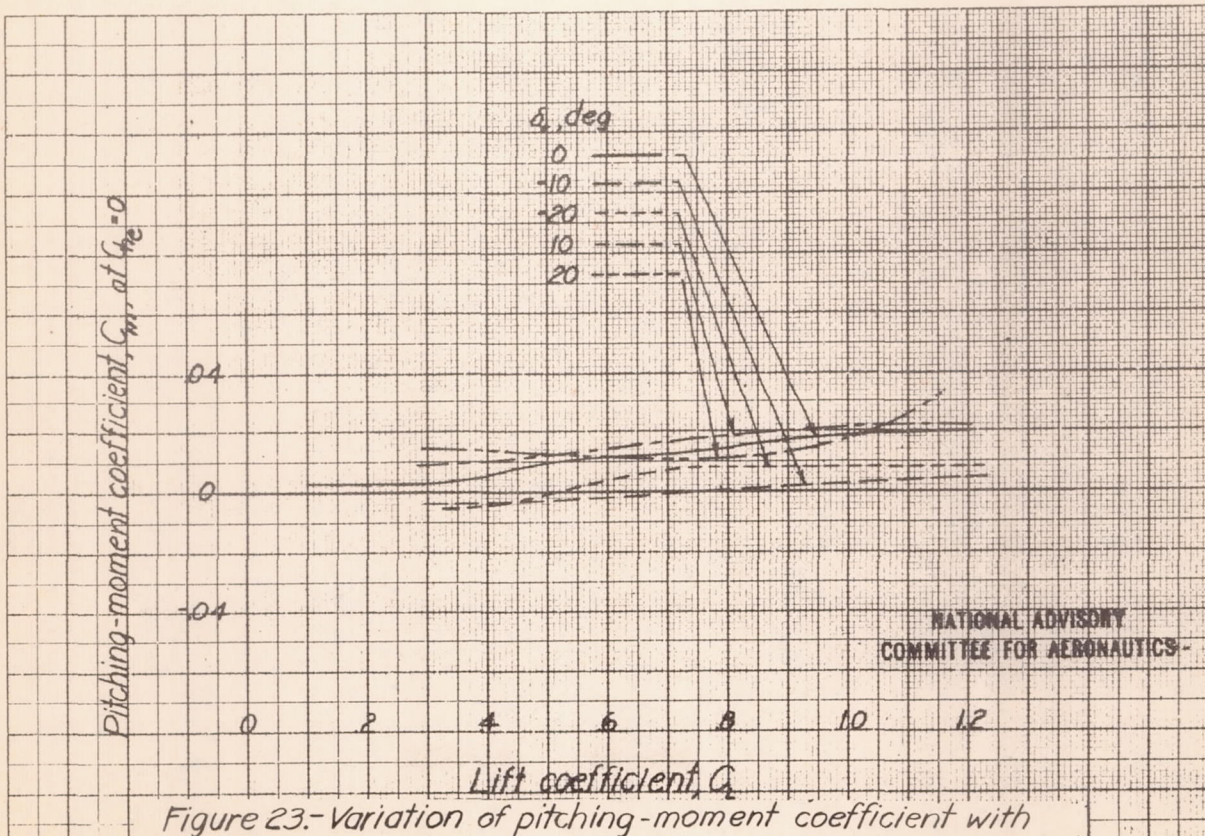


Figure 23.-Variation of pitching-moment coefficient with lift coefficient for different tab settings. Stick free; large-span slats installed; elevon sealed; center of gravity at 27.5 percent MAC.

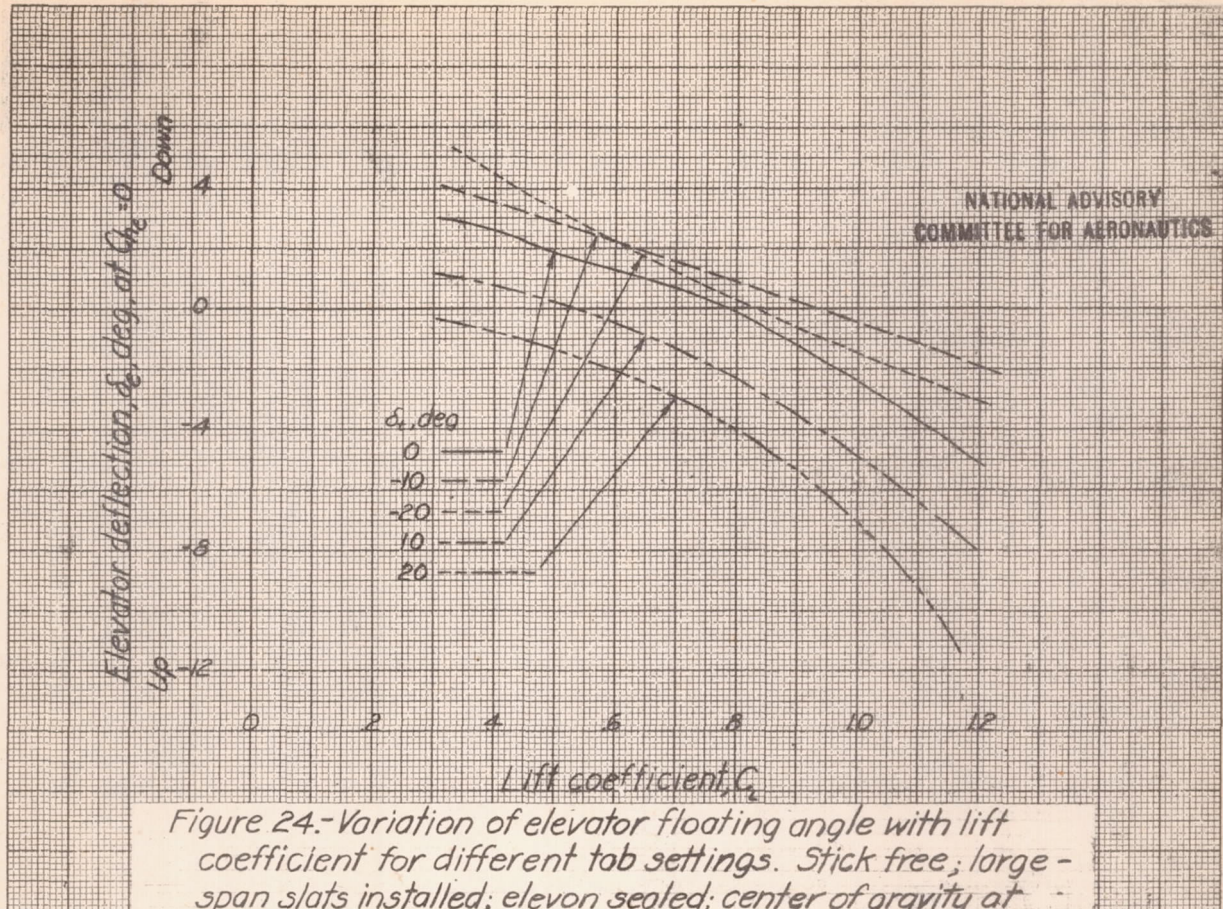


Figure 24.-Variation of elevator floating angle with lift coefficient for different tab settings. Stick free; large-span slats installed; elevon sealed; center of gravity at 27.5 percent MAC.

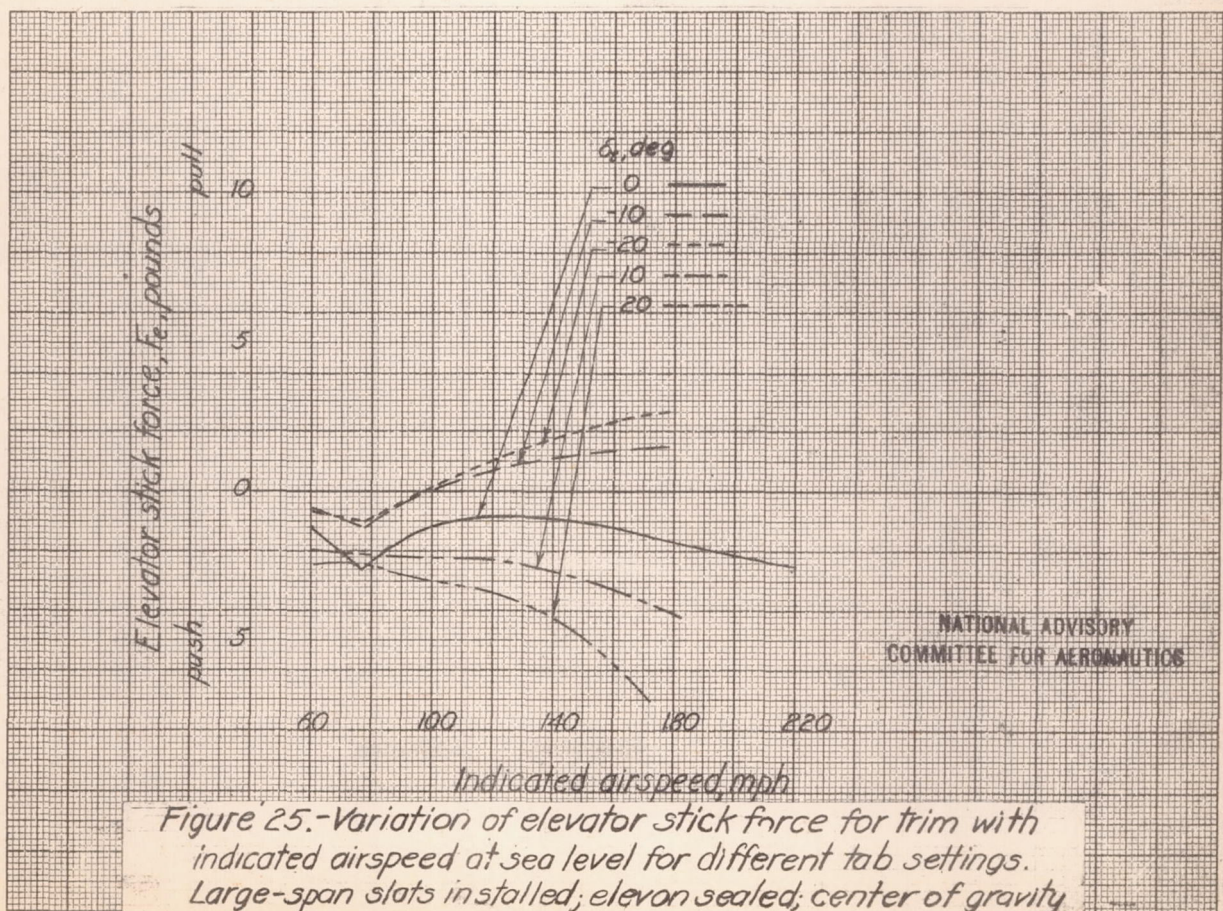
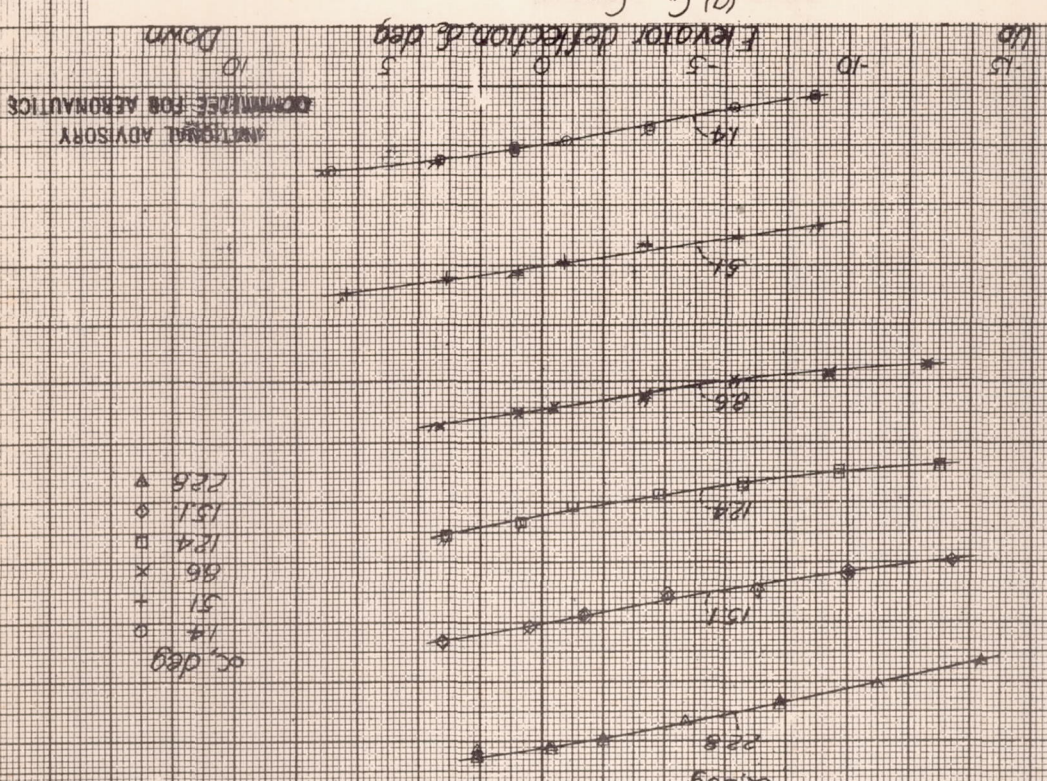
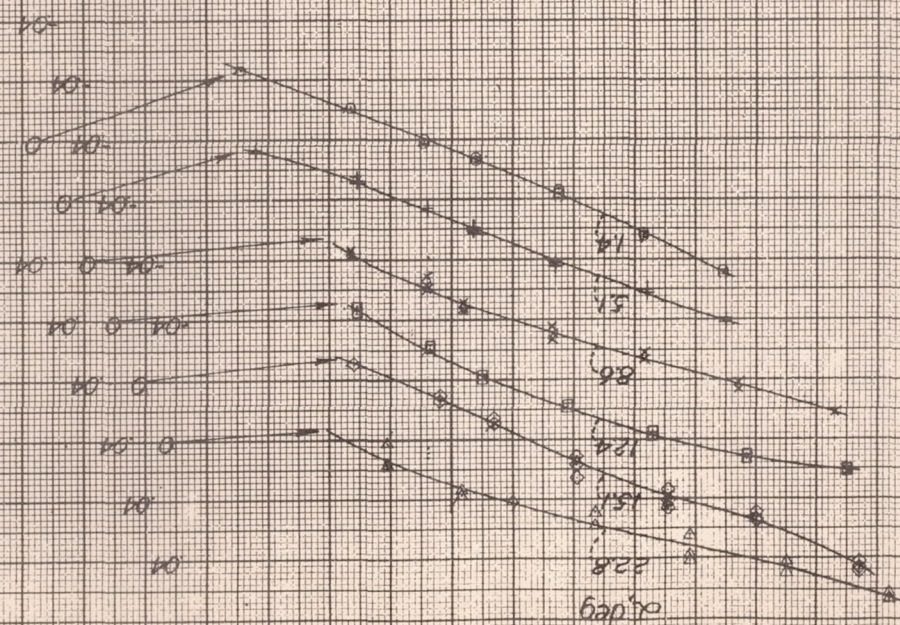


Figure 25.-Variation of elevator stick force for trim with indicated airspeed at sea level for different tab settings. Large-span slats installed; elevon sealed; center of gravity at 27.5 percent MAC.

Figure 26.—Effect of elevator deflection with the elevator seal removed on the aerodynamic characteristics of the airplane. Slats removed, tail neutral.



Pitching moment coefficient C_m



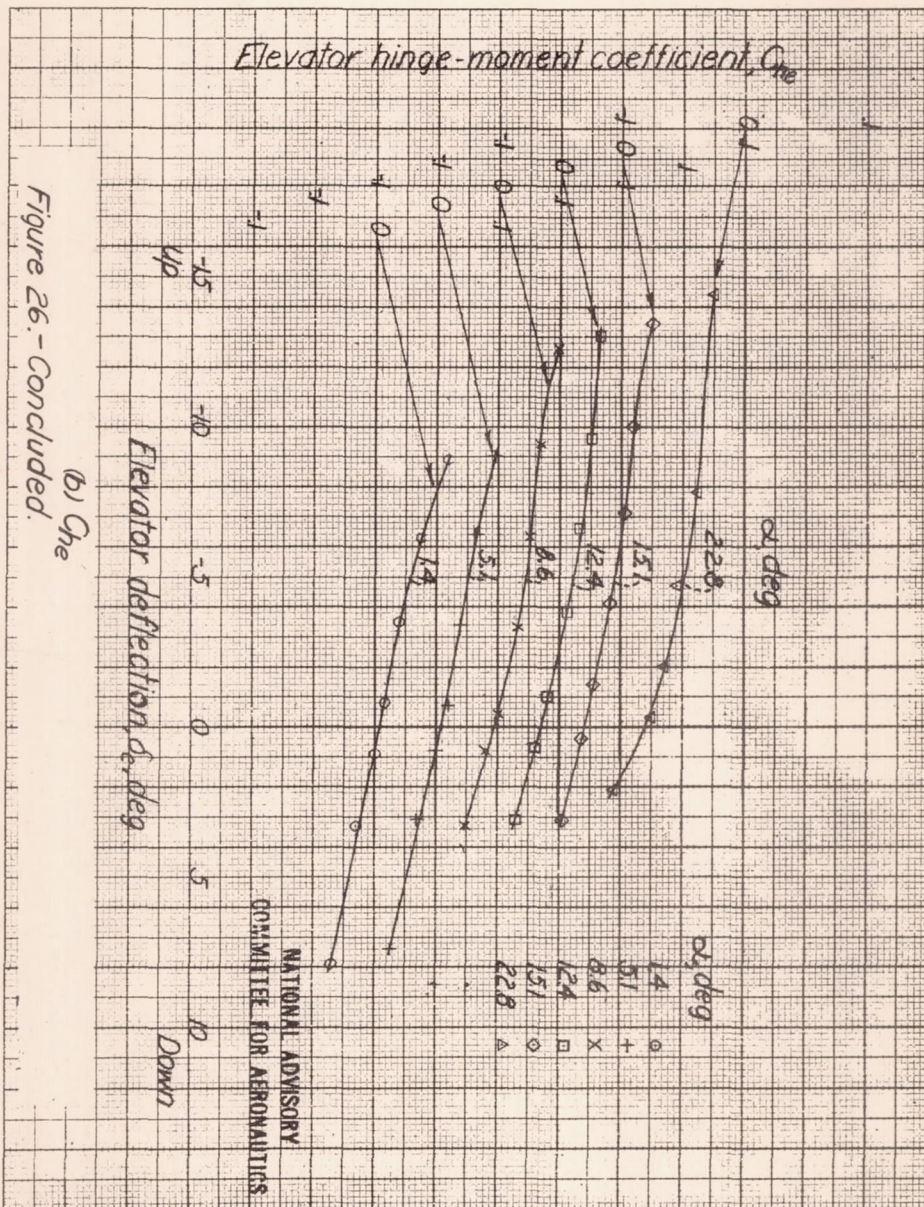


Figure 26.-Concluded.

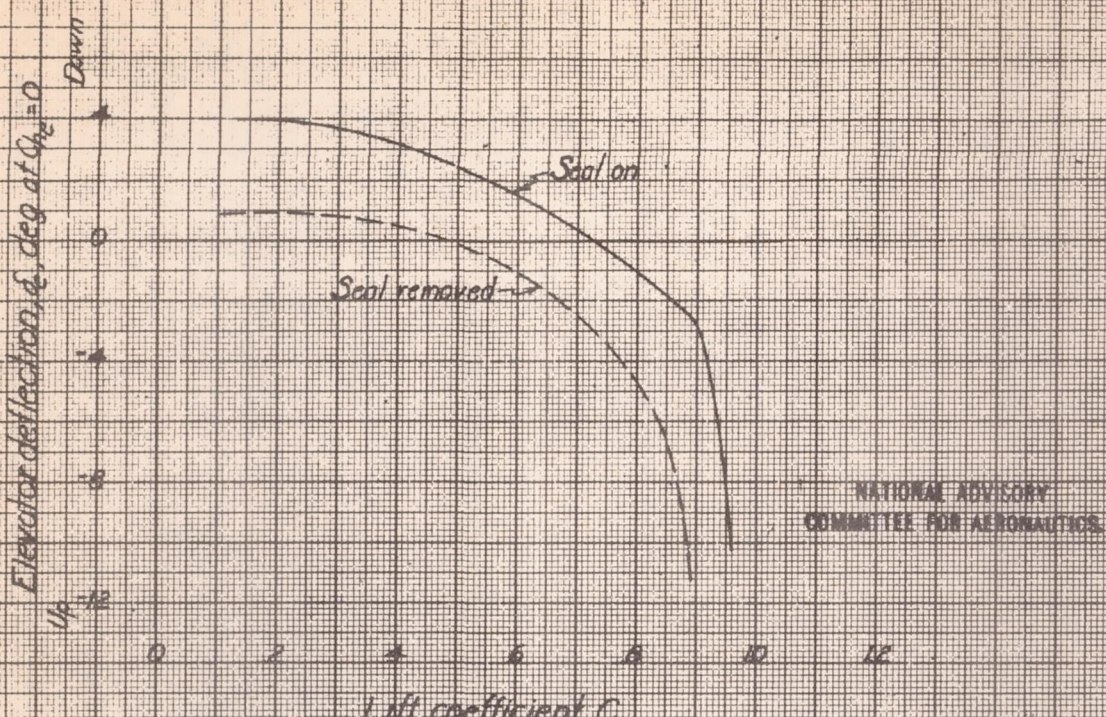


Figure 27.-Effect of the elevon seal on the elevator floating angle. Stick free; slats removed; tab neutral; center of gravity at 27.5 percent MAC.

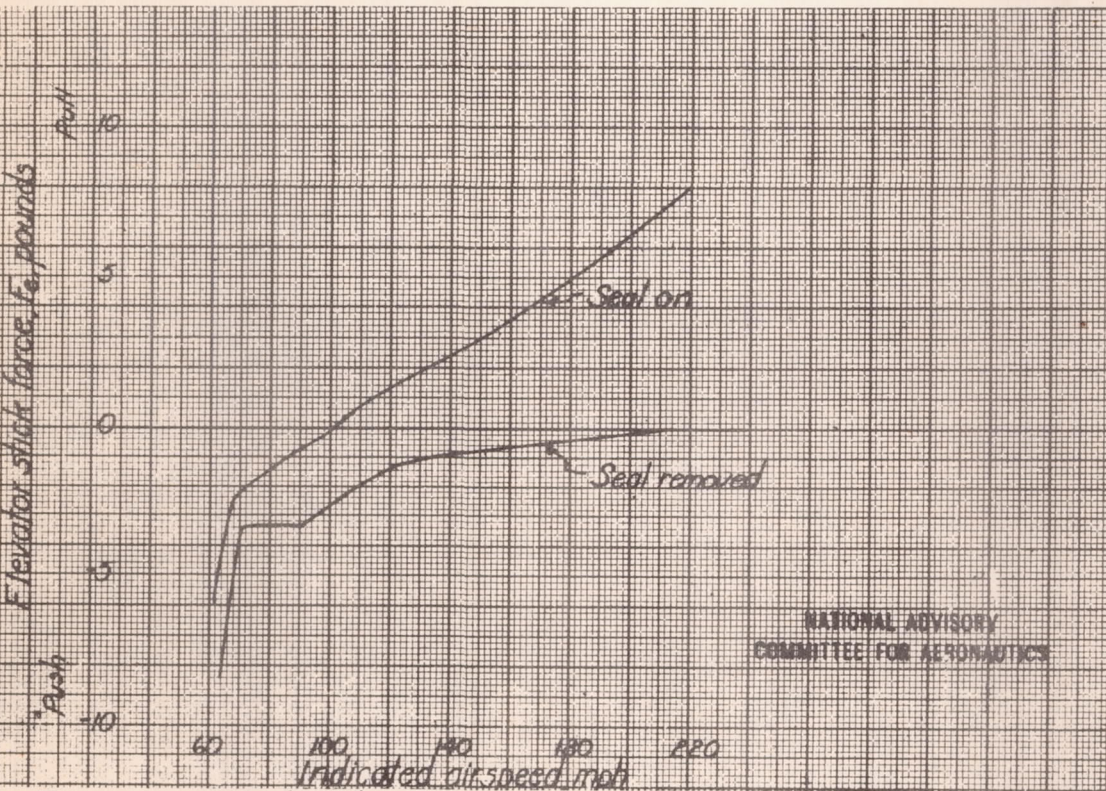


Figure 28.-Effect of the elevon seal on the variation of elevator stick force for trim with indicated airspeed at sea level. Slats removed; tab neutral; center of gravity at 27.5 percent MAC.

Pitching moment coefficient C_Q

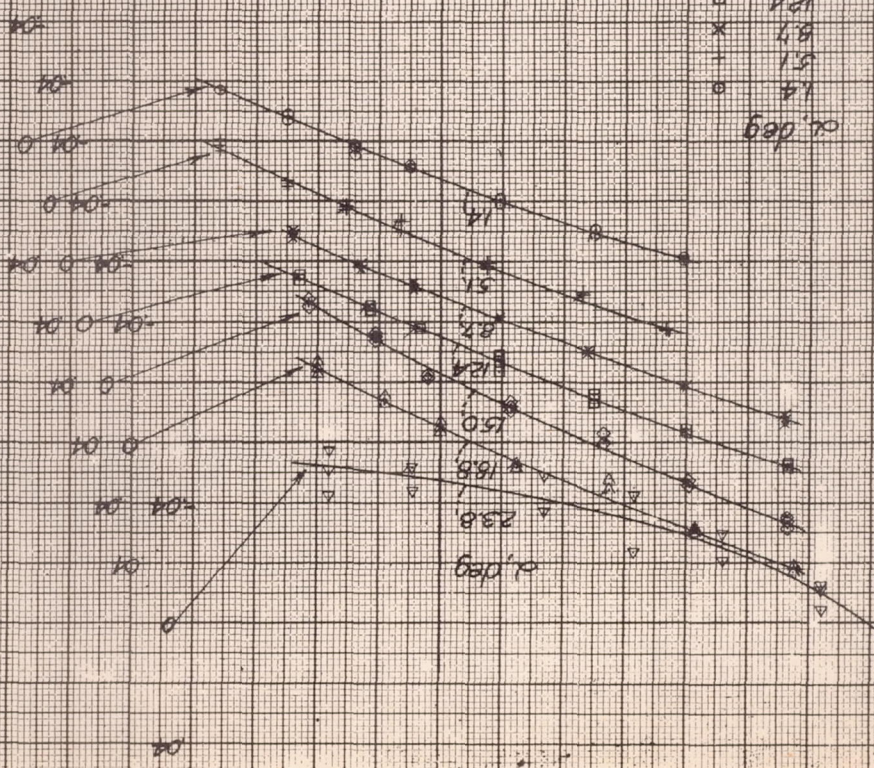


FIGURE 29.—Effect of elevator deflection with the elevator removed on the aerodynamic characteristics of the airplane. Large-span slats installed; tail neutral.

bevelled elevon installed.

the airframe. Large-span slats installed; tail neutral.

seal removed on the elevon installed.

Elevator deflection: up, down.

COMMITTEE FOR AERONAUTICS

NATIONAL ADVISORY

Elevator deflection: up

bevelled elevon installed.

the airframe. Large-span slats installed; tail neutral.

seal removed on the elevon installed.

Elevator deflection: up, down.

COMMITTEE FOR AERONAUTICS

NATIONAL ADVISORY

Elevator deflection: down

bevelled elevon installed.

the airframe. Large-span slats installed; tail neutral.

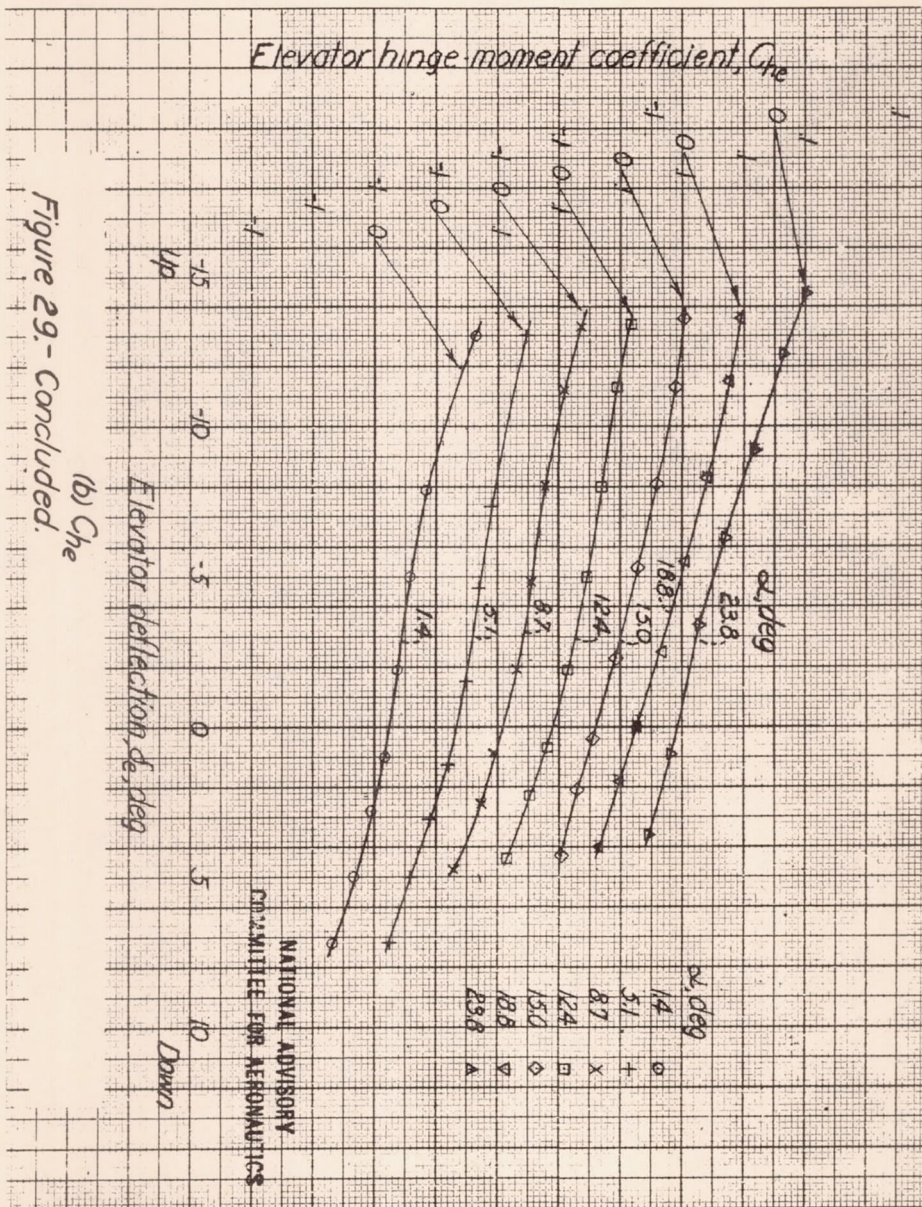
seal removed on the elevon installed.

Elevator deflection: up, down.

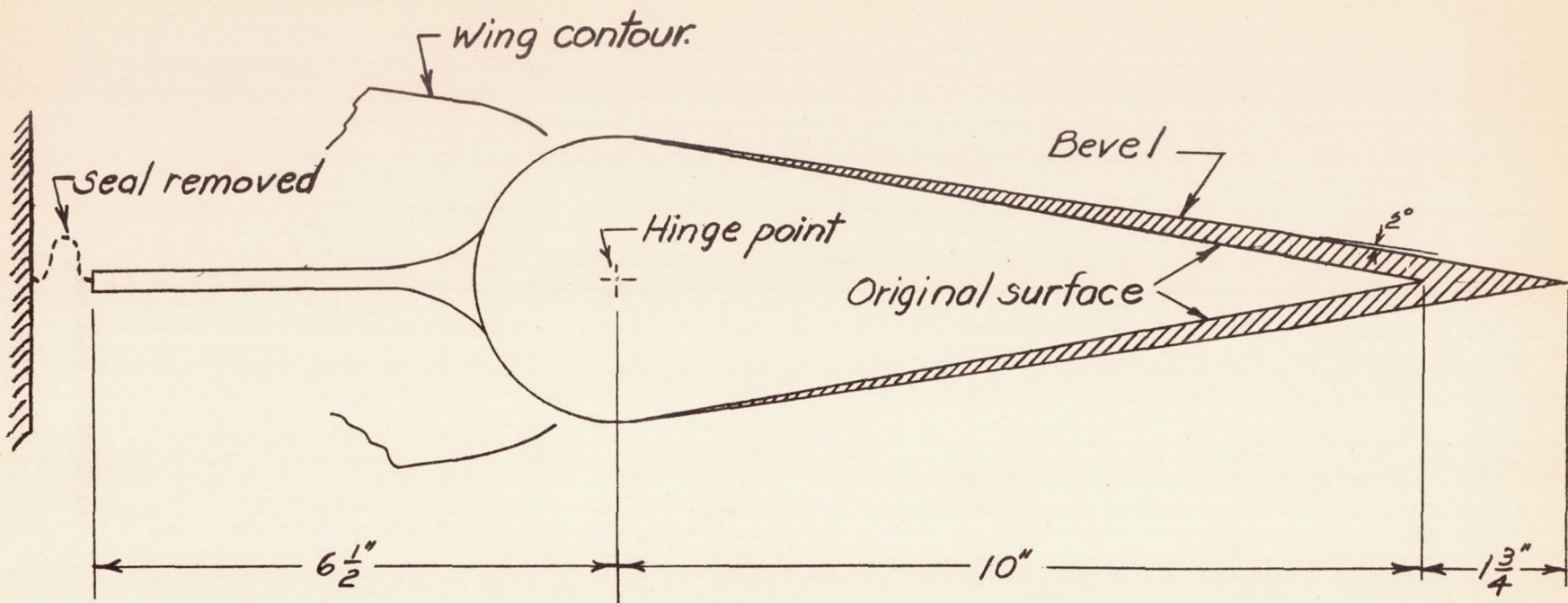
COMMITTEE FOR AERONAUTICS

NATIONAL ADVISORY

lift coefficient C_L

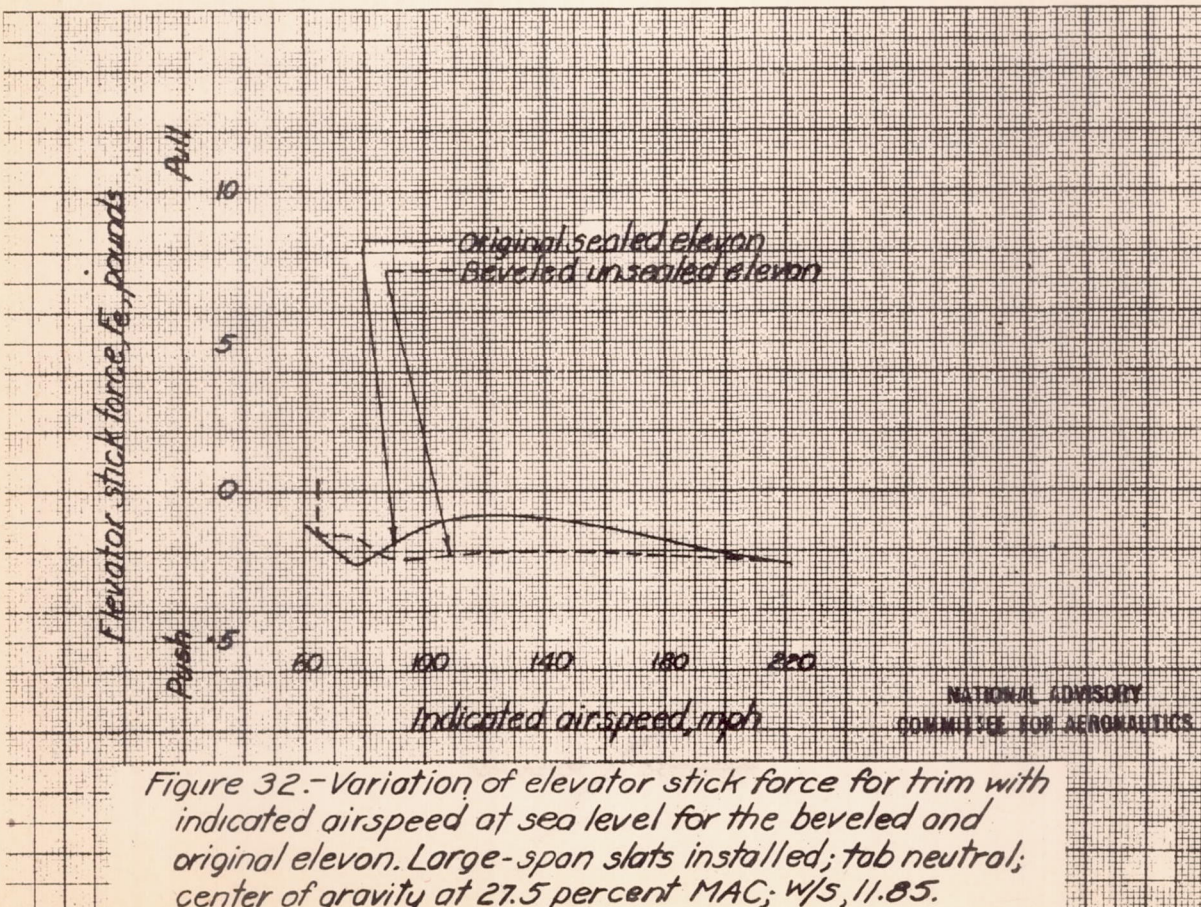
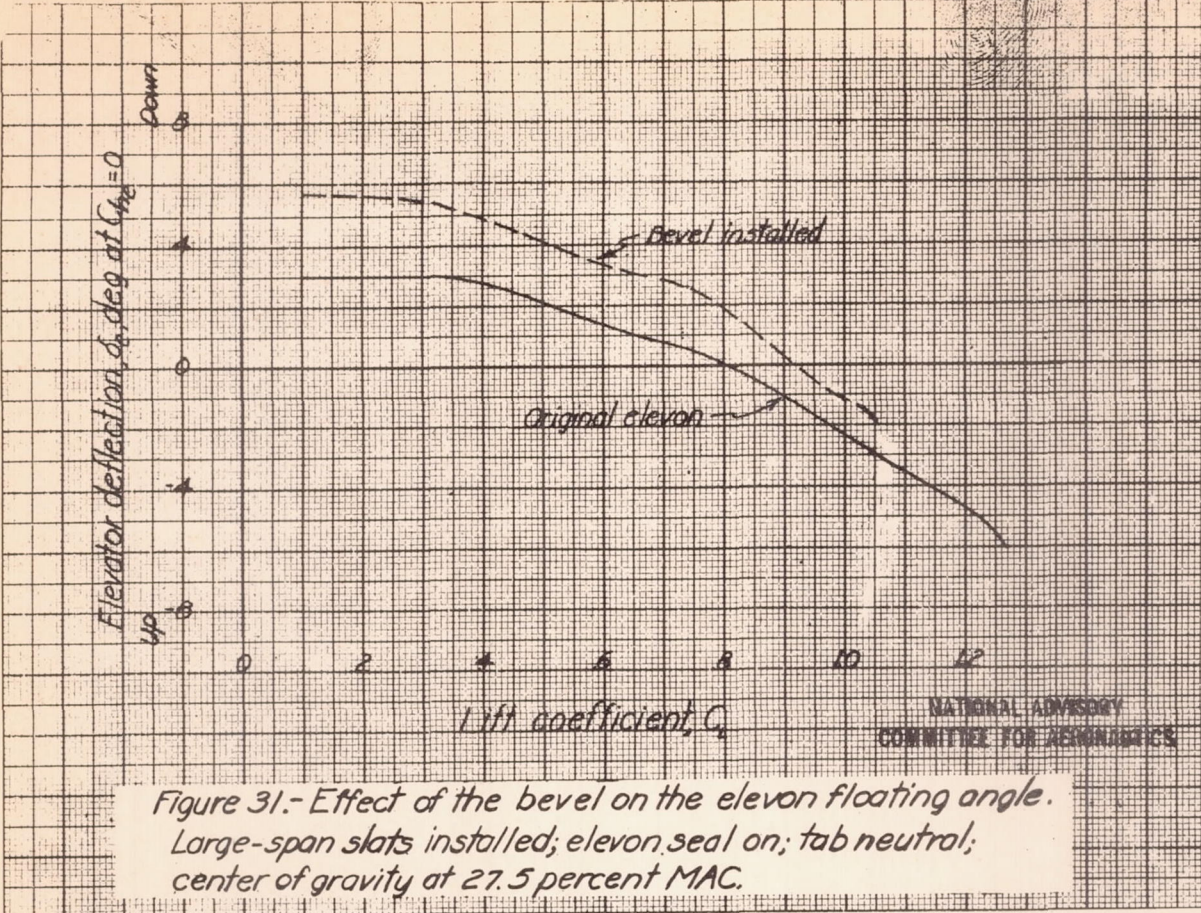


(b) Che
Figure 29.- Concluded.



NATIONAL ADVISORY
COMMITTEE FOR AERONAUTICS

Figure 30.- Sketch of the beveled elevon for the MX-334 airplane.



46555
FIGURE 33.—Effect of aileron deflection on C_L , C_n , and C_d
with the airplane in yaw. $\delta_a = 0^\circ$; large-span slots installed.
(a) $\alpha = 3.3^\circ$

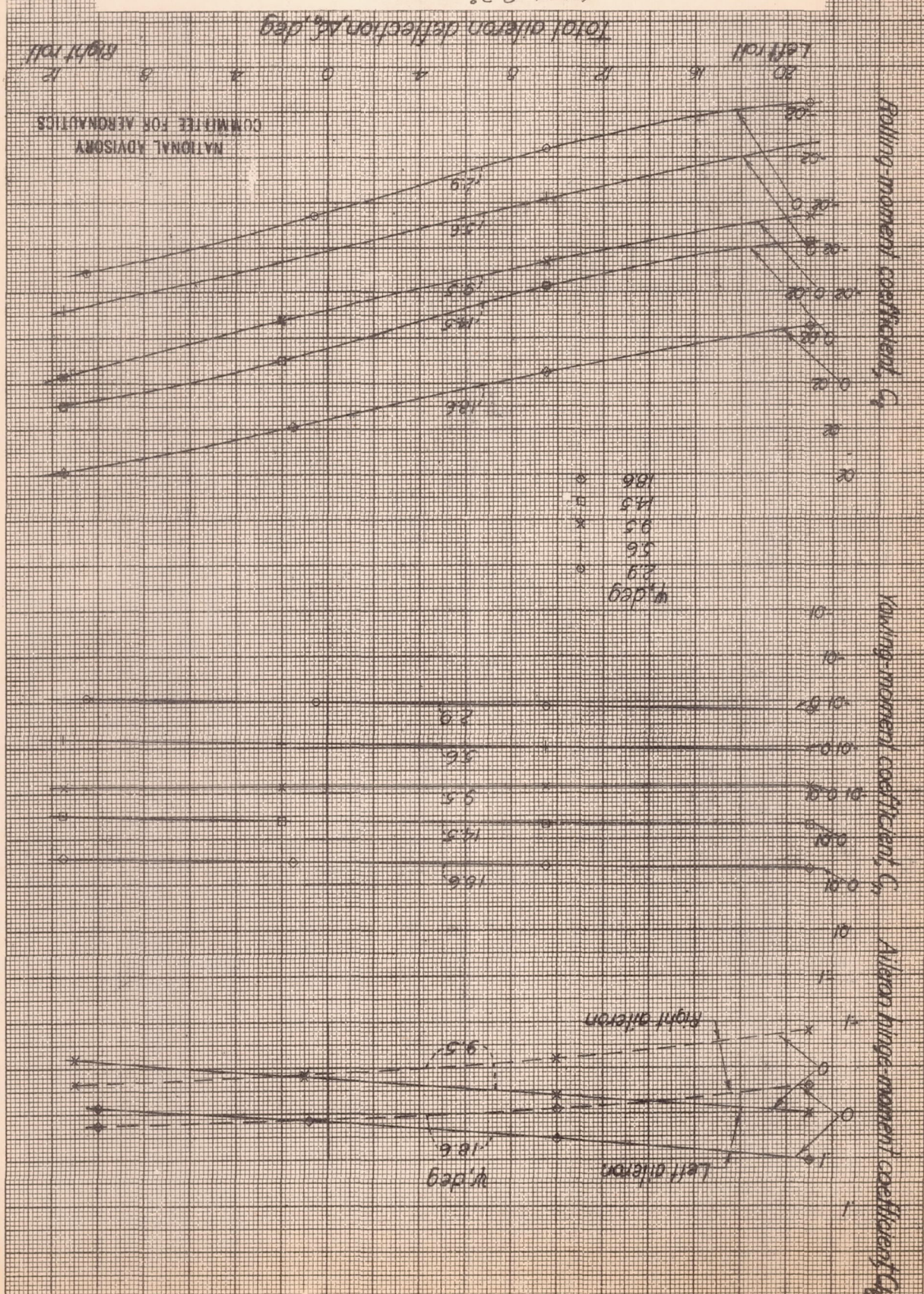


Figure 33.—Continued.

• 9.10.6.

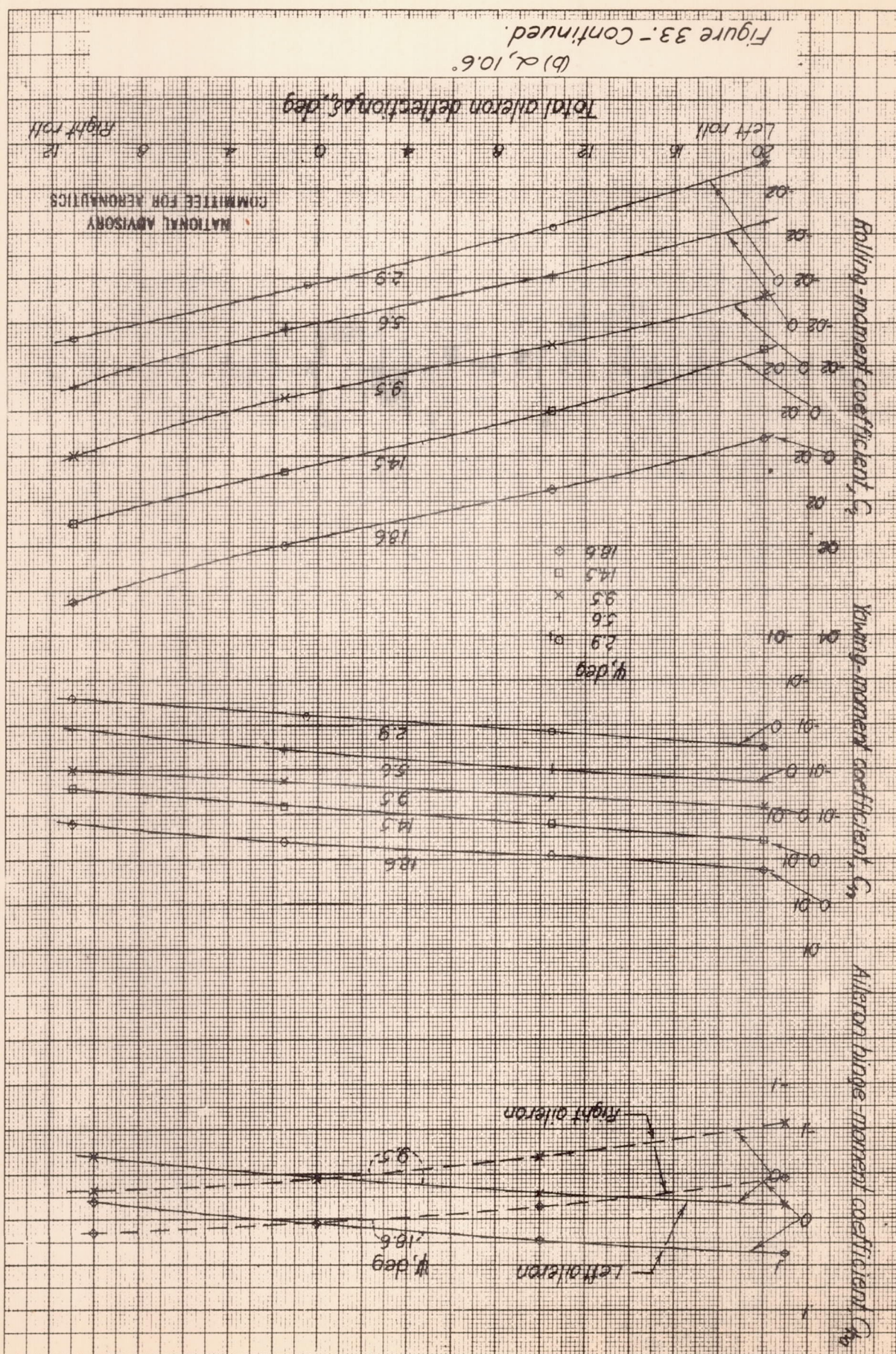


FIGURE 33.-Continued.

(C) 1969.

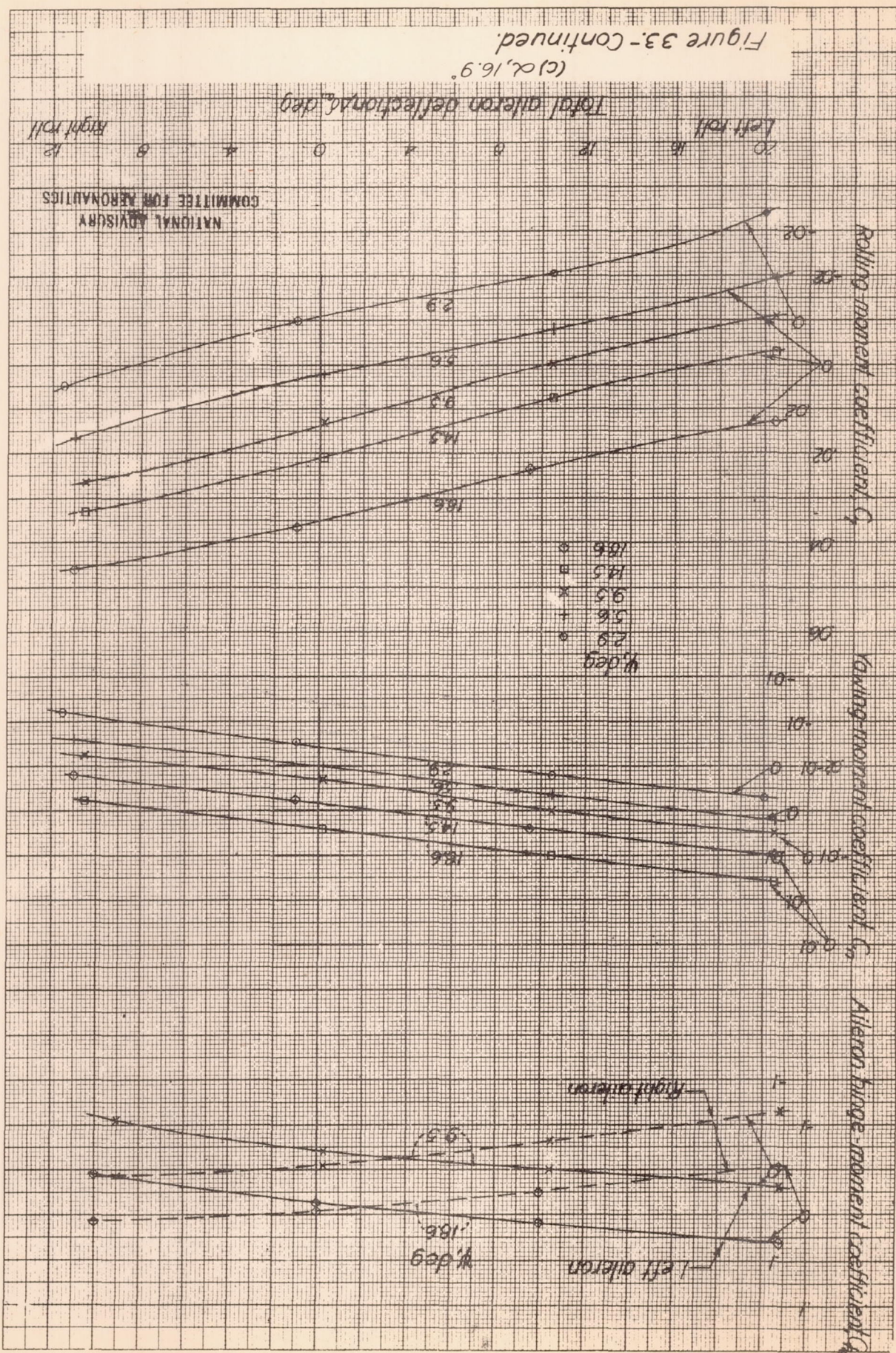
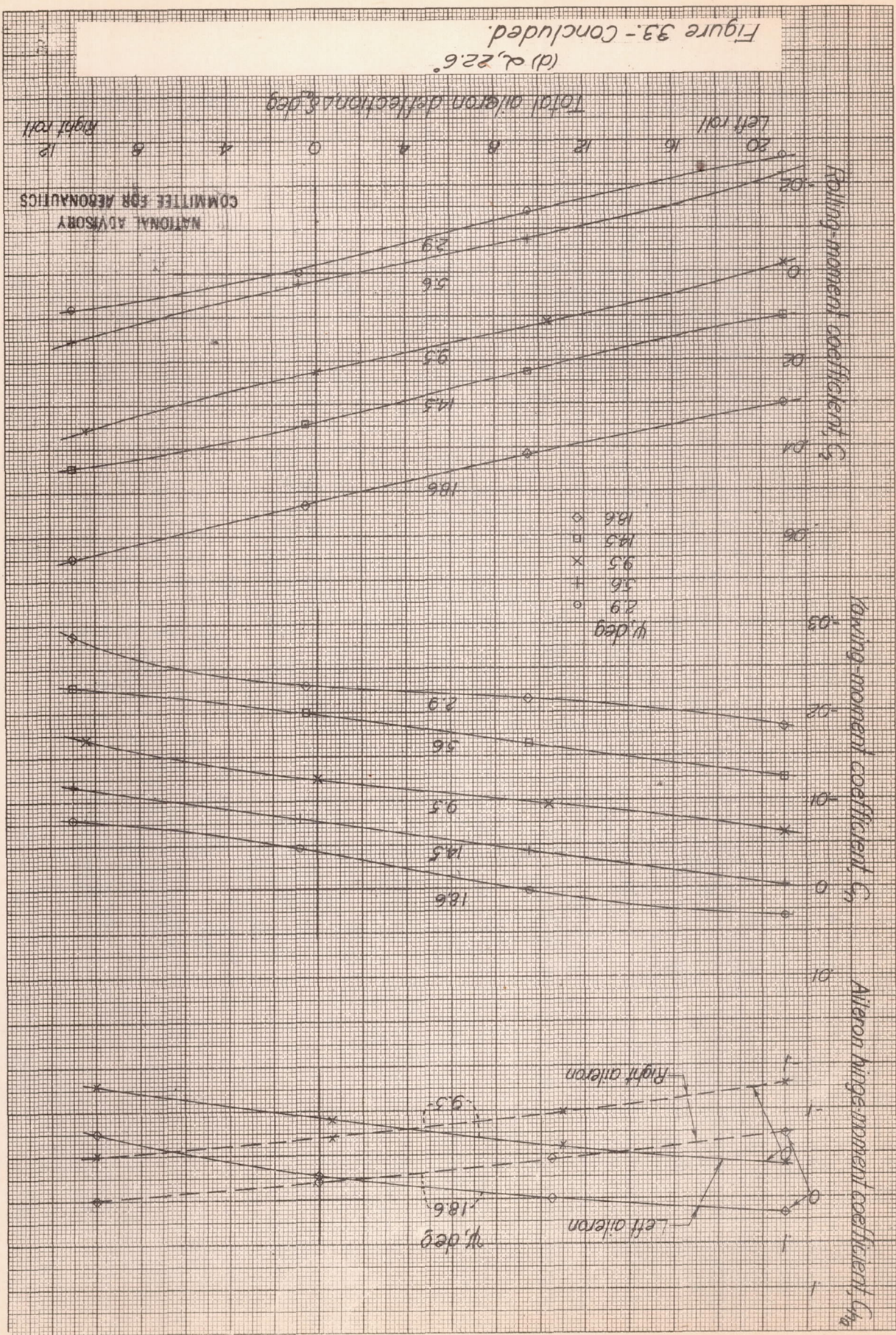


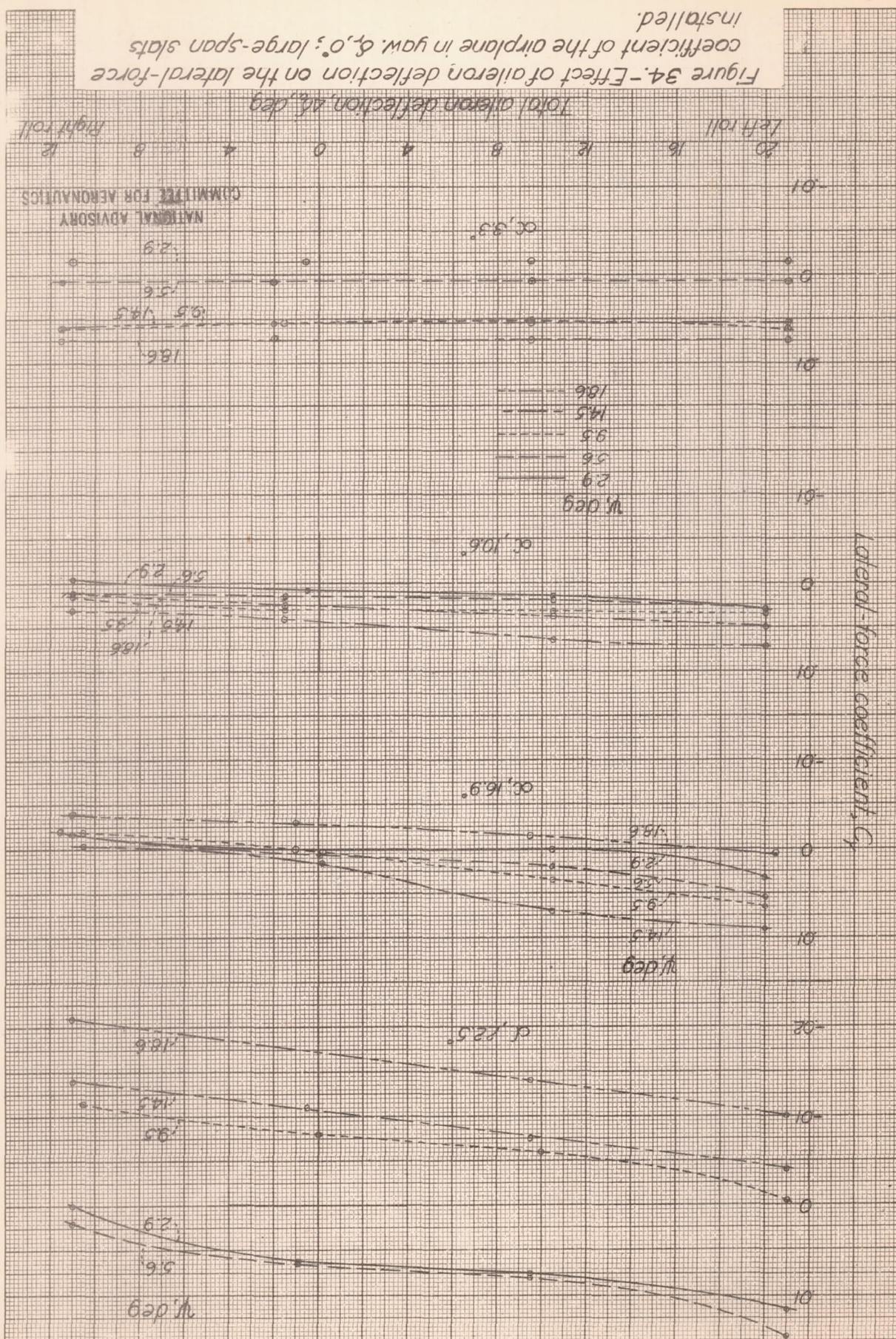
Figure 33.-Concluded.

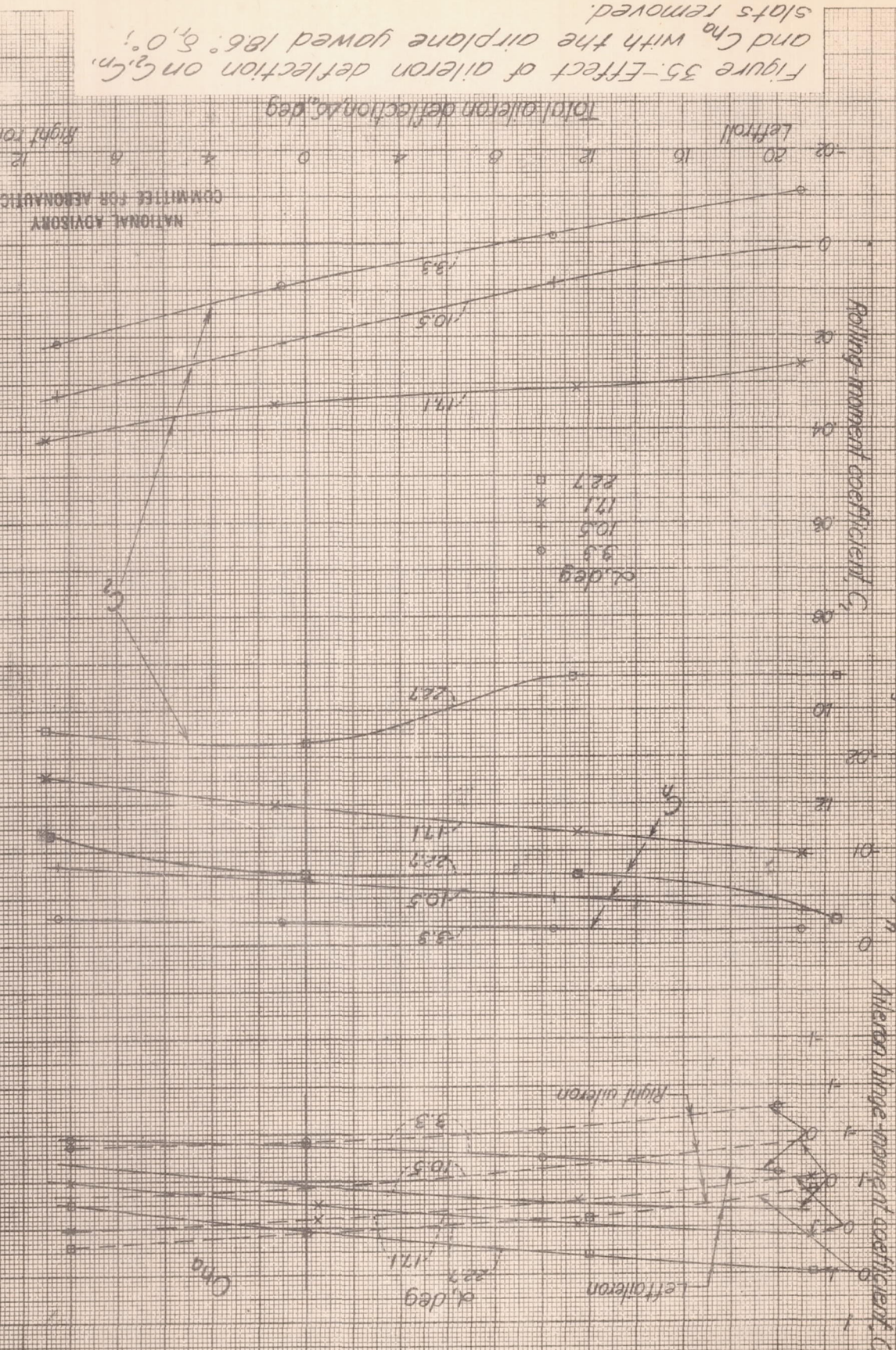
9.22.70 (P)



installed.

Figure 34.—Effect of aileron deflection on the lateral-force coefficient of the airframe in yaw. G_y/G_x ; large-span slats





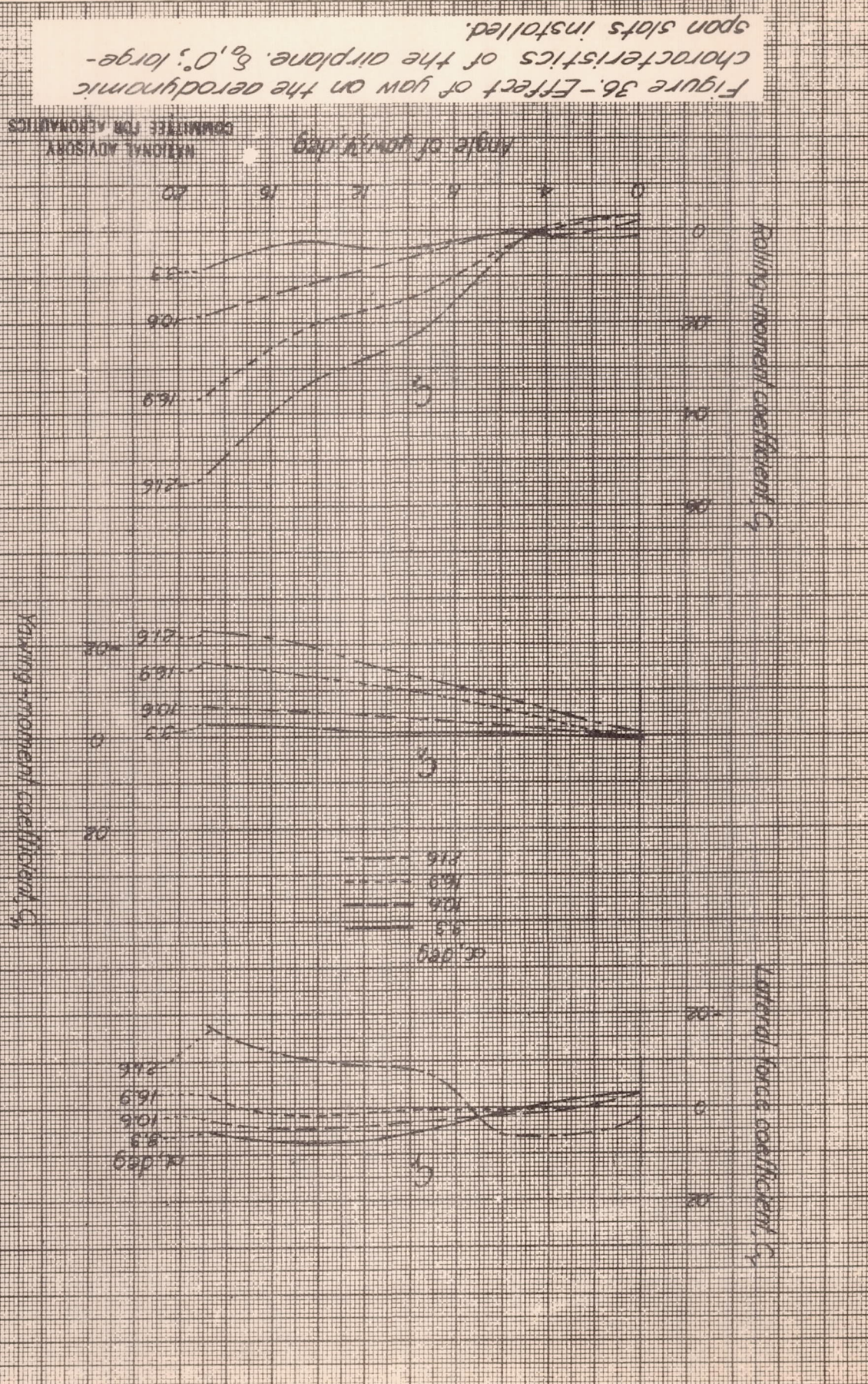
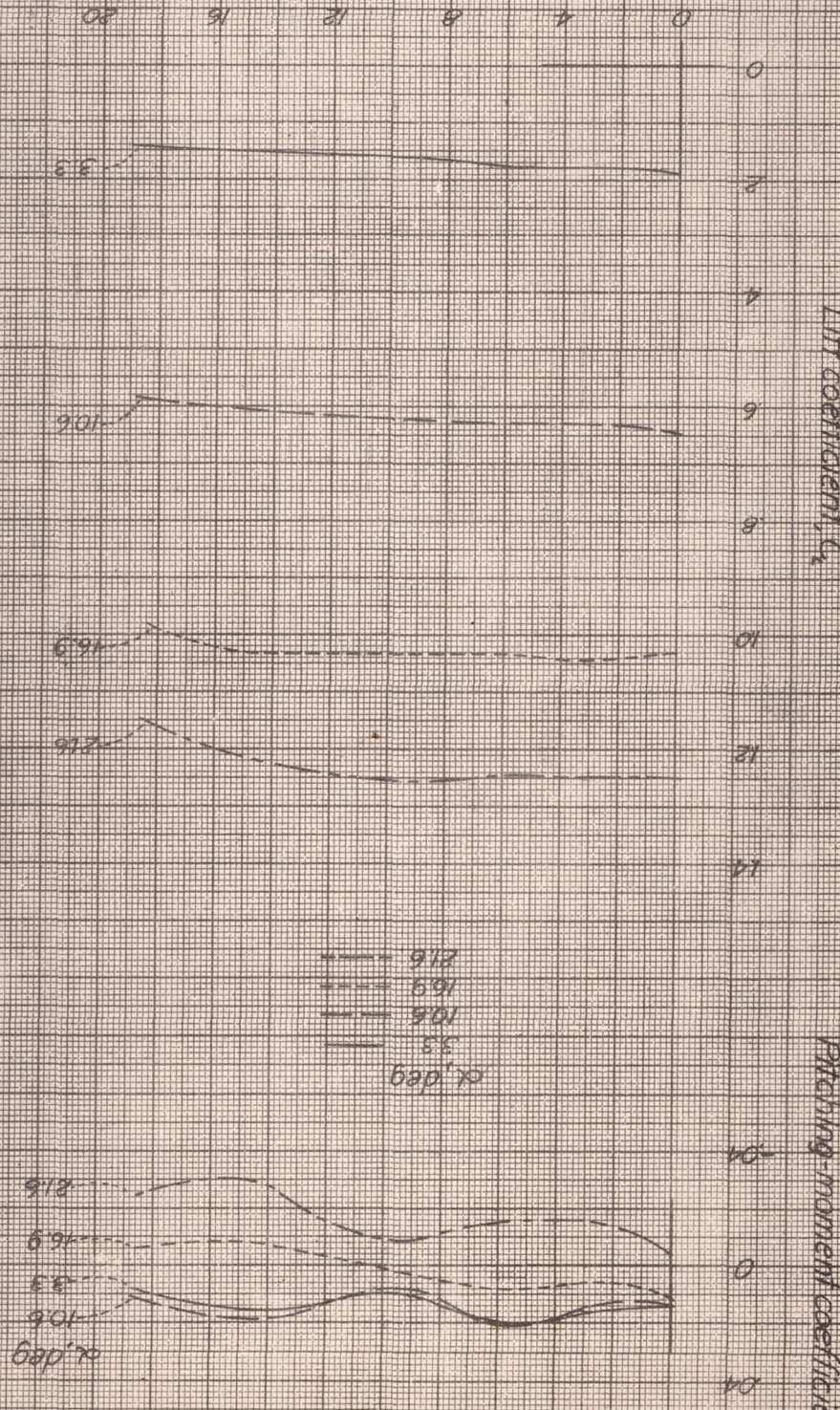


Figure 37 - Variation of lift coefficient and pitching moment coefficient with angle of yaw, θ , $0^\circ, 8^\circ, 16^\circ$. Large-span slots installed.

NATIONAL ADVISORY COMMITTEE FOR AERONAUTICS



NATIONAL ADVISORY AERONAUTICS
COMMITTEE FOR AERONAUTICS

Figure 3B—Effect of fins on the variations of
 C_x , C_n , C_y with C_l with the airfoil one showed δ_a .

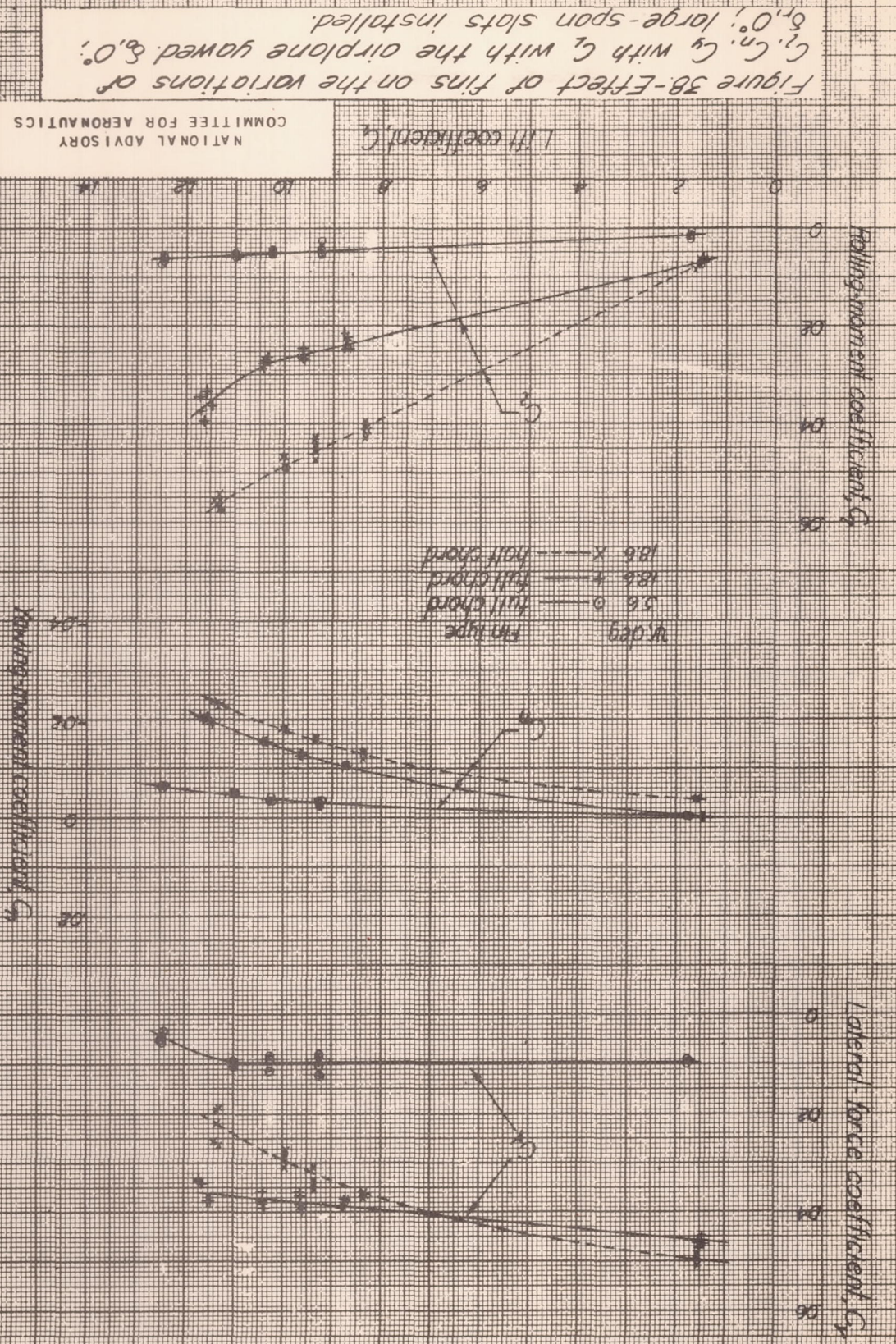


Figure 39.-The aerodynamic characteristics of the airplane showed 14.5° controls neutral; large-span slots installed.

NATIONAL ADVISORY AERONAUTICS
COMMITTEE FOR AERONAUTICS

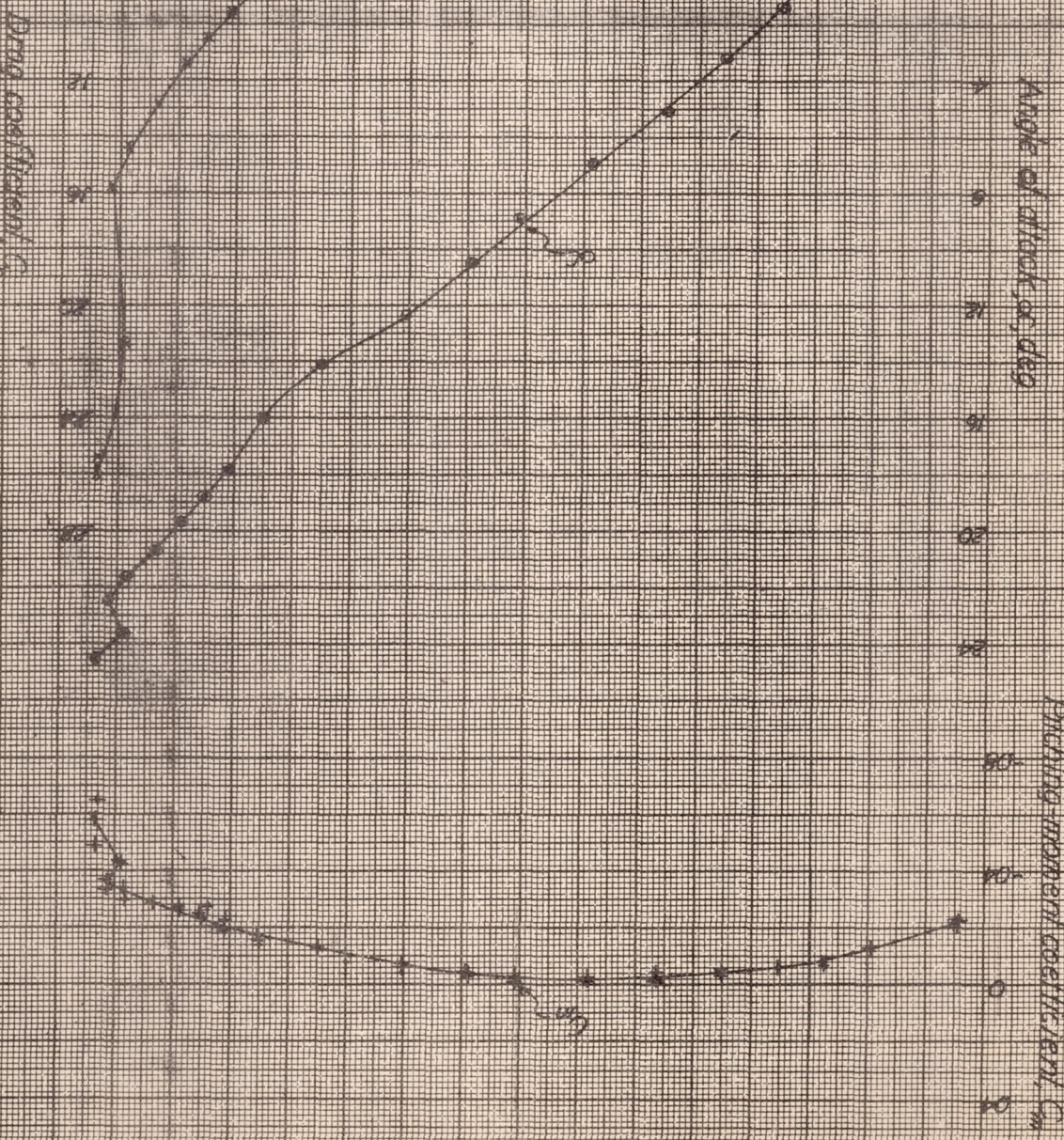
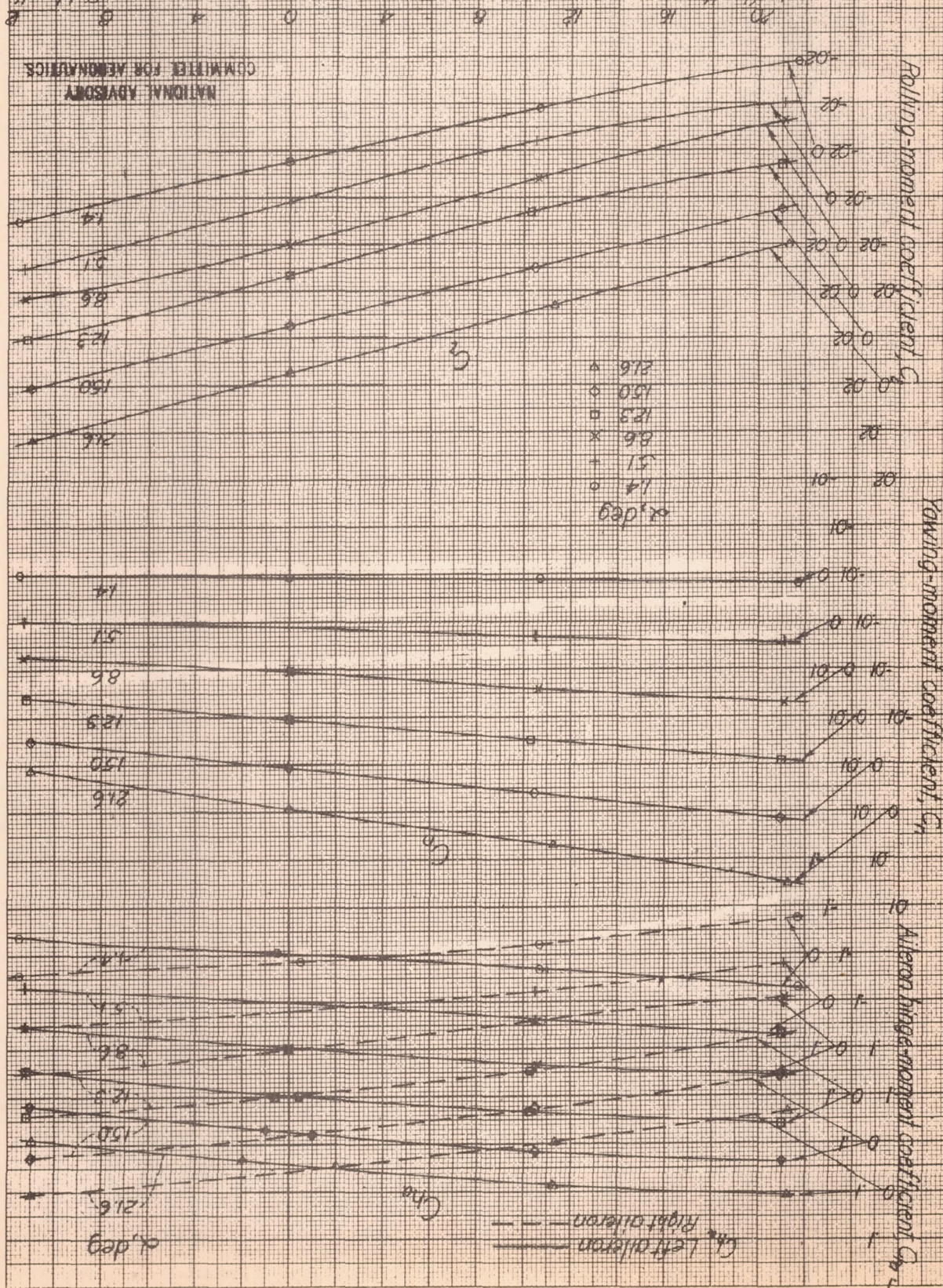


FIGURE 40.—Effect of aileron deflection on the aerodynamic characteristics of the airplane.
(a) Large-span slots installed.

Top aileron deflection angle

Right roll



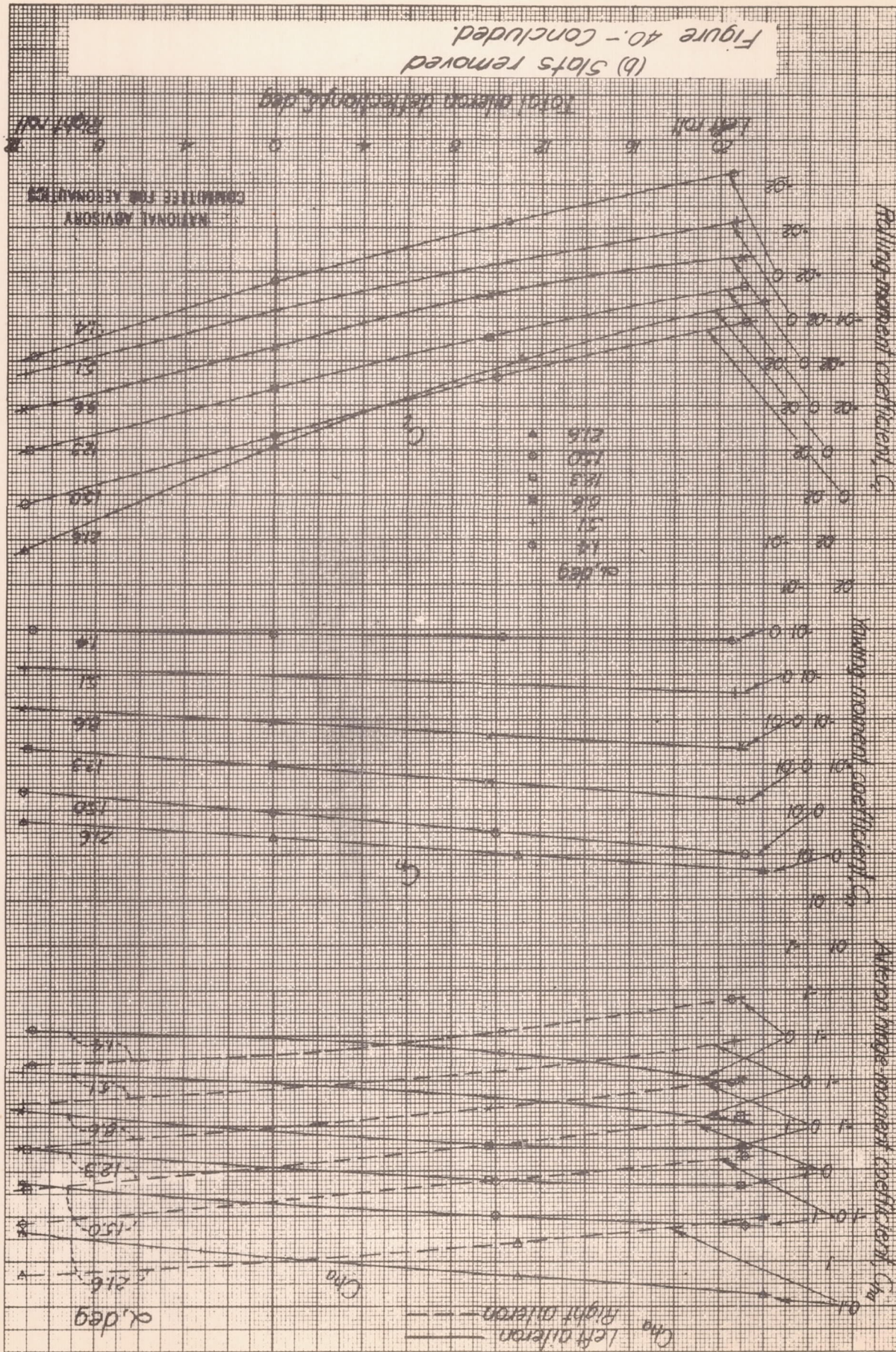


Figure 41.-Concluded.
(b) Slots removed

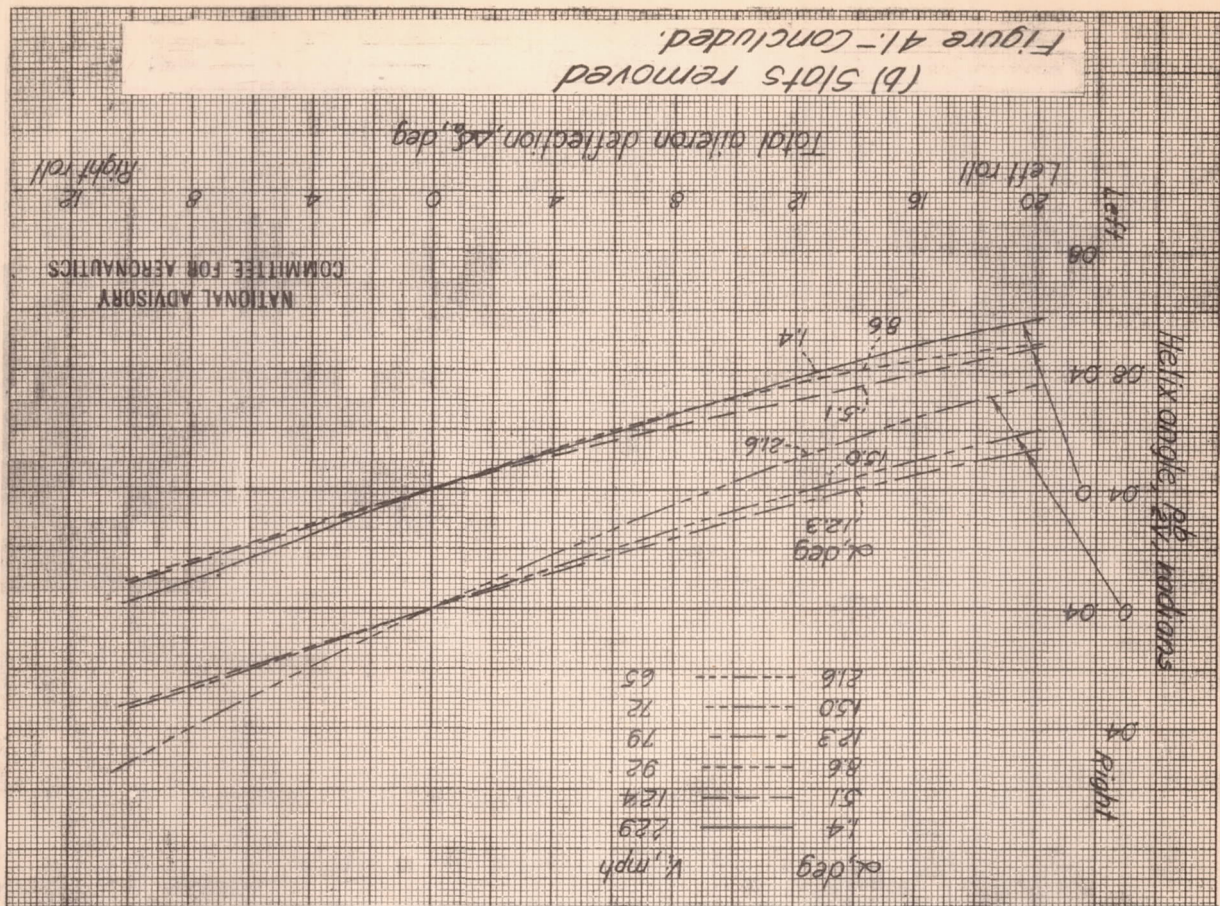
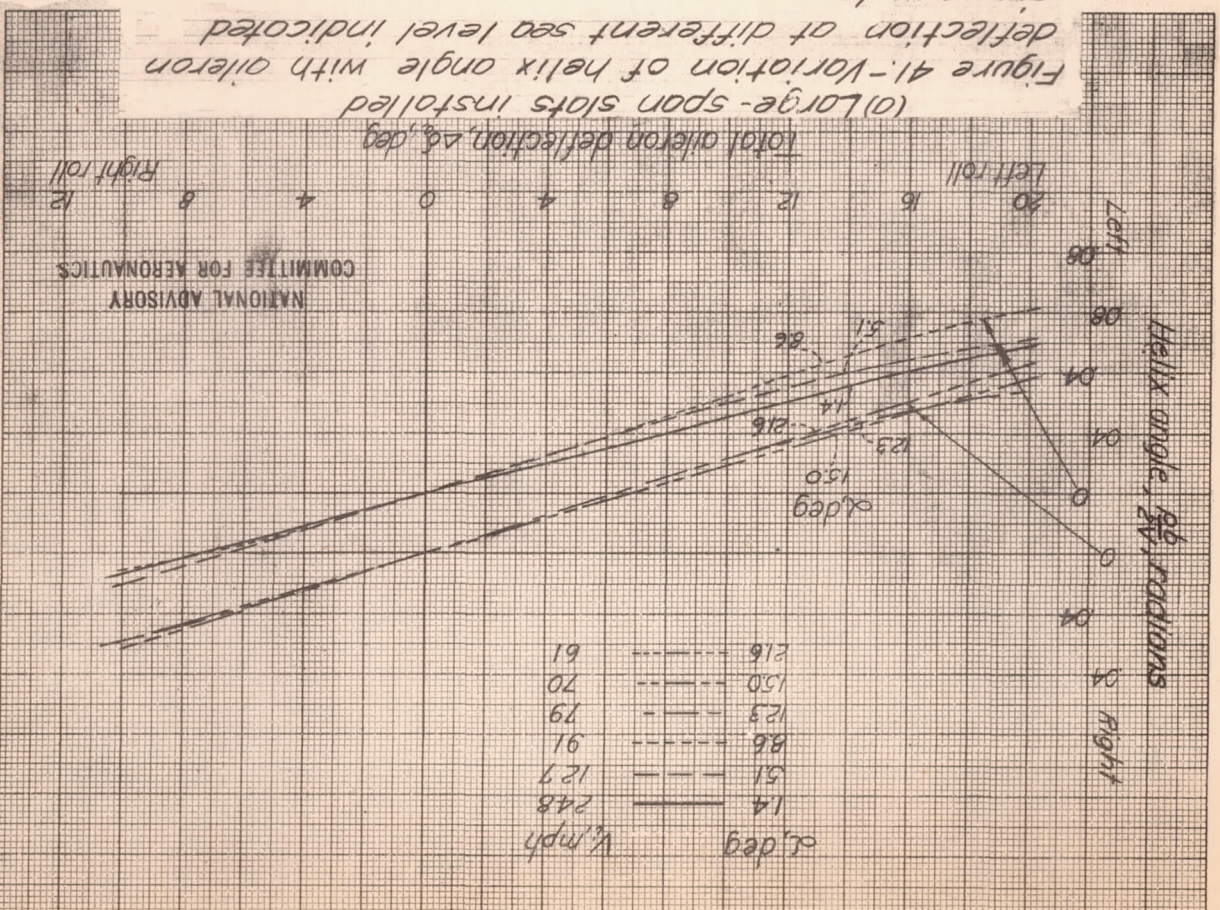


Figure 41.-Variation of helix angle with aileron deflection for different slot levels indicated air speeds.



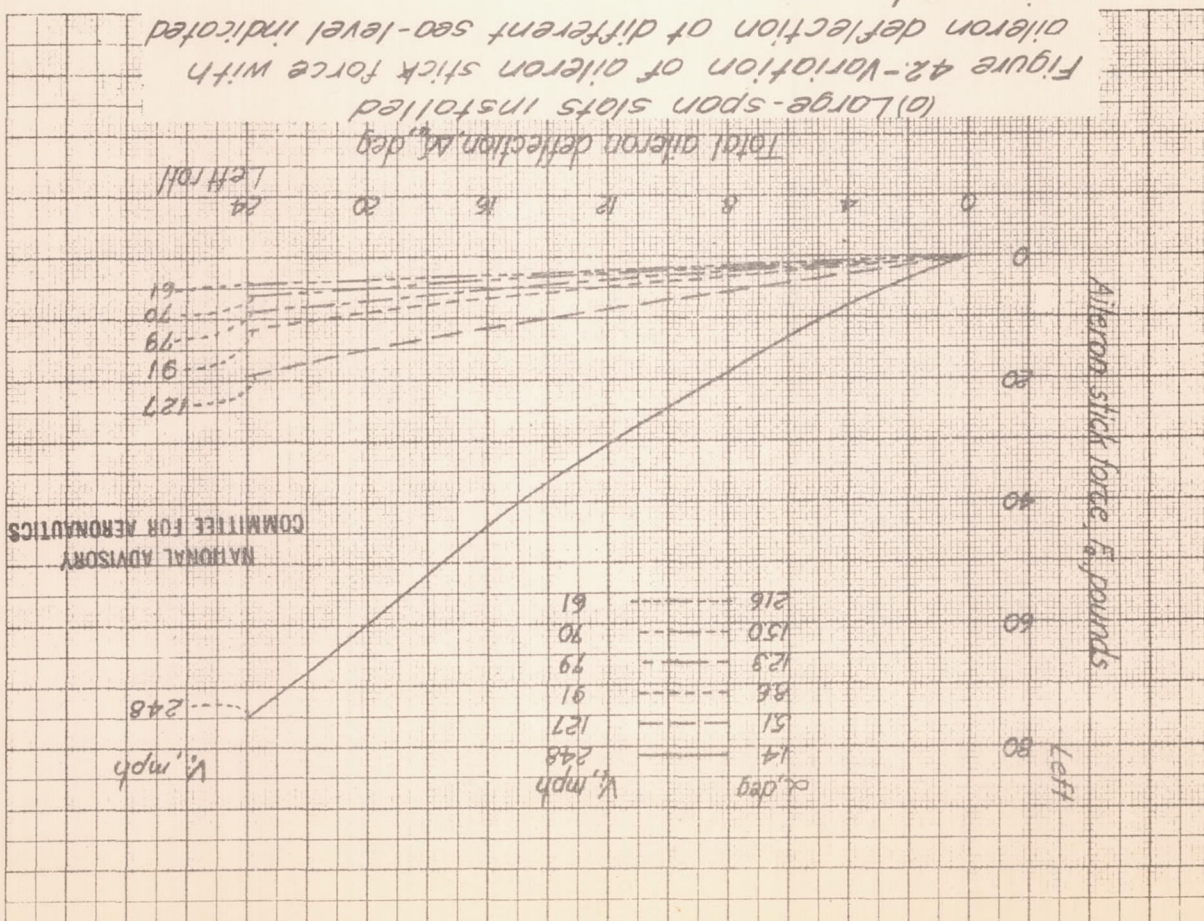
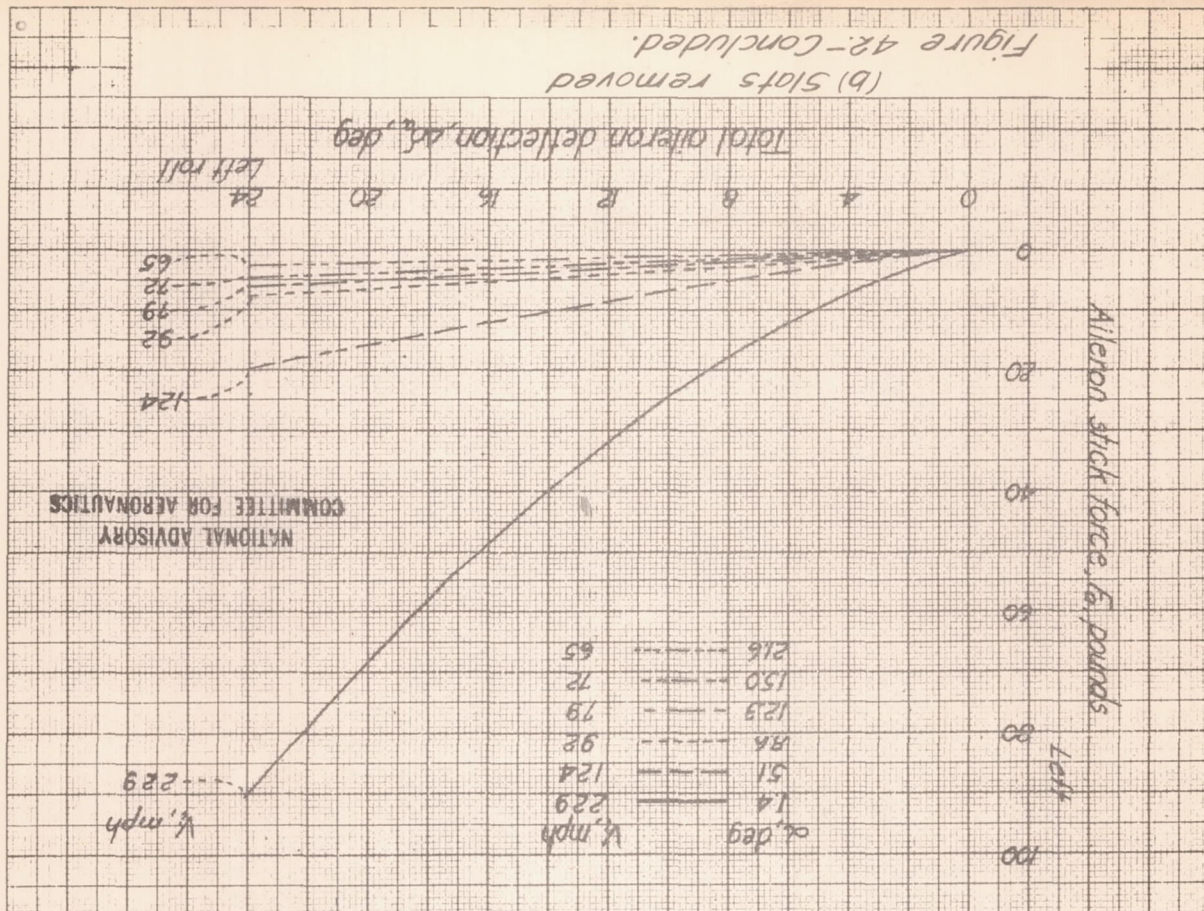
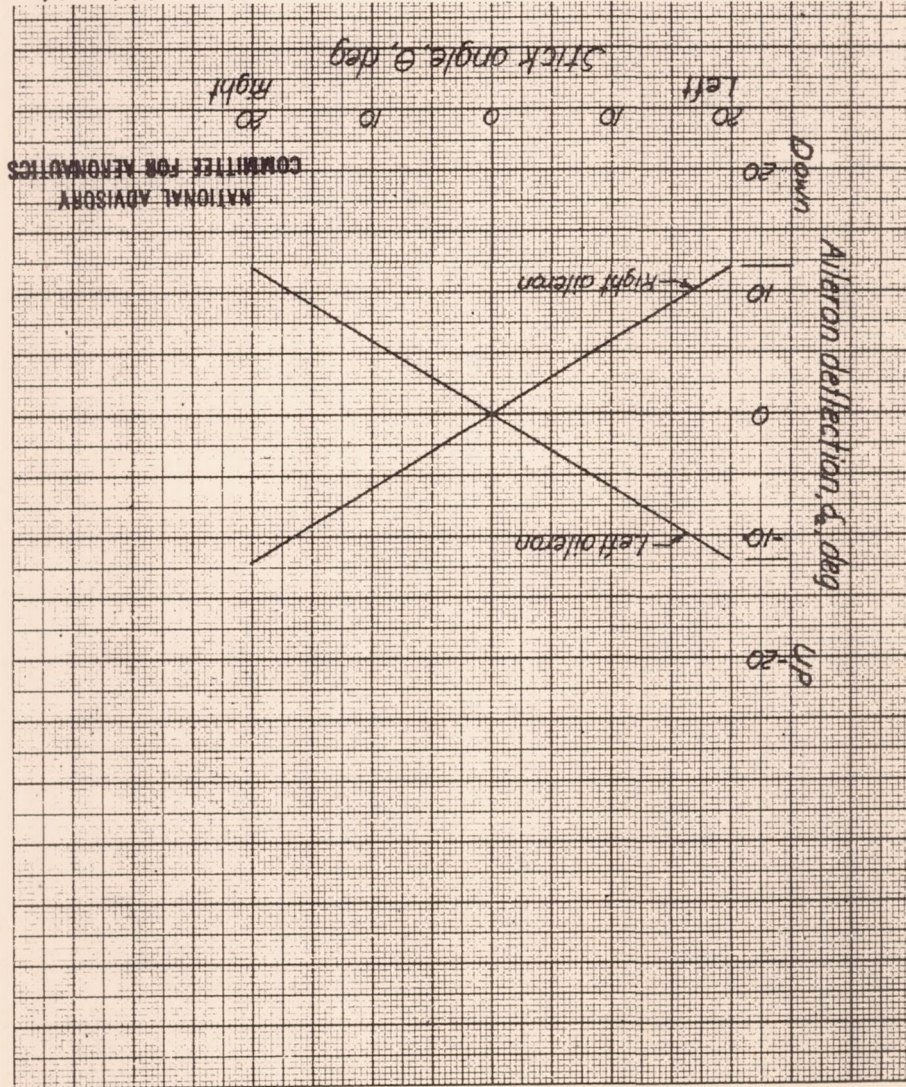


FIGURE 43.—LORIOTION OF STICK ANGLE WITH ALERON DEFLECTION FOR THE MX-334 AIRPLANE.



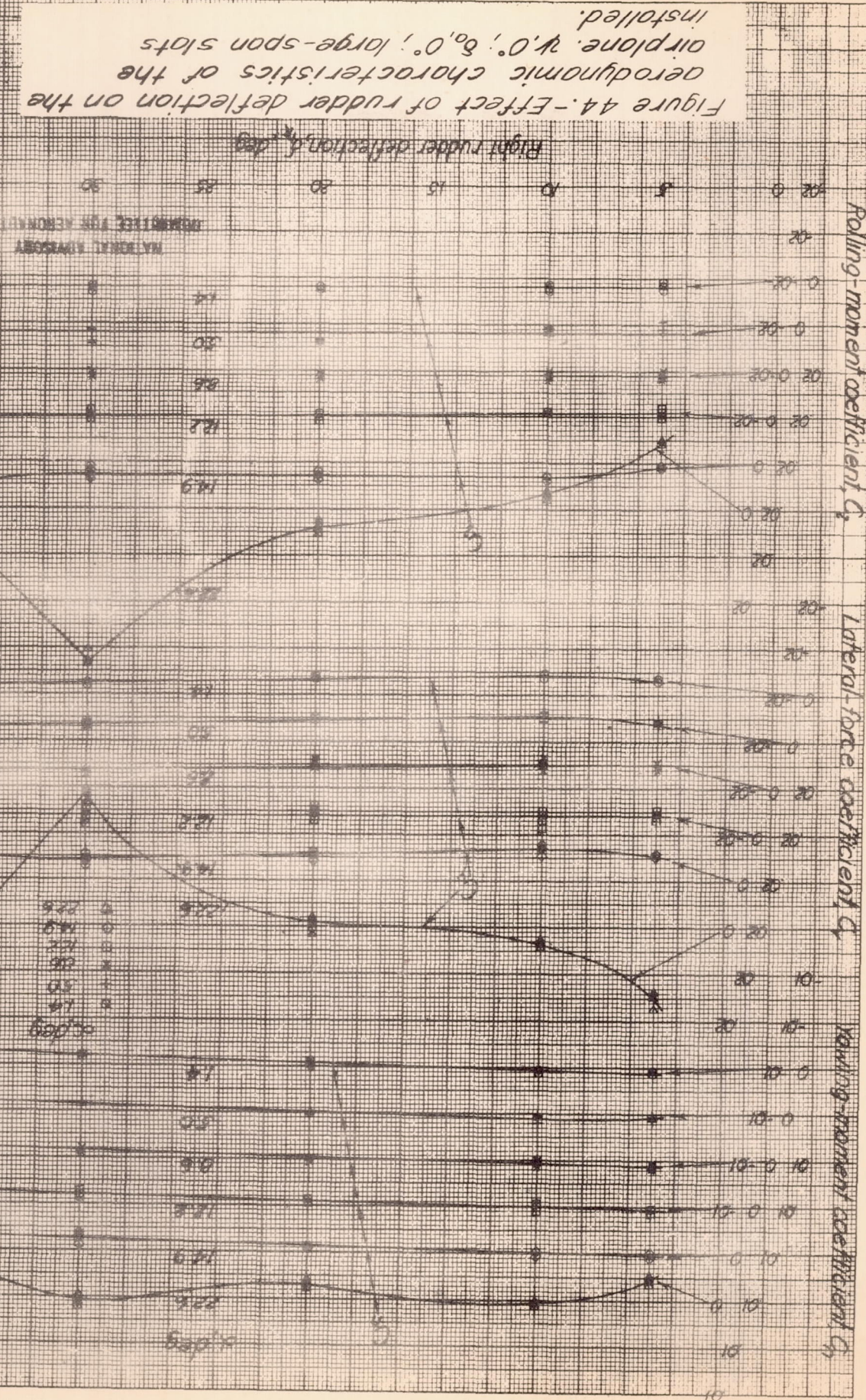


FIGURE 44.—Effect of rudder deflection on the aerodynamic characteristics of the airplane, $A.O.$, $B_0, 0^{\circ}$, large-span slots installed.

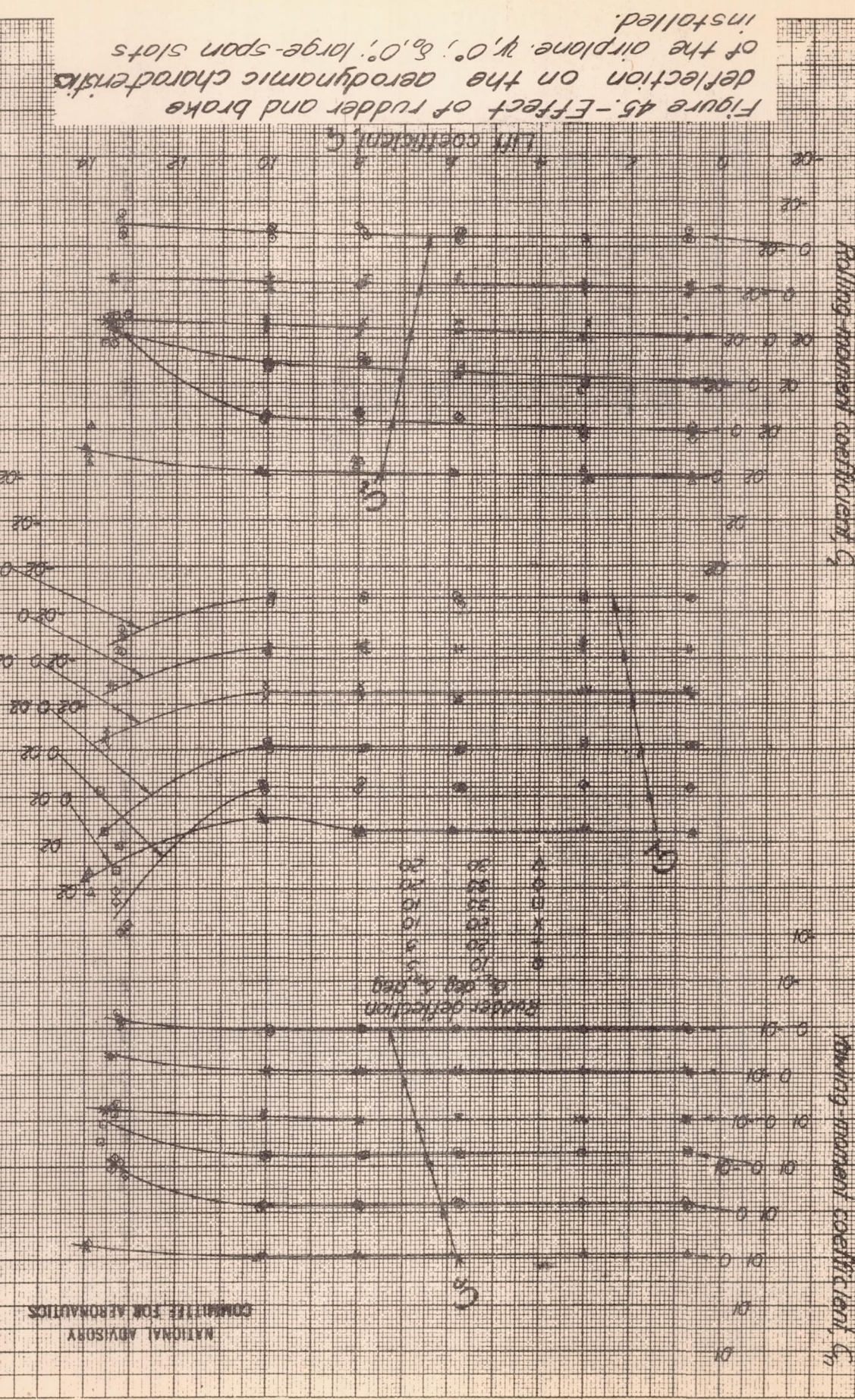
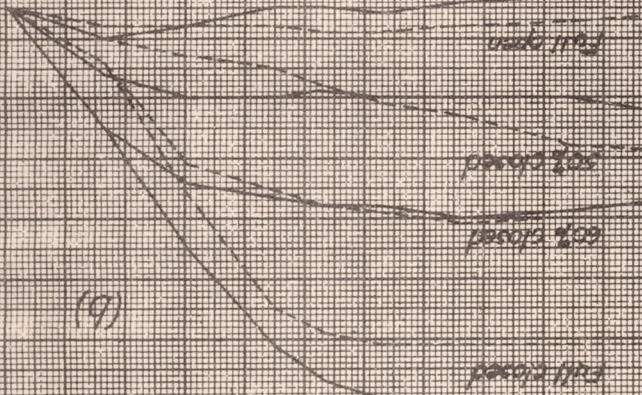


FIGURE 46 - Effect of inlet design on rudder deflection for four butterfly valve positions.
 (a) Original inlet (b) Modified inlet

CHARTS FOR ROLLING TESTS
WATER TANK 2000

Angle of attack, deg

0 2 4 6 8 10 12 14



(a)

Rudder deflection, deg

0 2 4 6 8 10 12 14

ROLL MOMENT COEFFICIENT

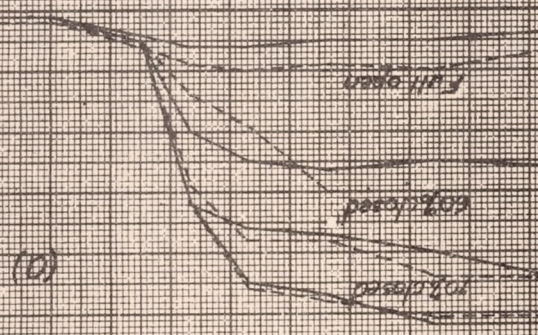
ROLL MOMENT COEFFICIENT

ROLL MOMENT COEFFICIENT

ROLL MOMENT COEFFICIENT

Angle of attack, deg

0 2 4 6 8 10 12 14



(b)

Rudder deflection, deg

0 2 4 6 8 10 12 14

ROLL MOMENT COEFFICIENT

ROLL MOMENT COEFFICIENT

ROLL MOMENT COEFFICIENT

ROLL MOMENT COEFFICIENT

Butterfly valve position

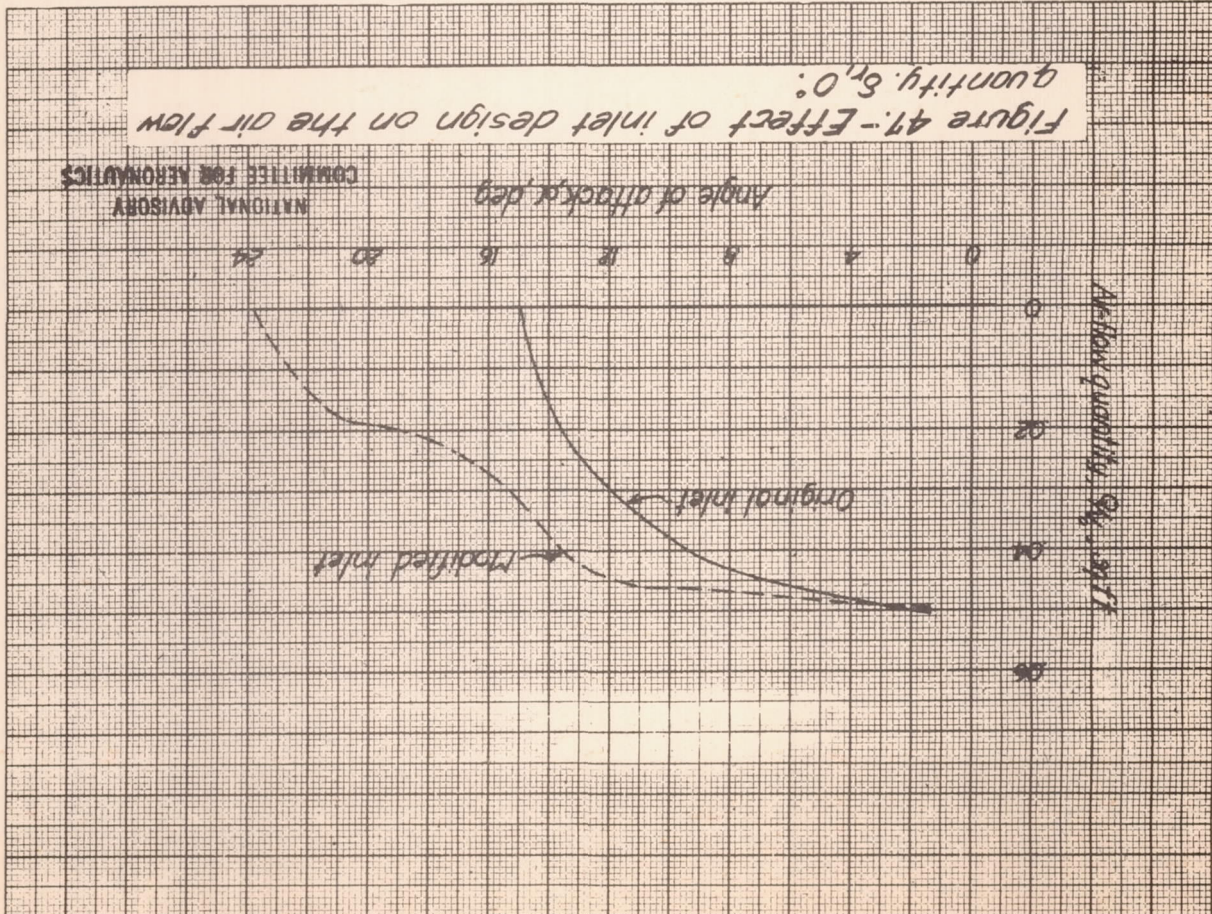
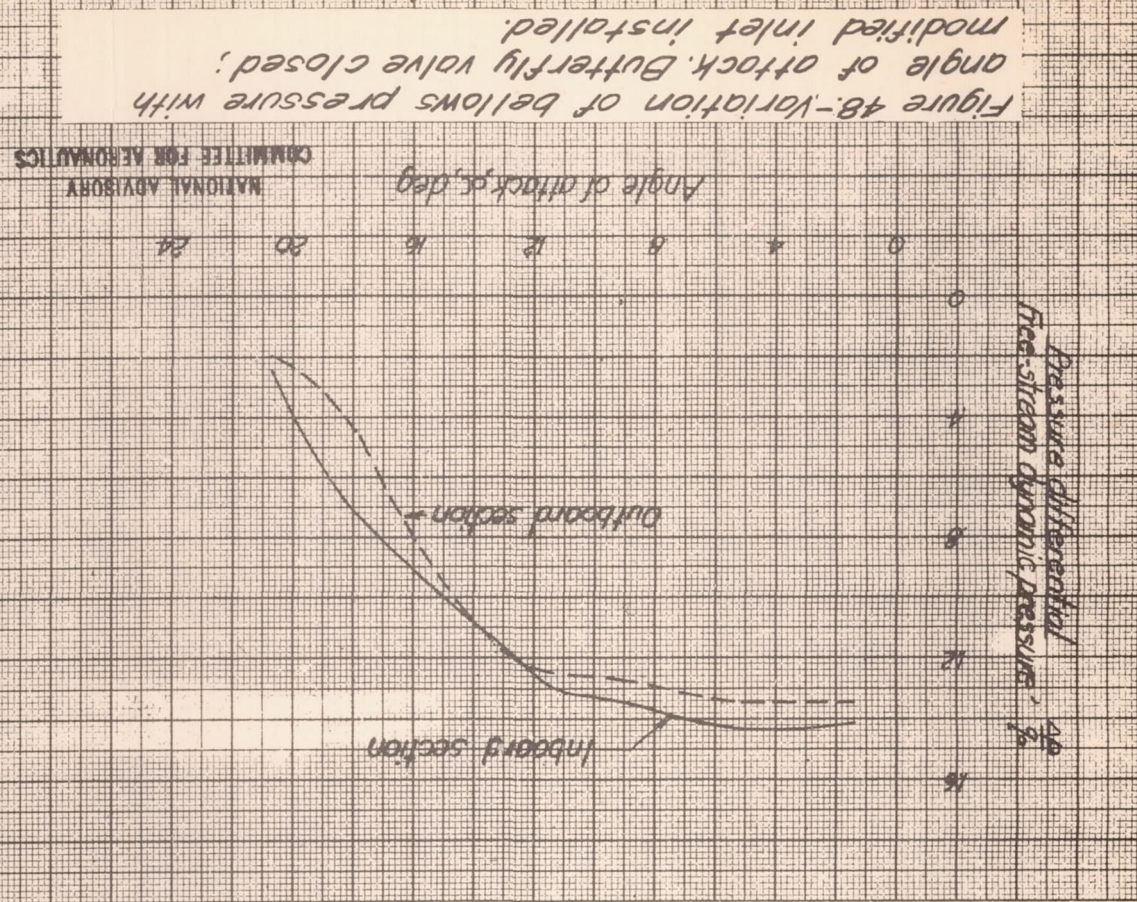


Figure 49. Variation of butterfly valve position with rudder deflection at several angles of attack.

